WAPD-TM-215
AEC RESEARCH AND
DEVELOPMENT REPORT

THE PERFORMANCE OF BASE-FORM ION EXCHANGERS FOR pH CONTROL AND REMOVAL OF RADIO-ISOTOPES FROM A PRESSURIZED WATER REACTOR SYSTEM

JULY 1960

CONTRACT AT-11-1-GEN-14

BETTIS ATOMIC POWER LABORATORY, PITTSBURGH, PA.,
OPERATED FOR THE U. S. ATOMIC ENERGY COMMISSION
BY WESTINGHOUSE ELECTRIC CORPORATION

DISCLAIMER

WAPD-TM-215
UC-4: Chemistry-General
TID-4500 (15th Ed.)

THE PERFORMANCE OF BASE-FORM ION EXCHANGERS FOR pH CONTROL AND REMOVAL OF RADIOISOTOPES FROM A PRESSURIZED WATER REACTOR SYSTEM

G. P. Simon • C. S. Abrams • W. T. Lindsay, Jr.

JULY 1960

Contract AT-11-1-GEN-14

Price $1.50
Available from the office of Technical Services,
Department of Commerce,
Washington 25, D. C.

BETTIS ATOMIC POWER LABORATORY
PITTSBURGH, PENNSYLVANIA
OPERATED FOR THE U. S. ATOMIC ENERGY COMMISSION BY
WESTINGHOUSE ELECTRIC CORPORATION

STANDARD EXTERNAL DISTRIBUTION

	No. Copies
UC-4: Chemistry-General, TID-4500, 15th Edition	559

SPECIAL EXTERNAL DISTRIBUTION

Manager, Pittsburgh Naval Reactors Operations Office, AEC	8
Director, Development Division, PNROO	3
Shippingport Atomic Power Station, C. S. Abrams	10
Westinghouse Research Laboratories, W. T. Lindsay, Jr.	10
Total	590

CONTENTS

	Page No.
I. INTRODUCTION	1
II. CONTROL OF pH BY BASE-FORM MIXED BEDS	2
A. Principles	2
B. Experience	4
C. Conclusions	6
III. REMOVAL OF FISSION PRODUCTS BY BASE-FORM MIXED BEDS	6
A. Preliminary Results	6
B. Laboratory Column Experiments	7
Experimental Procedures	9
Experimental Results	9
C. Equilibration Experiments	13
D. In-Pile Loop Test at Chalk River	18
E. Discussion	24
Monovalent Cations	24
Alkaline Earths	28
Halogens	29
Isotopes Forming Radiocolloids	29
IV. SUMMARY AND CONCLUSIONS	31
APPENDIX I: DESIGN AND TEST OF THE COLLIMATED AUTOMATIC COLUMN SCANNER	32
APPENDIX II: OPERATING HISTORIES OF LABORATORY ION EXCHANGE COLUMNS	40
A. NH_4OH - Form Columns	40
B. KOH - Form Columns	42
C. LiOH - Form Columns	44
APPENDIX III: DISTRIBUTION OF RADIOISOTOPES ON LABORATORY COLUMNS	50
APPENDIX IV: MULTISTAGE COLUMN THEORY INCLUDING RADIOACTIVE DECAY OF MICROCONSTITUENT	61
APPENDIX V: SURVEY OF HIGH pH OPERATION OF IN-PILE AND OUT-OF-PILE LOOPS	65
ACKNOWLEDGMENTS	69
REFERENCES	69

This report summarizes laboratory experiments and in-pile loop tests designed to evaluate, explain, and predict the performance of mixed-bed ion exchange columns in the base form for the control of radioisotopes in reactor coolants. The results of these tests are evaluated with the aid of a simple theory of column performance for absorption of radioactivity decaying ions, based on an approximate model for an ion exchange column. It is concluded that LiOH form resin will perform satisfactorily for both pH control and activity removal and that it is more effective than either KOH resin or NH_4OH resin for these purposes.

THE PERFORMANCE OF BASE-FORM ION EXCHANGERS FOR pH CONTROL AND REMOVAL OF RADIOISOTOPES FROM A PRESSURIZED WATER REACTOR SYSTEM

G. P. Simon, D. S. Abrams, and W. T. Lindsay, Jr.

I. INTRODUCTION

Side-stream purification systems were incorporated into the first pressurized water reactors as an aid in maintaining the coolant in as high a state of purity as possible. Mixed beds of strong acid cation-exchange resin in the hydrogen form and strong base anion-exchanger in the hydroxyl form were used in such purification systems.

These beds have the ability to remove dissolved, ionized material quite effectively by exchange with hydrogen or hydroxyl ion, to remove colloidal material from the water with moderate effectiveness by absorption on the large surface area provided by the resin bed, and to remove particulate matter with somewhat less effectiveness by acting as a bed filter. Thus, it was expected that practically all impurities in the coolant entering the purification side-stream would be removed by the ion exchange resin in the demineralizer.

The build-up of activity on pipe walls soon indicated that side-stream purification, at rates of the order of 10^{-4} system volumes per second, was not able to exert effective control over the slowly migrating inventory of particulate corrosion products accumulated in reactor plants operated with pure water as a coolant. It also became apparent that continuing radiation induced synthesis of ammonia from dissolved hydrogen, and nitrogen was able to perturb the coolant composition sufficiently to maintain a slightly basic condition if nitrogen was not excluded from the makeup water.

In-pile loop operations revealed the beneficial effects of a basic condition of the coolant in exerting more effective control over the insoluble corrosion products than was possible by simple demineralization and filtration of a portion of the coolant. Accordingly, resin beds in the purification system took on a new function—control of coolant pH to the desired level, now specified as pH 9.5 to 10.5. This required the use of mixed bed resins in the base form, i.e., with the cation resin regenerated with the appropriate alkali metal cation and the anion resin in the hydroxyl form.

It was desirable, concurrently, to retain the other functions of the purification system to remove all impurities other than the desired base.

However, the relative inability to control the insoluble material in the coolant system became of less concern because the concentration of particulate corrosion products in the coolant was markedly reduced by the use of strong base. Consequently, this becomes a relatively unimportant function of the purification system in coolant systems operating at high pH. The removal of freshly released corrosion products, which are still in the colloidal form, at a rate that would be competitive with the natural or radiation prompted transformation to insoluble material, remains a desirable objective for a side-stream purification system. However, it does not appear that effective competition can be achieved with practicable processing rates. This is especially true in high pH environments where it appears that the conversion to insoluble species proceeds at a somewhat greater rate than in pure neutral water. Thus, there remains one function for the purification system in addition to pH control—the control of the concentration of ionized or colloidal radioisotopes in the coolant to minimize radiation and radiological difficulties.

At the present state of the art, the ability of base-form mixed bed resins to perform this last function in the presence of a micro-concentration of a base was somewhat doubtful, and was the subject of this investigation. Ion exchange absorption of impurities depends on a favorable mass-action equilibrium for the exchange of ions in the aqueous phase with ions in the resin phase. The higher the concentration in the water of those ions which also nearly saturate the resin phase, the less favorable are the conditions for absorption of some other ionic species by the resin. Demineralizers, employing mixed resins of hydrogen-form cation resin and hydroxyl-form anion resins, work effectively for two reasons: hydrogen and hydroxyl ions are among the easiest to displace from the resin, and their concentration in neutral water is held to an extremely low value by their combination to form water.

Obviously, the situation is much less favorable for removal of ionized impurities from a high pH coolant by a base-form, mixed-bed resin. It is possible, however, that temporary residence in the bed of short-lived and moderate-lived ionized isotopes, due to an elution phenomenon, can be sufficient for considerable decay of these species, thus permitting effective control over their radioactivity in the coolant.

This report describes the work done to evaluate, explain, and predict the performance of base-form ion exchange beds in carrying out the two major functions of such beds in a side-stream coolant purification system—control of pH and control of the concentration of radioisotopes.

II. CONTROL OF pH BY BASE-FORM MIXED BEDS

A. Principles

A bed of base-form ion exchange resin in a bypass purification system provides a reservior of base from which leakage losses from the coolant can be replaced. In typical pressurized water reactors, with in-pile loops or out-of-pile loops, the ratio of resin volume to system volume may range from between 1 to 30 and 1 to 200. At 0.7 moles of base per liter of bulk wet resin volume, there will be from 233 to 35 times more total base in the resin bed than in the entire coolant at a concentration of 10^{-4} molar.

However, a well washed resin will not release base when a dilute base solution or even pure water is passed through the bed. Some other ionized material must be present in the influent to displace the base from the resin bed. It is the balance between the supply of the displacing ions and the rate of loss of the base from the coolant by leakage or sampling that allows control of pH by the presence of a bed of base-form resin. The displacing ions may originate from several sources. They may be in the makeup water, they may be produced by

corrosion, or they may be generated in the coolant by radiation-induced reactions. Makeup is normally demineralized. Hence, it is the last two processes which usually control release of base.

If the generation of displacing ions is pH-sensitive, it is possible that the system will be self-regulating. For example, if the concentration of ferrous ions in the coolant is higher at low pH values, because of increased release rates of corrosion products or higner solubility, any deviation toward low pH will be checked or reversed by the resulting increased rate of base release from the resin bed. Conversely, deviations toward pH values higher than the stable value will result in reduced base release rates, which, when coupled with higher losses in discharged or leaked water, will bring the base concentration back to the normal level, thereby increasing corrosion product release rate to normal also.

The equations describing the various processes can be written:

$$\frac{dC_1}{dt} = \frac{k_1 A}{V} - \beta C_1 - \frac{\ell_1 C_1}{V} - \alpha C_1, \quad (1)$$

$$\frac{dC_2}{dt} = \frac{k_2}{V} - \beta C_2 - \frac{\ell_2 C_2}{V} - \alpha C_2, \quad (2)$$

$$\frac{dC_B}{dt} = \beta(C_1 + C_2) - \alpha C_B, \quad (3)$$

where

V = volume of the coolant system.

C_1 = normality of the ionized corrosion products.

C_2 = normality of the ionized radiation produced in the coolant products.

C_B = normality of the base in the coolant.

k_1 = rate constant for the release of ionized corrosion products.

A = area of the corroding surface.

k_2 = rate constant for the production of ionized radiation products (ammonia).

β = rate constant for the absorption of ionized corrosion or radiation-produced products in the ion exchanger.

ℓ_1 = rate constant for the loss of ionized corrosion products by processes other than absorption in the ion exchange bed.

ℓ_2 = rate constant for the loss of radiation-produced products (ammonia) by processes other than absorption in the ion exchanger.

α = rate constant for water replacement.

Since β is usually much greater than α, the following will hold for the steady state:

$$C_B = \frac{(k_1 A + k_2) - \ell_1 C_1 - \ell_2 C_2}{\alpha V} \quad (4)$$

Experiments in which release of corrosion products from carbon steel have been measured at various pH values indicate that K_1 is dependent on the base concentration C_B, and is lower at higher values of C_B. Similarly, it would appear from various qualitative observations that ℓ_1, the rate constant governing conversion of ionized corrosion products to non-ionized products, also depends on the pH and is higher at higher pH values. No evidence exists one way or the other concerning the pH dependence of k_2 and ℓ_2, rate constants governing the formation and dissociation of ammonia by radiation. If it is assumed that there is no effect of pH on these rates, it is then apparent that self-regulation of pH can occur only in systems where ionized corrosion products control the rate of release of base from the bed, i.e., where C_1 is much greater than C_2. This will be the case only in plants in which makeup water is degassed, so that the concentration of dissolved nitrogen gas is very low.

This is not to imply, however, that the pH may not be easily controlled in other systems, for the balance between input and loss of base is very sluggish and control of pH within a range of one unit allows the base concentration to vary by a factor of 10.

As will be seen from later discussion in this report, most cations will easily displace lithium from IR-120 cation resin. Thus, if the resin is in the LiOH form and ammonia production is considerable, the bed may be almost completely converted to the NH_4OH form after an extended period of use. This situation was actually found at the conclusion of an extended power run with an operating reactor. Analyses of cored sections of the resin at the end of the run showed that 60% of the total capacity was taken up by NH_4^+ ions and 31% by Li^+, with the ammonium ions more concentrated in the uppermost parts of the bed. Small amounts of potassium, sodium, and iron were also found on the bed.

All of the preceding discussion applies to cases other than ammonium hydroxide beds. In this case, of course, dissociation and formation of ammonia by radiation play a direct role in establishing the steady-state level of ammonia concentration, while supply of ammonium hydroxide from the reservoir in the resin bed is regulated only by the supply of ionized corrosion products or impurities in the makeup water.

B. Experience

Little is yet known about the parameters in Eq (4) and their dependence on pH. It does appear, however, that ℓ_1/V, the rate constant describing conversion of ionized corrosion products to non-ionized forms, is large relative to β, the purification rate constant, so that a large fraction of the corrosion products initially released in ionized form is not absorbed by the ion exchanger. Thus, the net rate of formation of ionized corrosion products that can be observed in connection with ion exchanger operation is a small part of the total rate of corrosion product formation.

A survey was made of several in-pile and out-of-pile loop tests to determine the performance of LiOH and KOH beds in these loops for pH control. It was found that difficulty had been encountered in control of pH only in cases where leakage was excessive or where the loops were drained frequently. This is understandable, since it could hardly be expected that the net release of corrosion products would be high enough to displace base from the bed at a rate sufficient to keep up with a very high rate of loss of base from the coolant.

Some of the tests during which the loops operated for reasonably long periods of time without requiring direct addition of base are summarized in Table I. Although the data on pH and leak rate are qualitative at best, it is nevertheless interesting to calculate the apparent net rate of absorption of ionized corrosion products by the ion exchangers by using Eq (4). Ammonia formation is taken to be negligible, and the ionized corrosion products are assumed to be largely Fe^{++}. Although the results given in the table are of a believable order of magnitude, it is possible that the pH may have been falling steadily during the time without addition, and the calculated values of net ionized corrosion product release rate may be high. Nevertheless, it appears that it is possible for corrosion to release ionized material at a sufficient rate to control pH, at least in a system without an excessive water replacement rate.

The LiOH resin bed used during the extended power run mentioned previously picked up during its 4700-hr life an amount of ferric iron corresponding to a 0.13 mg Fe/dm^2-mo net release rate. According to Eq (4), this rate could have controlled the pH at about 10 in a system with a water replacement rate of about 4×10^{-4}/hr, equivalent to an average leak rate of about 1.4 gph in a 3500 gallon reactor coolant system. The actual

TABLE I

PERIODS OF OPERATION OF IN-PILE LOOPS WITHOUT ADDITION OF BASE TO COOLANT

Loop and Test	Time without Addition (hr)	pH Range	Base	Surface Area (ft^2)	Material	Leak Rate (cc/hr)	Calculated Net Release Rate of Ionized Corrosion Products* (mg Fe/dm^2-mo)
X-1-d	700	9.5-10.5	KOH	112	Stainless steel	10	0.02
X-1-j	600	9.5-10.5	KOH	112	Stainless steel	150	0.3
X-2-a	1000	9.5-10.5	KOH	112	Stainless steel	160-240	0.4
X-2-f	1200	9.5-10.5	KOH	112	Stainless steel	400	0.8
X-3	1000	10.0	KOH	112	Stainless steel	125	0.25
					Average for stainless loops		0.35
CR-VI-A	1000	9.5-10.5	KOH	112	Carbon steel	1700-4000	5.5

* Based on average pH 10 and average leak rates.

leak rate was much higher than this value, but despite this, the exchange of radiation-produced ammonia on the resin bed released enough additional lithium hydroxide to hold the pH within the desired range. The leak rate had to average about 36 gph to account for the loss of lithium hydroxide observed when the resin bed samples were taken for analysis before discharge.

As seen from Eq (4), the equilibrium base concentration is proportional to K_1A/V. Comparison between various systems must therefore take into account the nature of the material (which determines K_1) and the ratio of surface area to volume A/V. Although β, the purification flowrate constant, is usually maintained at the same value in loops as is employed in reactor plants, the values of A/V vary from system to system.

C. Conclusions

Release rates observed for carbon steel (Refs 1 and 2) in high pH environments lead to the assumption that in systems fabricated predominantly from stainless steels, the net release rate of ionized corrosion products is not greater than 0.1 mg Fe/dm^2-mo at pH 10. A system without ammonia formation will be able to hold this pH, provided the ratio of corroding surface area to water replacement rate is from 5900 to 8800 ft^2/gph, and depending on whether the iron is absorbed as the ferric or ferrous ion. Ratios in this range require a reasonably tight system. Additional base is required if the leak rates are high. This may be supplied by direct addition, either as a concentrate or by adjustment of the pH of the makeup water, or by establishing conditions such that ammonia will form and displace the required base from the resin bed.

Of course, direct addition will be necessary initially and after draining and refilling of a large fraction of the plant volume, since release of base from the bed will be gradual under normal circumstances.

In PWR, it has been necessary to add LiOH only in connection with additions of large volumes of water associated with plant cooldown and draining and refilling of loops. During steady operation, pH was maintained without additions between 9.7 and 9.9 for periods up to 2000 hours.

III. REMOVAL OF FISSION PRODUCTS BY BASE-FORM MIXED BEDS

A. Preliminary Results

As discussed previously and in Appendix IV, there is good reason to believe that the apparent or effective performance of mixed-bed ion exchangers in the base form should be better for short-lived isotopes than for long-lived ones. One of the first indications of this effect came from the X-1-h defected UO_2 fuel specimen test in the X-1 loop at Chalk River (Ref 3). A study of the performance of the ion exchanger in the loop purification system was undertaken during this test.

The ion exchanger was initially in the hydrogen-hydroxyl form. It consisted of a bed of MB-1 resin about 76 cm deep, with about 350 cc total bed volume. Flow loading of this bed was normally 15 gpm/ft^2, equivalent to a contact time of 0.5 min. No base was deliberately added to the loop coolant. Samples of the bed influent and effluent were taken regularly and analyzed for Cs^{136}, Cs^{137}, Cs^{138}, Cs^{139}, and I^{131}. In addition, samples of coolant were obtained for gas analyses to determine the Xe^{138} content. The purpose of this work was to determine the reason for the relatively low decontamination factors for gross activity that had been regularly reported from this and similar tests in which hydrogen-hydroxyl resin had been used.

More pertinent to the subject of this paper, however, was an interesting occurrence, fortuitously observed during this study. This occurrence evidences itself in Table II in which the decontamination factors for I^{131}, Cs^{136}, Cs^{137}, Cs^{138} (corrected), and Cs^{139} are given, along with the results

of measurement of the conductivity of the loop water during the 19-day bed test.

It is apparent from Table II that the cation-resin part of the mixed bed, at least, became exhausted by some impurity, probably by ions of an alkali metal or ammonia. Although no ion exchanger effluent conductivity determinations were made, unfortunately the loss of control of loop water conductivity clearly shows that the bed was saturated with some ionized material in the macro-concentration range. Decontamination factors for the two long-lived cesium isotopes, 37-y Cs^{137} and 13-d Cs^{136}, began to fall on the sixth day of the test, indicating approaching exhaustion of the bed. The decontamination factors for these isotopes reached unity at about the same time that the bed lost all control over loop water conductivity. The good apparent removal of the shorter-lived isotopes, 32-m Cs^{138} and 9.5-m Cs^{139}, was not affected by these changes. Since the time required for transit of water through the bed was on the order of 1 min, it is clear that the large decontamination factors for these isotopes must have been the result of hold-up while the cesium ions were repeatedly exchanged between water and resin phases. Eight-day I^{131} was effectively exchanged throughout the period of observation. (Compare these results with the later study of LiOH-form resin during the Chalk River X-1-L test, as shown in Fig. 3.)

Othor preliminary work, reported earlier (Ref 4), showed that activity breakthrough and conductivity breakthrough occur simultaneously when a dilute solution of KOH containing Cs^{137} is passed through a mixed-bed resin column in the H-OH form for a sufficient time to convert the bed to KOH resin. When the same experiment was carried out with LiOH solutions, activity breakthrough did not occur, although the processing of solution was continued well beyond the point at which the pH and conductivity of the column effluent became equivalent to that of the influent. These two results show that the resin has preference for Cs^+ over Li^+, while the preference for Cs^+ over K^+ is much less if, indeed, the preference is not reversed in the latter case. It follows, therefore, that K^+ is also preferred in the resin phase over Li^+. It also appears that Li^+ could not have been the exhausting cation during the X-1-h test described above.

B. Laboratory Column Experiments

The information described above, although of a preliminary nature, indicates that a base-form resin bed may control some radioisotopes by acting as a holdup volume for short-lived species. The data, however, is not sufficient to determine whether base-form resin beds can exert effective control over the concentration of ionized radioisotopes in a reactor coolant system. Two requirements are necessary for an affirmative answer to this question: First, the radioisotope in question must have a half-life on the order of or greater than the "purification half-life" (usually about 2 hours); and, second, the bed must have a decontamination factor on the order of 2 or greater. As shown in Appendix IV, it is predicted that isotopic exchange of monovalent radioisotopes from a pH 10 solution will result in a continuing decontamination factor of e, or greater, for half-lives of 8 days or less if the bed is equivalent to 10 or more equilibration stages. For this case, therefore, effective control would be exerted over the concentration of such radioisotopes having half-lives between 2 to 3 hours, and 8 days. The laboratory column experiments described in this section were undertaken to obtain additional data from which the effectiveness of control of the purification system could be predicted for the more important fission products expected in the coolant of pressurized water reactors. Ideally, the results of experiments with long-lived isotopes should be interpretable in terms of the constants K_c and n of the theory of Appendix IV, so that predictions can be made for performance of resin beds in control of shorter-lived isotopes of the same elements. This objective was not entirely achieved, as is explained later in this section under the heading Discussion.

TABLE II

DECONTAMINATION FACTORS FOR SPECIFIC ISOTOPES AND LOOP WATER CONDUCTIVITY DURING THE 19-DAY FILTER BED TEST PORTION OF THE X-1-h TEST

Day of Test	Time of Day	Decontamination Factors					Loop Water Conductivity (μmho/cm)	Remarks
		I^{131}	Cs^{136}	Cs^{137}	Cs^{138}*	Cs^{139}**		
1	1327	7.8×10^3	7.7×10^3	6.3×10^3	21	$>1.5 \times 10^3$	1.0	Flow loading 15 gpm/ft^2
2	0927	1.4×10^3	1.4×10^2	1.3×10^2	40	$>1.5 \times 10^3$	1.0	
2	1322	2.6×10^4	1.5×10^2	1.5×10^2	$>9 \times 10^6$	$>8 \times 10^2$	1.0	
3-5	8/22	--	--	--	--	--	1.0	Purification flow interrupted
6	1003	9.4×10^3	1.4×10^2	95	53	ND	0.97	Flow loading 7.5 gpm/ft^2; Contact time about 1 min
6	1033	5.1×10^3	1.2×10^2	82	32	ND	0.97	
6	1354	1.2×10^4	54	31	15	ND	0.97	
6	1453	3.5×10^3	36	25	17	ND	0.97	
9	1249	2.9×10^3	6.8	5.2	53†	$>2 \times 10^3$	0.80	
11	0938	9×10^3	7.5	4.4	17	ND	0.7	Cation resin approaching exhaustion; control of loop water conductivity lost.
16	1356	8.7×10^3	3.9	2.4	4×10^2	ND	1.2	
17	--	ND	ND	ND	ND	ND	2.1	
18	--	ND	ND	ND	ND	ND	6.8	
19	1015	ND	0.86	0.72	ND	$>1.6 \times 10^3$	10.6	
19	--	ND	ND	ND	ND	ND	41.7	

ND — Not determined

* Corrected for growth from Xe^{138}. Two types of Xe^{138} analyses were performed. These are designated as "bulb analyses" and "bottle analyses". The reported results are based on "bottle analyses" except where designated otherwise. Results are probably minimum values.

** Cs^{139} was never positively detected after the ion exchanger. All decontamination factors are minimum values.

† Based on "bulb analyses". No "bottle analyses" available for this day.

Experimental Procedures

Procedures followed those used in previous work (Ref 4). The ion exchange columns consisted of a mixture of two parts by volume of IRA-400 in the hydroxyl form to one part by volume of IR-120 in the appropriate cation form, giving a one-to-one cation-to-anion equivalent ratio. They are referred to in this report as base-form, mixed-bed resin columns. The bed dimensions were 1.05-cm diameter by about 76 cm (30 in.) deep, and each contained about 66 ml of wet settled resin. Some additional work was done with shorter columns of the same diameter but 12.5 cm (5 in.) long, containing about 11 ml of wet settled resin. Influent solutions were prepared in about 25-liter batches and were adjusted to the desired pH with the appropriate base after addition of the radioactive isotopes.

The following radioisotopes were obtained from Oak Ridge National Laboratory:

Sr^{90}-Y^{90} — carrier-free, as $SrCl_2$ in 1-N HCl

Zr^{95}-Nb^{95} — carrier-free, as oxalate complex in 0.5% oxalic acid

Ru^{106}-Rh^{106} — carrier-free, as $RuCl_3$ in 6-N HCl

Cs^{137}-Ba^{137} — carrier-free, as CsCl in 1-N HCl

Ce^{144}-Pr^{144} — carrier-free, as $CeCl_3$ in 1-N HCl

With the exception of Zr^{95}-Nb^{95}, the solutions were used as-received, with dilution by factors on the order of 10^6 in preparation of the process solutions. The Zr^{95}-Nb^{95} solution was converted to the nitrate after destruction of the oxalate complex and then diluted in the same way as the other radioisotopes.

All solutions were processed through individual glass columns at a flowrate equivalent to an area flow loading of 7.5 gpm/ft^2. Flow was maintained by gravity head, supplemented by rubber-tubing pumps. No attempt was made to obtain completely continuous operation. Flow was often stopped evenings, weekends, and over long holidays. Samples were taken periodically from the column influent and effluent streams. The relative concentrations of the radioisotopes in the samples were determined by evaporating to dryness and beta-counting in methane-flow proportional counters having efficiencies of about 15% for Sr^{90}. Decontamination factors are the ratios of influent to effluent radioactivity concentrations, the determinations having been made on equivalent geometrical and efficiency bases. Radiation from various levels in the columns was regularly monitored with an uncollimated, portable ionization chamber.

Experimental Results

Three tests were run with resin in the NH_4OH form, using SR^{90}-Y^{90}, Cs^{137}-Ba^{137}, and Ce^{144}-Pr^{144} as the added radioactivities. The influent solution was adjusted to pH 9.5 with NH_4OH. The operating histories of the columns are given in Table III and its referenced Tables. The number of column equivalents passed through each column was calculated on the basis of the total ammonia content of the solution, including non-dissociated base. As in all subsequent calculations of column equivalents, the capacity of the resin was assumed to be 0.7 eq/liter of wet settled resin.

TABLE III

NH_4OH-BED OPERATING HISTORIES

Activity	pH	Approximate Bed Length (cm)	Table
Sr^{90}-Y^{90}	9.5	76	XXV
Cs^{137}-Ba^{137}	9.5	76	XXVI
Ce^{144}-Pr^{144}	9.5	76	XXVII

TABLE IV

KOH-BED OPERATING HISTORIES

Activity	pH	Approximate Bed Length (cm)	Table
Sr^{90}-Y^{90}	10.3	76	XXVIII
Cs^{137}-Ba^{137}	10.3	76	XXIX
Ce^{144}-Pr^{144}	10.3	76	XXX

The results of the tests with Sr^{90}-Y^{90} must be considered questionable, since no effort was made in the counting procedure to distinguish between Sr^{90} and Y^{90}. It is quite probable, as is discussed later, that the apparent breakthrough of this activity in the effluent of the NH_4OH and KOH difficulties (Table IV) is not to be expected with the Cs^{137}-Ba^{137} and Ce^{144}-Pr^{144} activities, because sufficient time had elapsed between sampling and counting to allow re-establishment of mother-daughter equilibrium in the effluent samples. The breakthrough of Cs^{137} at about 0.1 column equivalent in the KOH bed and the apparent impending breakthrough of Cs^{137} at about 0.3 column equivalent in the NH_4OH bed show that K^+ and NH_4^+ are preferred over Cs^+ in the resin phase, as will be discussed later. The results with Ce^{144} cannot be similarly interpreted, as also will be discussed later.

The column tests with LiOH-form resin were carried out in considerably more detail. Two column sizes were employed for this work: approximately 76 cm long and 12.5 cm long. Two concentrations of LiOH were used, corresponding to pH 9.5 and pH 10.5. Five activities were used: Sr^{90}-Y^{90}, Cs^{137}-Ba^{137}, Ce^{144}-Pr^{144}, Ru^{106}-Rh^{106}, and Zr^{95}-Nb^{95}. The operating histories of these columns are given in the tables and figures referenced in Table V.

TABLE V

LiOH-BED OPERATING HISTORIES

Activity	pH	Approximate Bed Length (cm)	Table	Figure
Sr^{90}-Y^{90}	9.5	76	XXXI	18
Sr^{90}-Y^{90}	10.5	76	XXXI	19
Sr^{90}-Y^{90}	10.5	12.5	XXXII	20
Cs^{137}-Ba^{137}	9.5	76	XXXIII	21
Cs^{137}-Ba^{137}	10.5	76	XXXIII	22
Cs^{137}-Ba^{137}	9.5	12.5	XXXIV	23
Cs^{137}-Ba^{137}	10.5	12.5	XXXIV	24
Ce^{144}-Pr^{144}	9.5	76	XXXV	25
Ce^{144}-Pr^{144}	10.5	76	XXXV	26
Ce^{144}-Pr^{144}	9.5	12.5	XXXVI	27
Ce^{144}-Pr^{144}	10.5	12.5	XXXVI	28
Ru^{106}-Rh^{106}	9.5	76	XXXVII	29
Ru^{106}-Rh^{106}	10.5	76	XXXVII	30
Ru^{106}-Rh^{106}	10.5	12.5	XXXVIII	31
Zr^{95}-Nb^{95}	9.5	76	XXXIX	32
Zr^{95}-Nb^{95}	10.5	76	XXXIX	33
Zr^{95}-Nb^{95}	10.5	12.5	XL	34

As with the KOH and NH_4OH resin tests with Sr^{90}-Y^{90}, the results of tests with this activity are questionable because of probable separation of Sr^{90}. This possibility was checked some time after termination of the runs (Table XXXI), with the 76-cm column operating with Sr^{90}-Y^{90} in pH 10.5 LiOH solution. An additional batch of solution was prepared and passed through this column. Samples

were taken after at least five liters had been processed. Decay data were obtained on both the influent and effluent samples. The decay curves were analyzed with the aid of a value of 1.8 established by R. S. Gilbert of Bettis for the ratio of counting efficiency of Y^{90} to that of Sr^{90} in a methane-flow proportional counter of the type used for this work. The results of this extension of the processing of the Sr^{90}-Y^{90} column are given in Table VI.

It is apparent that neither the influent nor the effluent solutions were at equilibrium when sampled. Strontium was removed selectively from the influent solution with good effectiveness, while Y^{90} was actually released from activity previously deposited in the column. Consequently, the apparent breakthrough shown for Sr^{90}-Y^{90} in the data of Tables XXV, XXVIII, XXXI, and XXXII and Figs. 18, 19, and 20 probably is due entirely to Y^{90} leakage and not Sr^{90}. The behavior of Y^{90} is similar

TABLE VI

ADDITIONAL OPERATION OF Sr^{90}-Y^{90} COLUMN AT pH 10.5 WITH LiOH

Column Size - 1.05 cm ID x 76 cm deep

Flow Loading - 7.5 gpm/ft^2

Sample	Influent	Effluent No. 1	Effluent No. 2	Effluent No. 3	Effluent No. 4
Gross activity at sampling time (cpm/ml)	14,500	92,000	110,000	98,000	10,000
Gross activity at equilibrium (cpm/ml)	31,000	180	190	150	180
Sr^{90} activity at sampling time (cpm/ml)	11,100	64.4	68	53.6	64.4
Y^{90} activity at sampling time (cpm/ml)	3400	9.1×10^3	1.1×10^4	9.7×10^3	9.9×10^3
Total number of column equivalents processed	--	1.470	1.480	1.485	1.490
Sr^{90} decontamination factor	--	172	163	206	172
Y^{90} decontamination factor	--	0.36	0.31	0.35	0.34

Note: Activity concentrations were determined by analysis of decay curves, using a value of 1.8 for the ratio of Y^{90} to Sr^{90} counting efficiencies.

to that of Ce^{144}-Pr^{144}, as could be expected. However, since no previous effort was made to count the Y^{90} effluent samples at fixed times after passage through the columns, the data in this case are purely qualitative indications of Y^{90} breakthrough.

No such difficulty is to be expected for the Ru^{106}-Rh^{106} activity because of the short half-life of Rh^{106}. In the Zr^{95}-Nb^{95}, equilibrium could not have been re-established if any separation occurred; however, it is probable that the two isotopes behave similarly in this case. (The results of the tests with the LiOH-form columns are considered later in this section under the heading Discussion.) It is immediately apparent, however, that Cs^{137} continued to be removed with reasonable effectiveness up to about 1.8 column equivalents, thus indicating preference for Cs^+ over Li^+ in the resin phase.

Although activity distribution on the columns was monitored regularly with an uncollimated ionization chamber, all the data obtained in this way are not reproduced here. The distribution of activity on long columns of LiOH-form resin at the end of the tests is shown in the figures listed in Table VII. Distributions obtained by use of the Table VII uncollimated instrument are compared with the more accurate data obtained with a collimated scanning device, described in Appendix I, to show the qualitative agreement between the curve shapes obtained in these two ways. This agreement supports the qualitative conclusions, based on uncollimated column surveys, in previous work (Ref 4). However, any quantitative interpretation of the distribution, as attempted later in this section, requires the use of the more accurate results obtained by the collimated scanner.

The radiation profiles correctly reflect the distribution of the parent radioisotopes on the column in each case, because the measurements shown in the figures were obtained after a sufficient time had elapsed since absorption of the activity and stopping of solution flow to allow mother-daughter equilibrium to be re-established.

A special test, conducted with I^{132}, was somewhat different from the previously described work. Uncertainty as to the oxidation state preferred by radioiodine in high-temperature, high pH water (Ref 2) led to the following experiment.

TABLE VII

DISTRIBUTION OF ACTIVITY ON LiOH-FORM RESIN BEDS

Activity	pH	Approximate Bed Length (cm)	Type of Instrument	Figure
Sr^{90}-Y^{90}	9.5 and 10.5	76	Collimated	35
Sr^{90}-Y^{90}	9.5 and 10.5	76	Uncollimated	36
Cs^{137}-Ba^{137}	9.5 and 10.5	76	Collimated	37
Cs^{137}-Ba^{137}	9.5 and 10.5	76	Uncollimated	38
Ce^{144}-Pr^{144}	9.5 and 10.5	76	Collimated	39
Ce^{144}-Pr^{144}	9.5 and 10.5	76	Uncollimated	40
Ru^{106}-Rh^{106}	9.5 and 10.5	76	Collimated	41
Ru^{106}-Rh^{106}	9.5 and 10.5	76	Uncollimated	42
Zr^{95}-Nb^{95}	9.5 and 10.5	76	Collimated	43
Zr^{95}-Nb^{95}	9.5 and 10.5	76	Uncollimated	44

Two 3-liter autoclaves, previously exposed to a pH 10 solution of LiOH at 540°F for 500 hr, were used as sources of the radioactive solutions to be processed. An amount of Te^{132}-I^{132} activity was added directly to pH 10 LiOH solution held at 540°F in one of the autoclaves. The other autoclave, containing the same solution, was cooled down, the Te^{132}-I^{132} was added, and the autoclave was reheated. The two autoclaves were piped so that solution could be taken from either one, passed through a cooler, and then passed through a small ion exchange column containing 41 ml of wet settled resin. It had been found previously that Te^{132} is rapidly and almost completely adsorbed on stainless steel surfaces in contact with high-temperature water, while 2.4-hr I^{132} produced by decay of the adsorbed 67-hr Te^{132} is released to the water in nearly quantitative yield. Thus, the I^{132} was exposed only to the influence of the high-temperature, high pH environment and not influenced in its choice of oxidation state by the presence of prejudicial oxidants or reductants.

The entire contents of the first autoclave, to which the activity had been added after cooling, were passed through the column, and then the contents of the second autoclave were also processed. The flow-rate was equivalent to an area flow loading on the column of 7.5 gpm/ft^2.

Samples of the influent and effluent were obtained and analyzed by two different procedures:

1) Carrier iodide was added to an aliquot of the sample and precipitated with silver nitrate. The precipitate was dried and counted in a beta-proportional counter. A second aliquot was taken 24 to 48 hr later and treated in the same way. The I^{132} activity was determined from the first aliquot, and the Te^{132} activity was determined from the second aliquot, correcting for chemical yield in each case.

2) Carrier iodide was added to an aliquot of the sample. This was oxidized to iodate, then reduced to I_2, extracted into CCl_4, and re-extracted into water as the iodide. It was then precipitated with silver nitrate, dried, and counted in the same way as in the first procedure. Similar methods were used with another aliquot, after standing, to allow mother-daughter equilibrium to be established for Te^{132} determinations.

Similiar results were obtained from the two procedures, indicating that I^{132} probably was present as the iodide in the samples at the time of precipitation in the first procedure.

The results are given in Table VIII. Values for I^{132} and Te^{132} have been corrected for decay from the time of sampling. The short half-life of I^{132} makes the correction a rather large one in this case. Thus, the decay curves were interpreted in such a way as to give a maximum value for I^{132} concentration in the effluent consistent with the decay data. High decontamination factors were observed for I^{132} from the first autoclave; the activity had been added after cooling and the autoclave reheated. Moderate decontamination factors were observed for I^{132} from the second autoclave, to which the activity had been added by direct bomb addition while hot. The reason for the difference in results is not known, but it may be related to the period of time elapsed between addition of the activity and processing of the contents of the autoclave through the column. The results do not show that radioiodine is effectively absorbed by resin from a pH 10 LiOH solution, at least during processing of the number of column volumes used in this test. The results for Te^{132} are rather meaningless, but they do show that I^{132} was the major activity in the processed solution, as expected.

C. Equilibration Experiments

A series of experiments was carried out in an attempt to determine the equilibrium constant for the exchange reaction

$$M' + LiR \rightleftarrows M'R + Li^+,$$

TABLE VIII

RESULTS OF SPECIAL TEST WITH I^{132}-Te^{132} IN LiOH SOLUTION

Column Volume - 41 ml wet settled resin
Flow Loading - 7.5 gpm/ft^2
Solution pH - 10

	Sample 1*	Sample 2*	Sample 3**	Sample 4**	Sample 5**
Number of column volumes processed	39	54	68	80	100
I^{132} activity concentration in the influent (cpm/ml)	2.74×10^4	3.24×10^4	2.66×10^3	3.43×10^3	3.62×10^3
I^{132} activity concentration in the effluent (cpm/ml)	<9	<2	<37	<36	<45
I^{132} decontamination factor	$>3 \times 10^3$	$>1.6 \times 10^4$	>72	>95	>85
Te^{132} activity concentration in the influent (cpm/ml)	0	0	80	186	7
Te^{132} activity concentration in the effluent (cpm/ml)	0	0	65	52	56
Te^{132} decontamination factor	--	--	1.2	3.6	--

* First autoclave (cold addition).
** Second autoclave (hot addition).

where M' is a trace radioactive species, and R represents the resin. As defined in Appendix IV, the distribution coefficient R for the trace species is given by

$$R = \frac{C'_w}{X_r} = \frac{C_w}{K_c}$$

for a monovalent trace species, where

C'_w = the equilibrium concentration of the trace species in the water phase (mols/cc),

X'_r = the equilibrium mole fraction of the trace species in the resin phase,

C_w = the equilibrium concentration of the major species in the water (mols/cc), and

K_c = the (non-thermodynamic) equilibrium constant, related to the thermodynamic equilibrium constant as shown in Appendix IV.

Since the composition of lithium-form cation resin after equilibration with a solution containing a trace radioactive species in LiOH solution is essentially unchanged, the mole fraction X'_r is equal to the mole ratio of trace species to lithium in the resin phase.

Thus,

$$K_c = \left(\frac{C_w}{C'_w}\right)\left(\frac{N'_r}{N_r}\right)$$

for a monovalent species, where N_r and N'_r are the number of moles of the major and trace species per unit quantity of resin. Taking 1 g of vacuum-dried resin as the basis, the ratio $N'_r/C'_w N_r$ (= 1/R) can be expressed in units of (moles Li/cc)$^{-1}$ if N'_r is measured as cpm/g resin, N_r is measured as moles Li/g resin, C'_w is measured as cpm/cc water, and the activity measurements are made on comparable counting efficiency bases. Similar reasoning holds for divalent and trivalent trace species, as shown in Appendix IV.

The equilibration experiments were carried out with the same five activities used for the column experiments: Cs^{137}-Ba^{137}, Sr^{90}-Y^{90}, Ce^{144}-Pr^{144}, Ru^{106}-Rh^{106}, and Zr^{95}-Nb^{95}. Radioiodine, I^{131}, as the carrier-free iodide was used in a sixth test. The procedure was as follows. One hundred and ten milliliters of solution, containing the radioisotope and adjusted to pH 10 or 10.5 with LiOH, were placed in a small polyethylene bottle. The bottle was tightly capped and placed on a rotating tumbler in a water bath. Samples were taken regularly to monitor changes of pH and of the concentration of radioisotope in solution as the bottle surfaces equilibrated with the added solution. Six grams of vacuum dried MB-1 resin in the LiOH form were then added to the bottle, and equilibration of the solution with the resin was followed by additional water activity measurements. When it appeared that equilibrium had been reached, the solution was removed from the bottle and fresh LiOH solution, free of activity, was added and equilibrated with the non-active resin. Thus, equilibrium was approached from both directions.

The concentration of activity on the resin was calculated from differences between the amounts of activity added and the amounts found in the water at various stages of the experiment. Several activity balances were able to account for the total activity added with from 10 to 20% error; thus, the results are not highly accurate, but are satisfactory for rough comparison with similar values obtained from column experiments.

Several preliminary experiments showed that it was necessary to vacuum dry the resin to maintain the pH in the desired range after resin addition. Air drying the resin resulted in a marked drop of solution pH when the resin was added. The lithium content of the resin used for the experiments was determined and was found to be 2.1 millimoles of Li per gram of vacuum dried resin.

The equilibrium concentration of activity and of lithium in the resin and water phases are given in Table IX. Two repeat experiments were run with each activity. Lithium concentrations in the water were calculated from the measured values of solution pH after equilibration. Six grams of dried resin and 110 ml of solution were used in each test. The results from the experiments with Sr^{90}-Y^{90} are questionable, since no effort was made to distinguish between Sr^{90} and Y^{90} in the counting procedures, nor was the counting done at a fixed time after sampling. Thus, these results are subject to the same objections as are the column results for this activity, reported in the previous section. They are included in Table IX, nevertheless, to indicate the type of result found. In this case, it is quite probable that all the activity observed in the water after equilibration resulted from Y^{90}.

Values of K_c, as defined previously, were calculated for the two monovalent ionized species, Cs^{137} and I^{131}. These are given in Table X. Values of K_c for Sr^{90} were not calculated because of the above-mentioned uncertainties.

Note that the values of the constant for the second equilibration of each test (Table X) are higher than those for the first equilibration. It would appear either that complete equilibrium was not achieved or that the exchange was not completely reversible.

TABLE IX

EQUILIBRIUM CONCENTRATIONS OF ACTIVITY AND LITHIUM IN WATER AND RESIN PHASES OBSERVED IN RESIN EQUILIBRATION EXPERIMENTS

Room Temperature

Lithium Concentration in Resin = 2.1×10^{-3} moles/dry g (constant)

		First Equilibration*			Second Equilibration**		
Activity	Test No.	Activity Concentration in Water (cpm/ml)	Activity Concentration in Resin (cpm/g)	Lithium Concentration in Water (moles/ml)	Activity Concentration in Water (cpm/ml)	Activity Concentration in Resin (cpm/g)	Lithium Concentration in Water (moles/ml)
Cs^{137}-Ba^{137}	1	52	1.18×10^{6}	3.16×10^{-7}	100	1.18×10^{6}	7.94×10^{-7}
Cs^{137}-Ba^{137}	2	54	1.32×10^{6}	3.16×10^{-7}	91	1.3×10^{6}	7.94×10^{-7}
Sr^{90}-Y^{90}	1	392	1.18×10^{6}	7.94×10^{-7}	135	1.18×10^{6}	8.9×10^{-7}
Sr^{90}-Y^{90}	2	588	1.05×10^{6}	7.94×10^{-7}	154	1.05×10^{6}	8.9×10^{-7}
Ce^{144}-Pr^{144}	1	358	1.18×10^{6}	7.94×10^{-7}	220	1.18×10^{6}	7.94×10^{-7}
Ce^{144}-Pr^{144}	2	390	1.19×10^{6}	7.94×10^{-7}	210	1.18×10^{6}	1.0×10^{-6}
Ru^{106}-Rh^{106}	1	313	1.44×10^{6}	1.0×10^{-6}	270	1.43×10^{6}	7.9×10^{-7}
Ru^{106}-Rh^{106}	2	462	1.41×10^{6}	1.0×10^{-6}	331	1.40×10^{6}	7.9×10^{-7}
Zr^{95}-Nb^{95}	1	333	1.13×10^{6}	1.58×10^{-6}	141	1.12×10^{6}	7.94×10^{-7}
Zr^{95}-Nb^{95}	2	188	1.08×10^{6}	1.58×10^{-6}	96	1.08×10^{6}	8.9×10^{-7}
I^{131}	1	29	8.52×10^{5}	1.99×10^{-6} ++	+	8.52×10^{5}	1.0×10^{-6}
I^{131}	2	50	8.97×10^{5}	1.99×10^{-6} ++	+	8.97×10^{5}	1.0×10^{-6}

* All activity initially in water.

** All activity initially on resin.

\+ Probably erroneous results because of Sr^{90} separation on resin.

++ Hydroxyl ion concentration.

TABLE X

EQUILIBRIUM CONSTANTS FOR Cs^+ AND I^- EXCHANGE WITH LiOH-FORM MB-1 RESIN

Reaction	Test No.	K_c First Equilibration	K_c Second Equilibration
$Cs^+ + LiR \rightleftharpoons Li^+ + CsR$	1	3.41	4.45
	2	3.68	5.40
$I^- + ROH \rightleftharpoons RI + OH^-$	1	27.8	135
	2	17	107

* Activity initially all in water.
** Activity initially all on resin.

TABLE XI

DISTRIBUTION COEFFICIENTS FOR Ce^{144}-Pr^{144}, Ru^{106}-Rh^{106}, AND Zr^{95}-Nb^{95} OBSERVED IN EQUILIBRATION EXPERIMENTS

Activity	Test No.	R, First Equilibration*	R, Second Equilibration**
Ce^{144}-Pr^{144}	1	6.4×10^{-4}	3.9×10^{-4}
	2	6.9×10^{-4}	3.8×10^{-4}
Ru^{106}-Rh^{106}	1	4.6×10^{-4}	4.0×10^{-4}
	2	6.9×10^{-4}	4.9×10^{-4}
Zr^{95}-Nb^{95}	1	6.2×10^{-4}	2.6×10^{-4}
	2	3.7×10^{-4}	1.9×10^{-5}

* Activity initially all in water.
** Activity initially all on resin.

Note: Room Temperature.
Concentration of Lithium on Resin = 2.1×10^{-3} mols/dry gram.

$$R = \frac{C'_w}{X'_r} = \frac{\text{cpm/ml water}}{\text{cpm/g resin}} \times \text{mols Li/g resin.}$$

Equilibrium constants have not been calculated for the Ce^{144}-Pr^{144}, Ru^{106}-Rh^{106}, and Zr^{95}-Nb^{95} activities, since these almost certainly do not exist in basic water as true ions. Consequently, the constants for the reversible exchange with lithium ions are rather meaningless in these cases. Nevertheless, the distribution coefficient R, defined previously, is a measure of the capacity of the resin for adsorption of trace radiocolloids. This coefficient is more likely to be independent of base concentration in the water, over pH ranges within which the activities exist as colloids, than is the corresponding coefficient for trace ions. Thus, the values of R observed in the equilibration experiments are tabulated in Table XI. These will be shown to be useful in the later section titled Discussion. Note that the values of R are invariably less for the second equilibration than for the first equilibration

of each test. As for cesium and iodine, this appears to indicate some degree of irreversibility or lack of complete equilibrium.

D. In-Pile Loop Test at Chalk River

In-pile pressurized water loop tests of deliberately defected UO_2 fuel specimens made it possible to monitor the performance of a LiOH-form ion exchanger for removal of fission products from the loop coolant. The ion exchange columns are usually replaced frequently during in-pile defect tests to allow analyses to be made for the radioisotopes accumulated on the resin. However, one ion exchange column was kept in operation for 46 days during the X-1-L test in the X-1 loop in the NRX Reactor at Chalk River, Ontario, to monitor the performance of this column over an extended period of time.

This column contained 223 "air dried" grams of MB-1 resin in the LiOH form in a column, 1-in. ID by 36 in. long, with a bed volume of 465 cc. The lithium content of the resin was determined and found to be 2.31 meq/g of air dried resin. The bed operated at an average flowrate of 0.095 gpm, corresponding to a rather high area flow loading of 17.4 gpm/ft^2. The in-pile test section of the loop contained five PWR-type UO_2 fuel rods, one of which had been defected by drilling a 5-mil hole through the Zircaloy-2 cladding.

The pH and electrical conductivity of the column influent and effluent were regularly measured during the test period. The lithium content of the influent and effluent was also measured by flame photometry. Figure 1 gives a summary of the results of these measurements and also shows the variation of reactor power and ion exchange column flowrate during the test. Unfortunately, the three measurements of lithium hydroxide concentration in the influent were not completely self-consistent. This can be seen from Fig. 2 where the total number of column equivalents passed through the column, as calculated from electrical conductivity, pH, or lithium content measurements, is plotted as a function of time. The results have been selected arbitrarily from the pH measurements (which fall between the results of the other two measurements) as the basis for evaluating the performance of the column.

Radiochemical analyses were carried out regularly on both the column influent and effluent for the radioisotopes Cs^{136}, Cs^{137}, Sr^{89}, Ba^{140}, I^{131}, and I^{133}. These analyses were specific for the listed nuclides; no difficulties with mother-daughter equilibrium, as mentioned previously for Sr^{90}-Y^{90} laboratory column work, existed. The results of the radio-chemical analyses are given in Tables XII, XIII, XIV, XV, XVI, and XVII. Reactor power level, the total number of column equivalents of LiOH passed through the column (calculated from pH data), the column operating time, and calculated decontamination factors for the specific nuclides are also given in these tables.

Figure 3 shows the logarithm of the decontamination factor, as a function of the number of column equivalents passed through the column, for each of the analyzed radioisotopes. Note that both Cs^{136} and Cs^{137} removal performance fell rapidly. The decontamination factor for these isotopes reached a value of 2 (corresponding roughly to the maximum slope of an S-shaped breakthrough curve) at 3 column equivalents. After passage of 5 column equivalents, the decontamination factor for both of the cesium isotopes was approximately unity, except for occasional short intervals when release of these isotopes from the defected fuel rod increased markedly.

It is a characteristic of defected UO_2 fuel specimens, in a test of this type, that the release rate of soluble and gaseous fission products varies over a wide range when reactor power does not remain constant. Peak release rates are commonly observed when reactor power is increased; the release rate drops back to much lower values when reactor power is held constant. The ion exchange column acted as a "flywheel" in tending to hold the radiocesium concentration in the loop water to a constant value, absorbing extra cesium when the release rate

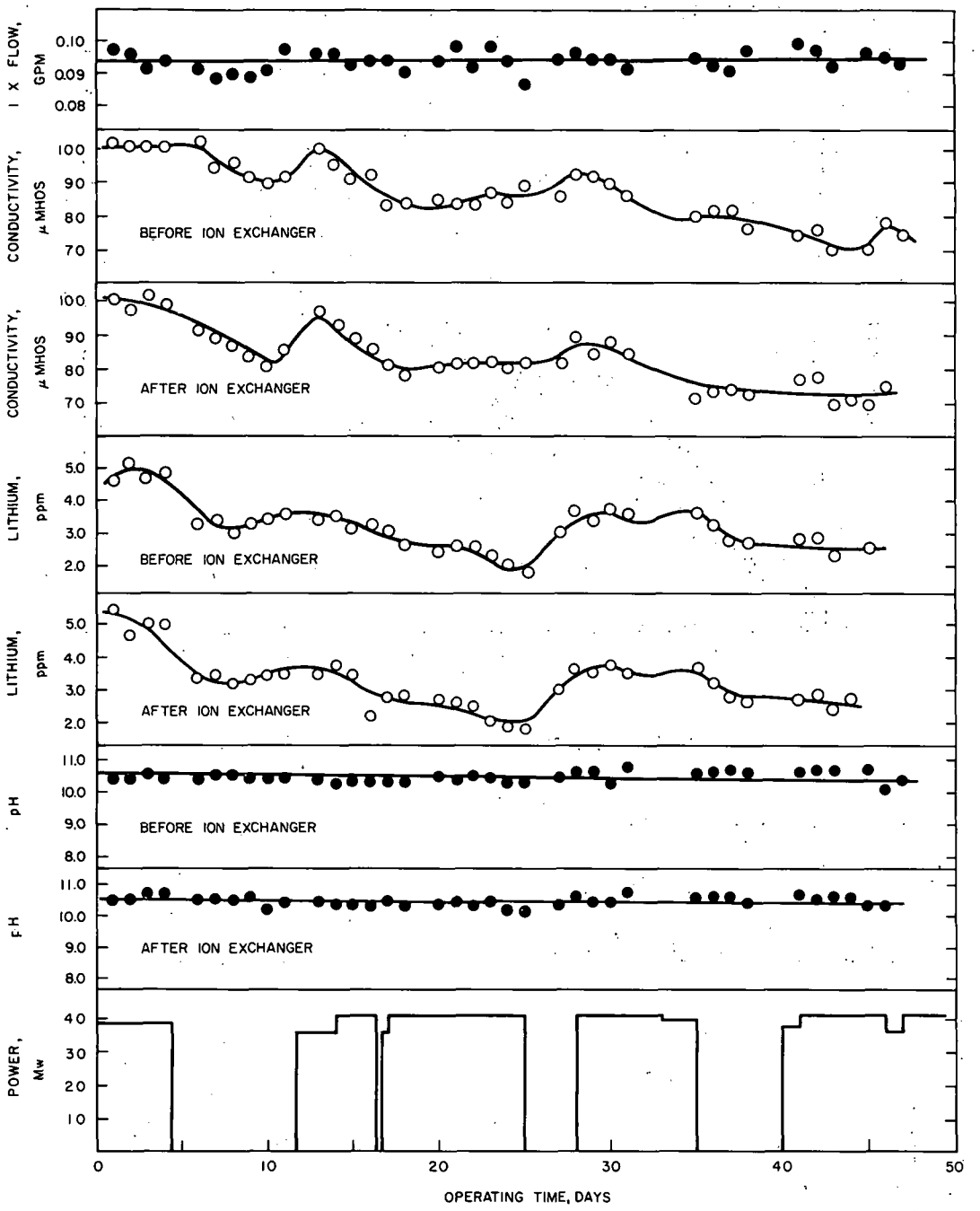

Fig. 1 X-1-L Loop Operation Summary with LiOH Resin

was high and releasing cesium when the release rate was low. This is the type of behavior to be expected according to the approximate theory developed in Appendix IV, because a peak in the column influent concentration will not result in peaking of the effluent concentration until sufficient time has elapsed for the elution wave to pass through the column. This time, according to the approximate theory, should be equal to GV_xK_c/QC_{wo}, where the symbols are as defined in Appendix IV. For this particular column, it should be the time required to process approximately 3 column equivalents of lithium hydroxide solution, since the initial cesium breakthrough maximum occurred after processing about that amount of solution.

It was not possible to carry out the radiochemical analyses at as many closely spaced intervals as

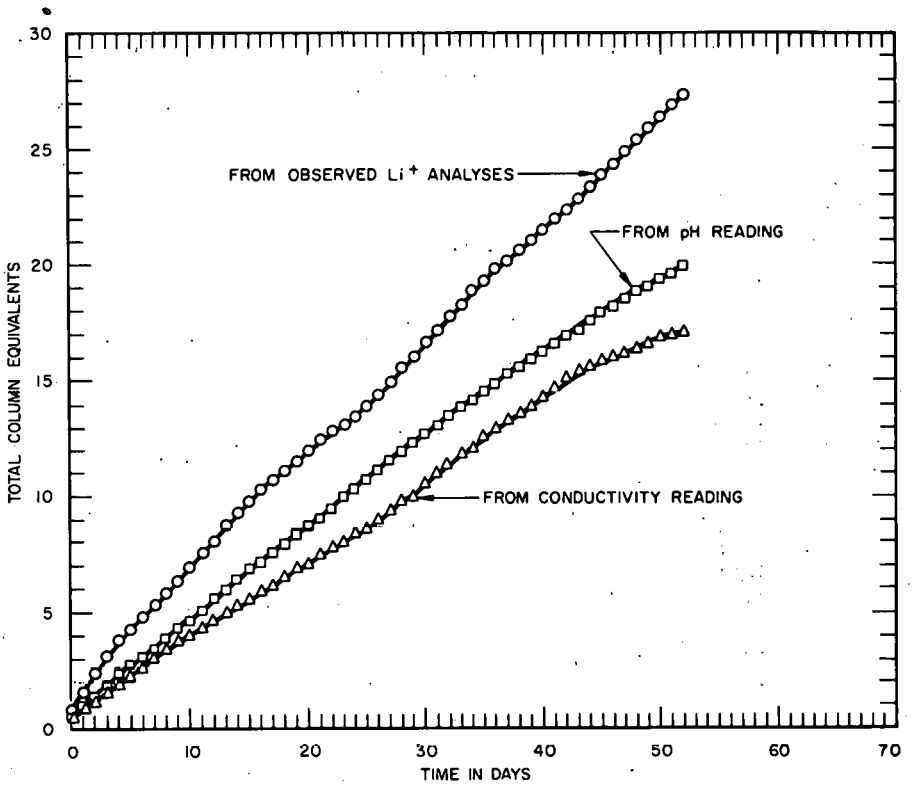

Fig. 2 X-1-L Loop Operation Summary with LiOH Resin

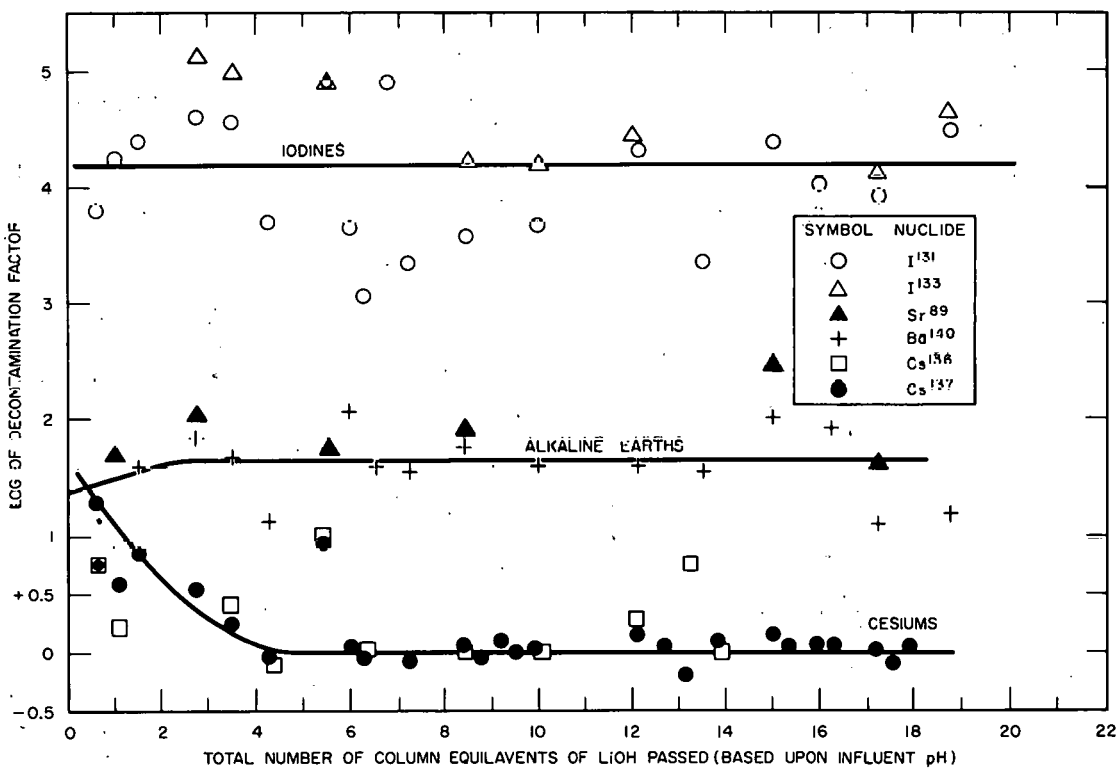

Fig. 3 Decontamination Factors Observed with LiOH Resin during X-1-L Loop Test

TABLE XII

BEHAVIOR OF X-1-L LOOP Cs^{137} ACTIVITY
DURING LiOH RESIN OPERATION

Operating Time (days)	Column Equivalents of LiOH*	Power (Mw)	Influent Activity (d/min-ml)	Effluent Activity (d/min-ml)	Decontamination Factor
1	0.65	38	2.96×10^3	2.14×10^2	13.8
2	1.0	38	1.01×10^3	2.54×10^2	4.0
3	1.5	38	4.24×10^3	6.17×10^2	6.9
6	2.75	0	7.78×10^3	2.30×10^3	3.4
8	3.5	0	5.75×10^3	3.29×10^3	1.8
10	4.3	0	3.75×10^3	4.02×10^3	0.93
13	5.6	35	6.25×10^4	6.87×10^3	9.1
14	6.0	40	9.2×10^3	8.58×10^3	1.07
15	6.3	40	1.11×10^4	1.13×10^4	0.98
16	6.8	40	1.82×10^5	1.47×10^4	12.4
17	7.2	40	2.68×10^4	2.90×10^4	0.92
20	8.4	40	3.08×10^4	2.98×10^4	1.03
21	8.75	40	3.92×10^4	4.02×10^4	0.97
22	9.2	40	4.70×10^4	3.76×10^4	1.25
23	9.6	40	4.36×10^4	4.26×10^4	1.02
24	10.0	40	4.52×10^4	4.39×10^4	1.03
27	12.1	0	7.73×10^4	5.34×10^4	1.45
28	12.7	40	6.71×10^4	6.00×10^4	1.12
29	13.1	40	2.00×10^4	3.33×10^4	0.60
30	13.5	40	1.49×10^5	4.24×10^4	3.5
31	13.8	40	6.03×10^4	4.98×10^4	1.21
35	15.0	0	6.30×10^4	4.40×10^4	1.43
36	15.3	0	6.48×10^4	5.90×10^4	1.08
37	15.9	0	6.99×10^4	6.06×10^4	1.15
38	16.3	0	6.52×10^4	5.70×10^4	1.14
41	17.2	40	6.24×10^4	5.95×10^4	1.05
42	17.6	40	7.73×10^4	9.53×10^4	0.81
43	17.9	40	6.68×10^4	5.93×10^4	1.13
46	18.8	35	1.03×10^4	6.22×10^4	0.165

* Column equivalents of LiOH based upon influent pH.

Note: Average ion exchange flow loading = 17.4 gpm/ft^2.
Average influent pH = 10.45.

TABLE XIII

BEHAVIOR OF X-1-L LOOP Cs^{136} ACTIVITY
DURING LiOH RESIN OPERATION

Operating Time (days)	Column Equivalents of LiOH*	Power (Mw)	Influent Activity** (d/min-ml)	Effluent Activity** (d/min-ml)	Decontamination Factor
1	0.7	38	2.6	0.45	5.8
2	1.0	38	0.71	0.41	1.7
8	3.5	0	6.7	2.7	2.5
10	4.3	0	3.3	4.2	0.8
13	5.6	35	62.3	5.6	11.1
15	6.3	40	10.9	10.9	1.07
20	8.4	40	24.5	23.0	1.06
24	10.0	40	33.2	31.9	1.04
27	12.1	0	71.7	34.5	2.1
29	13.1	40	14.3	2.5	5.7
31	13.8	40	42.8	45.0	0.95

* Column equivalents of LiOH based upon influent pH.

** All values expressed as corrected counts per minute per milliliter. Determined on gamma-spectrometer using the 0.82 Mev photopeak. Spectra run about one week after sampling, in general.

Note: Average ion exchange flow loading = 17.4 gpm/ft^2.
Average influent pH = 10.45.

would be required for positive identification of effluent activity peaks with the preceding influent activity peaks. Nevertheless, an inspection of Table XII does reveal several qualitative indications of this type of behavior, despite the confusion caused by frequent and randomly introduced influent activity peaks.

The decontamination factors for Ba^{140} and Sr^{89} remained in a moderate range throughout the test. The removal of these isotopes was always sufficiently complete for effective control of their concentration in the loop water. As was the case for the cesiums, fluctuations in the release rate played a role in causing variable decontamination factors for the barium and strontium isotopes. The removal performance for the two iodine isotopes, I^{131} and I^{133}, remained outstanding throughout the test, decontamination factors averaging on the order of 10^4. Here again, the influence of variable influent activity on the decontamination factor is apparent.

Viewed as a qualitative demonstration of LiOH-column performance, the results of this test reveal the following information:

1) Long-lived cesium radioisotopes will break through an LiOH column after passage of about 3 column equivalents of solution.

2) With the average pH of about 10.5 and the rather high area flow loading of this test, the

TABLE XIV

BEHAVIOR OF X-1-L LOOP I^{131} ACTIVITY
DURING LiOH RESIN OPERATION

Operating Time (days)	Column Equivalents of LiOH*	Power (Mw)	Influent Activity (d/min-ml)	Effluent Activity (d/min-ml)	Decontamination Factor
1	0.65	38	2.91×10^5	47	6.2×10^3
2	1.0	38	4.24×10^5	24	1.77×10^4
3	1.5	38	5.33×10^5	22	2.42×10^4
6	2.75	0	1.66×10^6	41	4.05×10^4
8	3.5	0	1.10×10^6	30	3.67×10^4
10	4.3	0	3.62×10^4	7	5.17×10^3
13	5.6	35	3.98×10^6	48	8.29×10^4
14	6.0	40	1.80×10^5	39	4.62×10^3
15	6.3	40	4.14×10^4	36	1.15×10^3
16	6.8	35	9.21×10^6	114	8.08×10^4
17	7.2	40	9.06×10^4	41	2.21×10^3
20	8.4	40	1.01×10^5	27	3.74×10^3
24	10.0	40	9.87×10^4	21	4.7×10^3
27	12.1	0	1.61×10^6	77	2.09×10^4
30	13.5	40	1.11×10^5	48	2.31×10^3
35	15.0	0	3.83×10^5	16	2.39×10^4
38	16.3	0	2.20×10^5	20	1.10×10^4
41	17.2	40	2.62×10^5	31	8.45×10^3
46	18.8	35	2.34×10^6	81	2.89×10^4

* Column equivalents of LiOH based upon influent pH.

Note: Average ion exchange flow loading = 17.4 gpm/ft^2.
Average influent pH = 10.45.

13-day half-life of Cs^{136} was too long for any appreciable decay of this isotope while being eluted through the column. It is probable that a normal flow loading of about 7.5 gpm/ft^2 and an average pH of 10 would increase the time required for passage of the approximately 3 column equivalents needed for elution sufficiently to give some apparent removal performance in the steady state for this 13-day isotope. Shorter-lived cesiums should show good apparent removal on the column.

3) Alkaline earths as long-lived as 54-day Sr^{89} will be removed effectively by an LiOH column. No breakthrough was apparent after passage of 18 column equivalents in a period of about 45 days. At lower flow loading and lower average pH, the time required to pass 18 column equivalents would be sufficiently great relative to the 54-day half-life of Sr^{89} to have assurance that effective control of this nuclide and all shorter-lived alkaline earth nuclides would continue indefinitely.

TABLE XV

BEHAVIOR OF X-1-L LOOP I^{133} ACTIVITY
DURING LiOH RESIN OPERATION

Operating Time (days)	Column Equivalents of LiOH*	Power (Mw)	Influent Activity (d/min-ml)	Effluent Activity (d/min-ml)	Decontamination Factor
1	0.65	38	6.62×10^5	ND	--
2	1.0	38	8.55×10^5	ND	--
3	1.5	38	7.98×10^5	ND	--
6	2.75	0	3.94×10^6	30	1.31×10^5
8	3.5	0	2.94×10^5	30	9.8×10^4
10	4.3	0	1.59×10^4	ND	--
13	5.6	35	4.07×10^6	93	4.38×10^4
14	6.0	40	2.72×10^5	ND	--
15	6.3	40	1.18×10^4	ND	--
16	6.8	35	1.0×10^7	125	8.0×10^4
17	7.2	40	1.91×10^5	ND	--
20	8.4	40	3.92×10^5	23	1.70×10^4
24	10.0	40	3.43×10^5	21.4	1.63×10^4
27	12.1	0	2.12×10^6	77	2.75×10^4
30	13.5	40	3.50×10^5	ND	--
35	15.0	0	6.99×10^5	ND	--
38	16.3	0	3.90×10^4	ND	--
41	17.2	40	8.66×10^5	62	1.40×10^4
46	18.8	35	4.34×10^6	100	4.34×10^4

* Column equivalents of LiOH based upon influent pH.

Note: Average ion exchange flow loading = 17.4 gpm/ft^2.
Average influent pH = 10.45.

4) All halogen radioisotopes will be effectively removed by an ion exchange column of LiOH-form resin, since 8-day I^{131} is the longest-lived nuclide of any importance in this class. Effective removal of radioiodine continued to be excellent throughout this 46-day test.

E. Discussion

Monovalent Cations

The monovalent cations Li^+, K^+, NH_4^+, and Cs^+ behave in dilute solutions at both high and low temperature almost according to expectations. Ionization is essentially complete, radiocolloid formation does not appear to occur, and difficulties with adsorption on surfaces from solutions are not pronounced. Thus, it is to this group that the multistage column theory of Appendix IV is perhaps most applicable. According to this theory, two parameters, an equilibrium constant (K_c) and the number of equilibration stages equivalent to the column (n), should be sufficient to describe approximately the performance of a column of a given resin type at a particular set of conditions of pH and flow loading for each pair of exchanging ions. They should also suffice to predict the apparent performance of a column

TABLE XVI

BEHAVIOR OF X-1-L LOOP Sr^{89} ACTIVITY
DURING LiOH RESIN OPERATION

Operating Time (days)	Column Equivalents of LiOH*	Power (Mw)	Influent Activity (d/min-ml)	Effluent Activity (d/min-ml)	Decontamination Factor
2	1.0	38	295	6	49.2
6	2.75	0	803	7.5	107
13	5.6	35	298	5.2	57.3
20	8.4	40	534	6.1	87.5
35	15.0	0	955	3.1	308
41	17.2	40	266	6.4	41.6

* Column equivalents of LiOH based upon influent pH.

Note: Average ion exchange flow loading = 17.4 gpm/ft^2.
Average influent pH = 10.45.

operating at the selected set of conditions for removal of shorter-lived isotopes of the same trace elements.

The case of trace Cs^+ absorption of LiOH resin, for which the most data are available, is considered first. Information of varying reliability concerning the value of K_c is available from four independent sources: equilibration experiments, operating histories of laboratory columns, radioisotope distribution on laboratory columns, and the performance of the loop ion exchange column during the Chalk River experiment. Despite the limitations cited earlier, the equilibration results are probably the most reliable, since no assumptions are required in this case about the value of n. The average of the values of K_c is 3.55, determined from the two duplicate experiments in which equilibrium was approached from an initial condition with the activity in the water. The two activity distribution curves, shown on Fig. 35 of Appendix III for the long laboratory columns operated at pH 9.5 and 10.5, allow a check of this value. The curve for the pH 10.5 column has a rather broad range for the maximum slope; however, the center of this range seems to be at about 35 cm. Using this value, the length of the column, and the number of column equivalents processed at the time the distribution curve was determined, a value of 3.5 is calculated for K_c from the equations given in Appendix IV. The maximum for the slope of the curve for the pH-9.5 column appears to fall at about 4.5 cm. This gives a value of 2.25 for K_c. The lower result obtained in this last case is not unexpected; the column certainly does not contain a large number of equivalent equilibration stages in the first 5 to 10 cm.

It is shown in Appendix IV that K_c for monomonovalent exchange is equal to the number of column equivalents processed at the time the maximum occurs in the slope of the breakthrough curve, provided that $n/(n-1)$ is approximately equal to one. Although the data obtained from the Chalk River test are somewhat variable because of large variations in influent activity, it does appear that C/C_o, the ratio of effluent to influent activity, reached a value of 0.5 at about 3 column equivalents. If the breakthrough curves were symmetrical, the maximum slope would be at $C/C_o = 0.5$. Thus, an approximate

TABLE XVII

BEHAVIOR OF X-1-L LOOP Ba^{140} ACTIVITY
DURING LiOH RESIN OPERATION

Operating Time (days)	Column Equivalents of LiOH*	Power (Mw)	Influent Activity (d/min-ml)	Effluent Activity (d/min-ml)	Decontamination Factor
1	0.65	38	150	7.5	20
2	1.0	38	177	4.1	43.2
3	1.5	38	163	4.2	38.8
6	2.75	0	248	3.6	68.9
8	3.5	0	185	3.9	47.5
10	4.3	0	90	6.7	13.4
13	5.6	35	93	1.8	51.6
14	6.0	40	120	1	120
15	6.3	40	149	3.7	40.3
16	6.8	40	222	3.8	58.5
17	7.2	40	183	5.2	35.2
20	8.4	40	184	3.1	59.4
24	10.0	40	202	5.2	38.9
27	12.1	0	504	13	38.7
30	13.5	40	170	4.8	35.4
35	15.0	0	264	2.5	106
38	16.3	0	135	1.6	84.3
41	17.2	40	108	8.5	12.7
46	18.8	35	92	5.9	15.6

* Column equivalents of LiOH based upon influent pH.

Note: Average ion exchange flow loading = 17.4 gpm/ft^2.
Average influent pH = 10.45.

value of 3 for K_c is obtained from this test. Furthermore, since n probably is not a large number in this case because of the high area flow loading of the column, the factor n/(n-1) will increase somewhat the value of K_c consistent with this test, possibly to as much as 4.

Figure 4 summarizes the results of the four laboratory columns operating with Cs^{137}-LiOH exchange by plotting C/C_o versus the number of column equivalents processed. The shorter columns begin to show leakage of Cs^{137} in the effluent at an early time, as would be expected for columns with a low number of equivalent equilibration stages. The short column that was operated at pH 10.5 shows the beginning of a rapid rise in C/C_o that is consistent with a maximum in the slope of this curve at about 3 column equivalents. This is in agreement with the Chalk River column results. The larger columns do not show any breakthrough up to 1.75 column equivalents. This fact is not inconsistent with the other results, for it is possible that a sharp

breakthrough could have occurred after passage of one or two additional column equivalents. The distribution curve for the pH-10.5 long column, shown in Fig. 37, certainly indicates that breakthrough was imminent at 1.75 column equivalents.

It appears from the foregoing discussion that a value between 3 and 4 can be assigned for K_c for Cs^+ exchange on LiOH resin. The other parameter n cannot be determined with the same degree of assurance. Only the two distribution curves shown in Fig. 37 allow an estimate to be made of the value of n. By assuming that the maximum activity level found on the column corresponds to resin equilibrated with the influent solutions, values of approximately 7 and 5 were calculated for n for the pH 9.5 and 10.5 column, respectively. This result indicates at once that the use of Stirling's approximation in the calculations is rather crude, and these values of n, therefore, can be considered only as very approximate numbers.

Only the column operating histories are available as a basis for estimating the corresponding parameters for Cs^+ exchange on NH_4OH and KOH resins. From Table XV it appears that Cs^{137} breakthrough occurred after passage of about 0.1 column equivalent of KOH solution through the KOH columns. The NH_4OH column was not taken to complete breakthrough with Cs^{137}. However, Table XXVI shows that activity was definitely beginning to appear in the effluent at the termination of the test at 0.224 column equivalents. It would be reasonable to assume that breakthrough would be well along at about 0.3 column equivalents.

Summarizing the above discussion, the approximate values for equilibrium constants for exchange reactions among Cs^+, Li^+, NH_4^+, and K^+ can be tentatively assigned according to Table XVIII.

To illustrate the significance of the constants in Table XVIII, the value of K_c for the reaction $Cs^+ + LiR \rightleftharpoons Li^+ + CsR$ is between 3 and 4. It is apparent that these four cations are ordered in the following way with respect to relative ease of displacement from IR-120 cation resin:

$$Li^+ > Cs^+ > NH_4^+ > K^+.$$

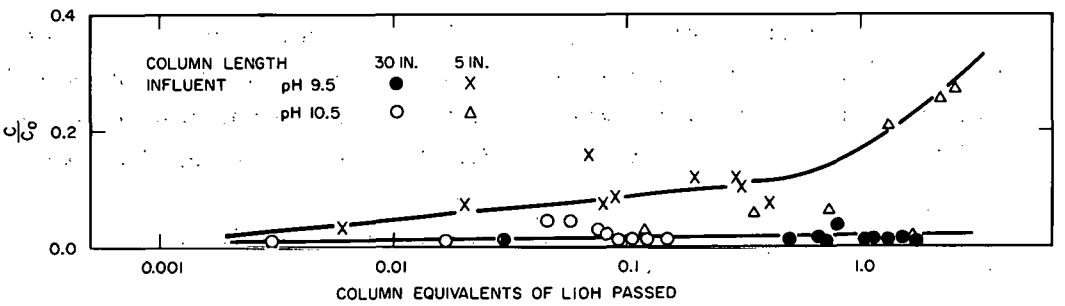

Fig. 4 The Exchange of Cs^{137}—Ba^{137} Activity on LiOH Resin

TABLE XVIII

APPROXIMATE EQUILIBRIUM CONSTANTS, K_c

Displacing Trace Cation	Initial Cation Resin Form			
	CsR	LiR	NH_4R	KR
Cs^+	1	3 to 4	~0.3	~0.1
Li^+	~0.25 to 0.33	1	~0.08 to 0.1	~0.025 to 0.033
NH_4^+	~3.3	~10 to 13	1	~0.33
K^+	~10	~30 to 40	~3	1

Thus, lithium-form cation resin is the most suitable of the four for use in a purification system ion exchanger because it will most readily absorb impurity or radioactive ions and will also most readily release lithium to maintain a high pH level.

If it is assumed that a 30-in. deep bed operating at 7.5 gpm/ft^2 area flow loading has about 6 equivalent equilibration stages for all of these mono-monovalent exchange reactions, it is possible to make predictions of bed performance by using the equations of Appendix IV. These predictions, while necessarily rather approximate, may be sufficiently accurate for plant engineering purposes. They will certainly be better than any predictions based on single stage "mixing-pot" theory or similar very crude approximations used heretofore.

Alkaline Earths

As mentioned previously, it is unfortunate that most of the results obtained from column operation and equilibration experiments are invalidated by failure to take into account deviation of the Sr^{90}-Y^{90} system from mother-daughter equilibrium. Thus, the plot of C/C_o for this activity, shown in Fig. 5, probably represents breakthrough of Y^{90} but not of Sr^{90}. As described earlier in this section under Laboratory Column Experiments, a short additional period of operation of the pH 10.5 column with Sr^{90}-Y^{90} activity in LiOH solution showed that Sr^{90} was still being removed with a respectable decontamination factor. The two distribution curves shown on Fig. 35, which are not subject to uncertainty about mother-daughter equilibrium, also indicate that Sr^{90} breakthrough was not imminent at the conclusion of operation of either the pH 9.5 or the pH 10.5 column.

The Chalk River experiment showed that moderately high decontamination factors were obtained for 54-day Sr^{89} and 12.8-day Ba^{140}, without any appearance of impending breakthrough, up to a processed volume of 18 column equivalents. Since it took only about 45 days to process this much solution, it is at once obvious that the magnitude of observed decontamination factors for 54-day Sr^{89} could not have resulted from decay of this isotope on passage through this column. Only one conclusion is possible—the magnitude of K_c for Sr^{++} exchange in LiOH resin must be such that more than 18 column equivalents of LiOH solution are required to elute Sr^{++} (and probably also Ba^{++}) through a 36-in. column.

The exact magnitude of K_c for this case cannot be ascertained from any of the experimental results reported in this document because the two distribution curves of Fig. 35 do not yield consistent

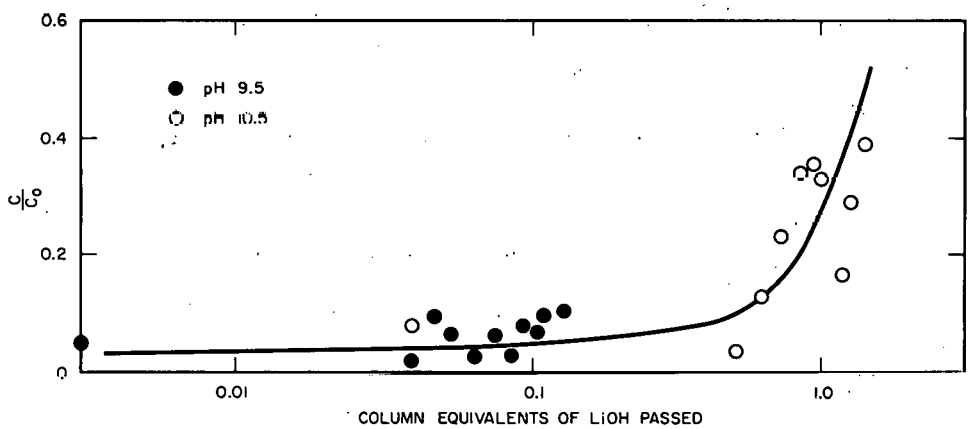

Fig. 5 Sr^{90}—Y^{90} Exchange on LiOH Resin

results. However, since Sr^{89} is the longest-lived alkaline earth radioisotope (other than Sr^{90}) likely to be encountered in pressurized water reactors, it can be concluded that LiOH resin will effectively control the concentration of alkaline earth activities in a system operating with LiOH in the coolant. Strontium-90 will eventually break through an LiOH column of course, but this will require the passage of a minimum of 18 column equivalents of solution. A resin bed would have a considerable period of useful life for Sr^{90} removal even if it were replaced after passage of this minimum number of column equivalents at an average pH of 10 and at 7.5 gpm/ft^2.

Halogens

Eight-day I^{131} is the longest-lived halogen nuclide of concern in pressurized water reactors. This isotope and other radioiodines are of considerable importance, since their concentrations must be effectively controlled to prevent excessively hazardous levels of airborne contamination from developing should leakage occur in confined locations. No laboratory columns were operated with I^{131}. However, the equilibration experiments show that K_c for the exchange reaction $I^- + ROH \rightleftharpoons RI + OH^-$ has a rather large value. An average of 22.4 for K_c is obtained from the two equilibration experiments in which the activity was initially all in the water. According to the equations of Appendix IV, therefore, about 22 column equivalents must be processed before breakthrough can occur.

The Chalk River column test showed that quite high decontamination factors, on the order of 10^4, were obtained for up to 18 column equivalents of processed solution with no discernible downward trend. Since it required only a little over five I^{131} half-lives to process this much solution, it is evident that the high observed decontamination factors could not have been the result of I^{131} decay on the column. Therefore, it can be concluded that iodine breakthrough would not have occurred even for stable iodine isotopes during passage of up to 18 column equivalents. If a value of 22 is adopted for K_c (probably a minimum value), it can be easily shown that very adequate apparent decontamination factors will be obtained for 3-day I^{131} and all shorter-lived halogen radioisotopes, even in the steady state after passage of many more than 22 column equivalents of solution, provided the base concentration in solution and the column flow loading are in the ranges normally used in pressurized water reactors.

The special experiment with I^{132} is helpful primarily in showing that radioiodine isotopes will exist in a chemical state in high-pH solution, which permits effective absorption by ion exchange columns. The results of this experiment also qualitatively demonstrate effective hold-up of radioiodine on the column, despite the presence of base in the solution being processed.

Isotopes Forming Radiocolloids

The operating histories of the laboratory columns used to process LiOH solution with Ce^{144}-Pr^{144}, Ru^{106}-Rh^{106}, and Zr^{95}-Nb^{95} activities are summarized in Figs. 6, 7, and 8 as plots of C/C_o vs the number of column equivalents of solution processed. It is at once apparent that the pH 9.5 and pH 10.5 solution results do not correlate with the number of column equivalents passed through the column. When it is recalled that the number of column equivalents per column volume in pH 10.5 solution is ten times that for pH 9.5 solution, it can be seen that breakthrough occurred at about the same number of column volumes of processed active solution for each pair of columns used with the same activity.

This behavior is to be expected for activities which exist as radiocolloids rather than as true ions in solution, since there is no reason to expect the base concentration of the solution to affect the results, except indirectly by altering the nature of the radiocolloid or the inadsorption capacity (as distinguished from the ion absorption capacity) of

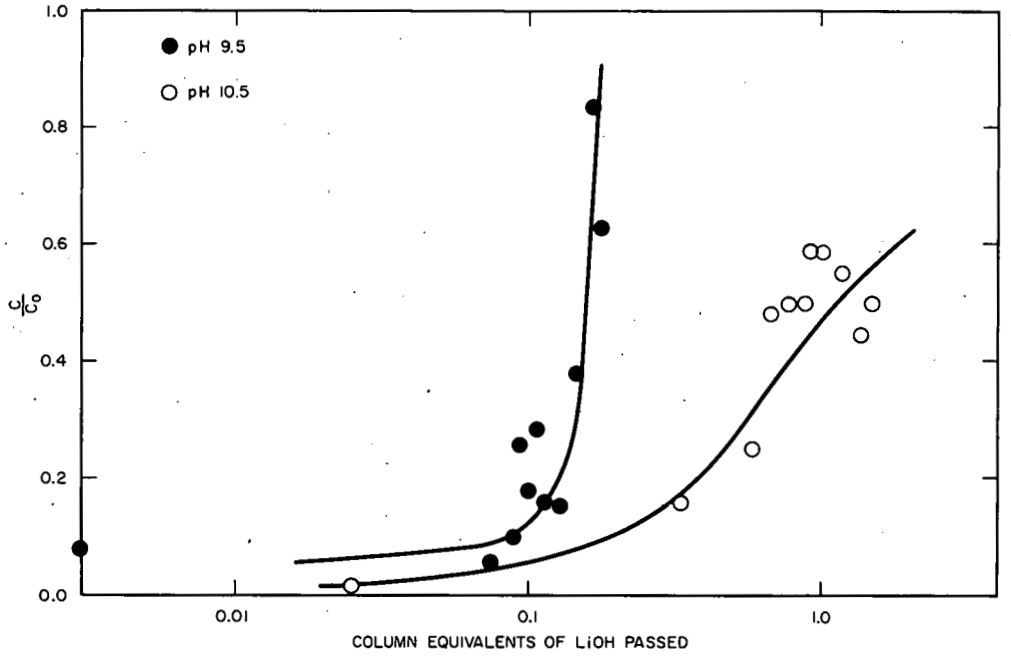

Fig. 6 Ce^{144}—Pr^{144} Exchange on LiOH Resin

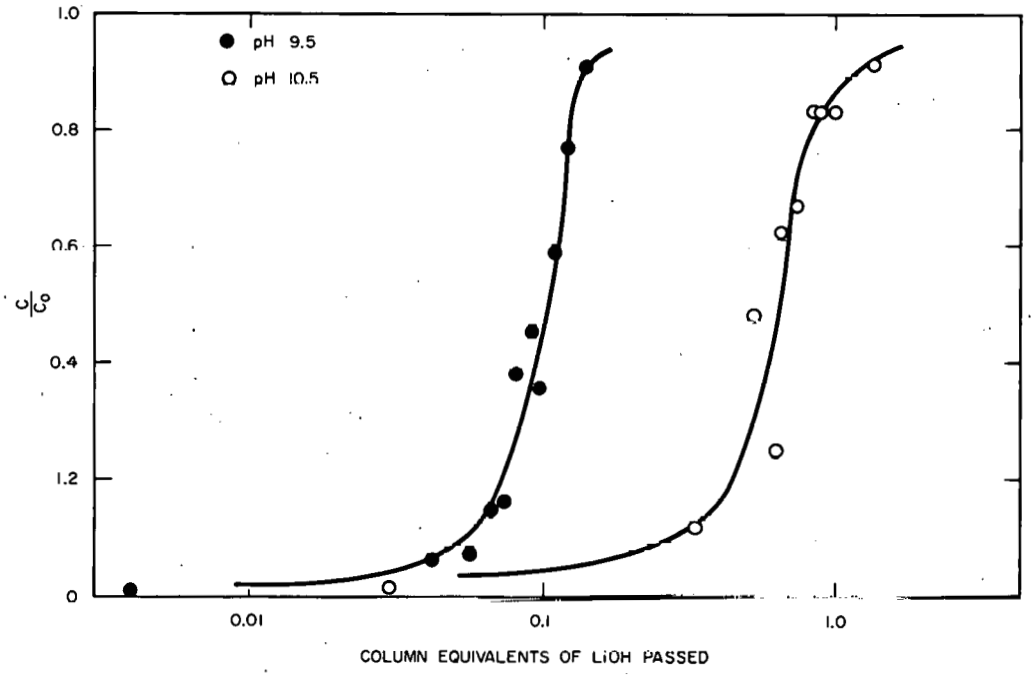

Fig. 7 Ru^{106} Rh^{106} Exchange on LiOH Resin

the resin. If it is assumed that neither of these two factors varies appreciably in the pH range 9.5 to 10.5 for the cerium, ruthenium, or zirconium activities, the approximate number of column volumes of active solution that will exhaust the adsorptive capacity of the columns can be calculated by using the distribution coefficients determined by the equilibration experiments with these activities. Thus, it is predicted that about 1000 to 1500 column volumes of active solution would be required for breakthrough of Ce^{144}-Pr^{144}, Ru^{106}-Rh^{106}, and Zr^{95}-Nb^{95} activities, with breakthrough occurring in the order cerium, ruthenium, zirconium. This is in fair qualitative agreement with the results

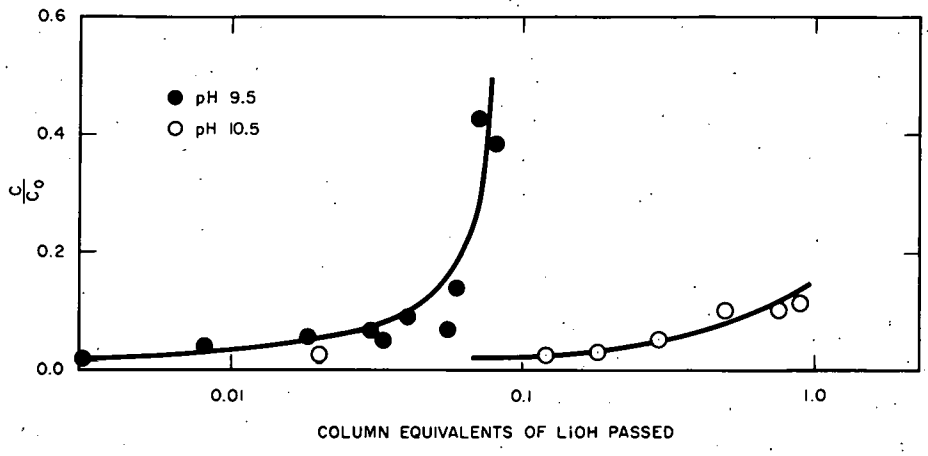

Fig. 8 Zr^{95}—Nb^{95} Exchange on LiOH Resin

for the 30-in. columns, as can be seen from inspection of Figs. 6, 7, and 8 and the tables and figures of Appendix II. The shorter columns show breakthrough at a very low number of column volumes of solution, however, indicating that equilibrium conditions for adsorption are not rapidly reached. This is hardly surprising for radiocolloidal species, which would be expected to diffuse slowly.

Further evidence for slow attainment of adsorption equilibrium for colloids is also presented by the fact that these species are typically found distributed in depth on ion exchange columns, even before breakthrough, instead of being concentrated in a relatively well-defined band moving down the column. The distribution curves of Appendix III do not show this too clearly since they were obtained after breakthrough had occurred. However, earlier observations do show a trend toward distribution in depth which can be interpreted as evidence for low capacity and slow attainment of equilibrium in columns treating solutions containing radiocolloids.

The fact that from 1000 to 2000 column volumes of active solution were required to exhaust the capacity of the laboratory columns cannot be used for quantitative prediction of plant ion exchanger performance for similar radiocolloid-forming isotopes, since the results obtained in the laboratory may be specific for the particular condition of the Ce^{144}, Ru^{106}, and Zr^{95} radioisotopes purchased for use in these experiments. It is quite possible that similar nuclides in reactor coolant would exhaust the adsorptive capacity of a plant purification ion exchanger somewhat differently. Nevertheless, it is to be expected that the radiocolloid-forming fission products will not be effectively removed or retained on base-form ion exchanger beds. This poor removal performance is not particularly disturbing, however, because such radioisotopes as those of the rare earths, ruthenium, zirconium, niobium, and tellurium are rarely found in basic reactor coolant in any significant concentration, the rate constant for adsorption of these isotopes on the surfaces of the primary system being much greater than the purification rate constant.

IV. SUMMARY AND CONCLUSIONS

The pH of circulating coolant systems can be effectively and conveniently controlled in the range pH 9.5 to 10.5 by the use of mixed-bed, ion exchange resins in the LiOH or KOH form if leakage and water makeup rates are not too high. Lithium is more easily displaced from LiOH resin than is potassium from KOH resin. This is especially true with respect to displacement by any ammonium ions that may be produced in the coolant by radiation reactions. Thus, the pH may be more easily controlled by LiOH resin than by KOH resin when water makeup rates are high.

Monovalent cations will not be retained on base-form resin beds processing solutions of LiOH, KOH, or NH_4OH. However, the rate of elution of these species will depend on the value of the equilibrium constant for the exchange reaction in question, and on the rate at which column equivalents of base solution are processed. In many cases, temporary hold-up on the column can result in sufficient decay of the radioisotopes so that the resin bed will have a good apparent decontamination factor, and will exert effective control over the concentration of such radioisotopes in a coolant system. Predictions of bed performance for specific cases may be made from equations developed in Appendix IV by using approximate parameters tentatively assigned in the section titled Discussion. These predictions will not be exact, but they may suffice for plant engineering purposes.

A bed of LiOH resin, with such dimensions and area flow loading as are typical of beds used in pressurized water reactors, will not continue to remove Cs^{137} from a basic influent of constant Cs^{137} concentration after passage of from 3 to 4 column equivalents of solution. However, the bed will act as a "flywheel," tending to maintain a relatively constant level of this isotope in the coolant system by absorbing extra Cs^{137} when release rates in the core are high, and discharging Cs^{137} when release rates in the core are low. The ratio of total Cs^{137} on the bed to total Cs^{137} in the coolant, when the bed and coolant are equilibrated, will be from 3 to 4 times the corresponding ratio for LiOH, or as high as from 200 to 300 in some reactor systems. Thus, LiOH resin will hold the concentration of even this long-lived isotope to much lower concentrations in the coolant than would be present if no purification system were employed.

Potassium hydroxide resin is from 30 to 40 times less effective in this respect, while NH_4OH resin is also less effective for this purpose than LiOH resin. Shorter-lived monovalent cations, from about 13-day half-life on down, will decay sufficiently during hold-up of a LiOH resin bed to be removed from the purification stream with fair to excellent decontamination factors, depending on the half-life. Beds of KOH and NH_4OH resin are less effective for this purpose.

All halogen radioisotopes will be effectively removed by an ion exchange bed of LiOH resin. The performance of KOH and NH_4OH resins in halogen removal has not been specifically determined but should be equally as good as LiOH resin.

Divalent cations, such as Sr^{++} and Ba^{++}, with half-lives of up to at least 50 days, will be removed effectively by LiOH resin. Beds of KOH and NH_4OH resin should also perform well for alkaline earth radioisotope removal.

Radioisotopes existing in the colloidal state in basic coolant will not be effectively removed by LiOH, KOH, or NH_4OH resin. Radiocolloidal daughters of ionized isotopes already absorbed on beds of LiOH, KOH, or NH_4OH resins may be released by the bed after they are produced in the bed by decay of the parent nuclide. Zirconium, niobium, yttrium, ruthenium, rhodium, and rare earth radioisotopes all exhibit evidence of colloidal behavior in basic solution.

A mixed bed of lithium-form IR-120 cation resin and hydroxyl-form IRA-400 anion resin, in a one-to-one anion-cation equivalent ratio, is probably the most effective base-form ion exchanger for fulfilling the dual functions of pH control and activity removal in pressurized water reactor coolant systems.

APPENDIX I: DESIGN AND TEST OF THE COLLIMATED AUTOMATIC COLUMN SCANNER*

Previous measurements of radioisotope distribution on the resin columns were carried out using

* G. P. Simon

an uncollimated ("Cutie Pie") survey instrument. This technique, although rapid, is not accurate because of the unknown and variable background correction. In addition, fine structure of the dependence of activity upon the distance down the column is missed because of the large radioactive area sampled at each measurement position. The column scanning device described in detail below was designed to overcome these difficulties. The G.M. tube is of small size and is shielded to reduce the background to a low fixed value. The shielding is arranged so that good collimation of the incident radioactivity is obtained. In addition, the travel and timing circuits are arranged so that the observed number of counts can be totalled for each 2 cm of travel or less.

The mechanical portion of the instrument is shown in Fig. 9. It consists of a carrier which moves in a vertical plane on smooth, 1/2-in. diam steel rods.

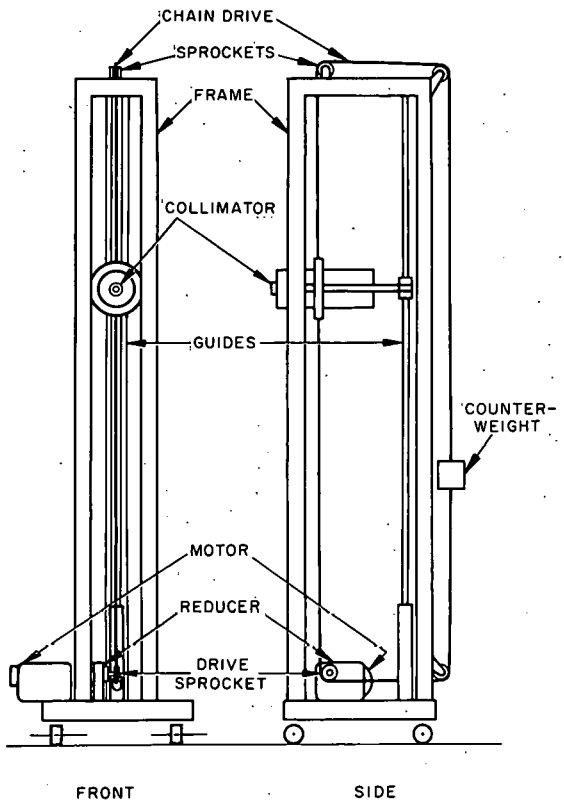

Fig. 9 Collimated Scanning Device

Friction between the carrier and rods is reduced by linear ball bushings permanently mounted in the carrier. The carrier is used to mount the radiation-sensitive head together with its appropriate shielding and collimation. The carrier is driven by a 1/4-horsepower motor which acts through a gear reducer on a chain drive. The linear speed of the carrier is fixed in this case at 0.56 cm/min.

The wiring diagram for the motor and the appropriate microswitches and relays are shown in Fig. 10. The circuit is arranged so that the carrier will move to a limit switch and then reverse its direction of travel so that, if left unattended, the system will monitor the ion exchange column or contaminated pipe section repeatedly until manually shut off. Using a 1-min counting time, the instrument produces 110 separate readings for each length of about 76 cm. An additional timer setting of 3-min allows readings to be taken for each 2.3 cm of travel.

Figure 11 is a block diagram of the electronic instrumentation associated with the scaling and recording functions of this system. The radiation-sensitive head consists of a G.M. tube (with a 2 mg/cm^2 window) and an appropriate shield.

The shielded G. M. tube is shown in Fig. 12. The equivalent lead shielding was calculated as a function of the angle the incident radiation makes with the axis of the G. M. tube. The results are given in Table XIX and shown in Fig. 13.

Upon completion and assembly of the device, a program was undertaken to evaluate its performance for the location of known sources. This was carried out by mounting known weights of radioactive crud at fixed positions. The results of these studies are reported in the following tables and figures:

Location of a Single Source, Table XX and Fig. 14
Location of Multiple Sources, Tables XXI and XXII and Figs. 15 and 16
Resolution of Adjacent Sources, Table XXIII and Fig. 17

Since these data indicate a fair degree of resolution, a run was carried out in which the sources were located only about 5 cm apart. This is as close together as the containers would allow. The observed data are given in Table XXIII and shown in Fig. 17. It is possible to separate the compound curve observed into three distinct sources, as shown by the superimposed broken line in Fig. 17. The source positions observed are compared with those measured, as shown in Table XXIV.

The results of these tests show that the G.M. tube and scanning system is capable of accurately showing differences in the distribution of radioactivity down an ion exchange column.

TABLE XIX

EQUIVALENT LEAD SHIELDING AS A FUNCTION OF INCIDENT ANGLE OF RADIATION

Angle of Incident Radiation (degrees)	Shielding Equivalent (inches of lead)
0	0
5	1.12
10	1.42
15	1.26
20	1.48
25	1.59
30	1.76
35	1.87
40	2.05
45	2.28
50	2.16
55	2.00
60	1.91

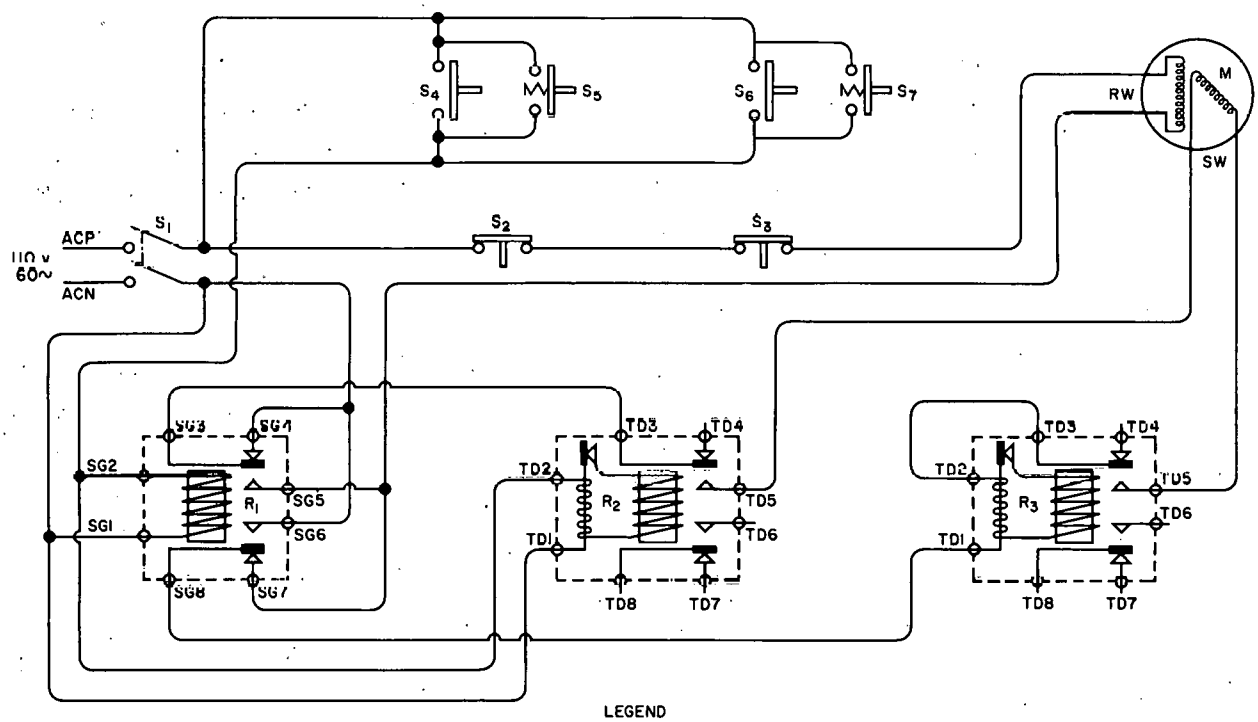

LEGEND

S_1 MAIN POWER SWITCH
S_2 BOTTOM EMERGENCY STOP (MICROSWITCH)
S_3 TOP EMERGENCY STOP (MICROSWITCH)
S_4 BOTTOM REVERSING SWITCH (MICROSWITCH)
S_5 PUSHBUTTON UP START
S_6 TOP REVERSING SWITCH (MICROSWITCH)
S_7 PUSHBUTTON DOWN START
R_1 110 v S.G. RELAY
R_2 & R_3 110 v TIME DELAY RELAY
M 1/4 HORSEPOWER MOTOR

Fig. 10 Wiring Diagram for Automatic Scanning System

TABLE XX

LOCATION OF SINGLE SOURCES

(All Readings Are Net Counts in Distance Traveled)

Travel (cm)	Source 53.5 mg Crud			Source 51.9 mg Crud			Source 181.9 mg Crud		
	A*	B*	Ave	A*	B*	Ave	A*	B*	Ave
9.9 - 10.6	81	71	76	57	80	68	167	200	183
10.6 - 11.3	107	103	105	92	95	93	213	261	237
11.3 - 12.0	149	167	108	108	146	127	292	315	303
12.0 - 12.7	198	200	199	148	217	183	375	480	427
12.7 - 13.4	296	282	289	236	288	262	521	785	653
13.4 - 14.1	332	324	328	398	327	362	726	1060	893
14.1 - 14.8	448	404	426	535	554	545	1007	1124	1061
14.8 - 15.5	650	765	707	500	593	546	1153	1692	1422
15.5 - 16.2	363	361	362	357	306	331	1747	1755	1751
16.2 - 16.9	252	322	284	307	307	307	1640	1112	1376
16.9 - 17.6	209	226	217	202	192	197	1109	1027	1068
17.6 - 18.3	152	161	156	129	140	135	951	678	814
18.3 - 19.0	103	114	108	112	102	107	670	492	581
19.0 - 19.7	86	53	69	67	49	58	500	315	407
19.7 - 20.4	--	--	--	57	59	58	329	279	304
20.4 - 21.1	--	--	--	--	--	--	220	260	240
21.1 - 21.8	--	--	--	--	--	--	157	203	180

* A scanned down; B scanned up.

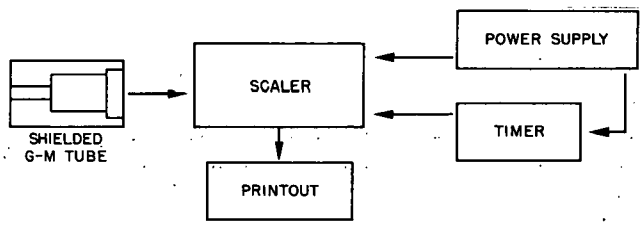

Fig. 11 Block Diagram of Electronic Instrumentation

TABLE XXI

LOCATION OF MULTIPLE SOURCES—FIRST RUN

Sources	Crud (mg)	Actual Position of Sources (cm)
A	51.9	15.9 - 16.2
B	181.9	20.2 - 20.8
C	53.5	26.1 - 26.4

Travel (cm)	Activity (Net Counts in Distance Traveled)	Travel (cm)	Activity (Net Counts in Distance Traveled)
10.4 - 11.0	270	22.2 - 23.0	1140
11.0 - 11.6	289	23.0 - 23.6	950
11.6 - 12.3	289	23.6 - 24.2	646
12.3 - 12.9	322	24.2 - 24.9	550
12.9 - 13.6	354	24.9 - 25.5	516
13.6 - 14.3	465	25.5 - 26.2	536
14.3 - 14.9	477	26.2 - 26.9	637
14.9 - 15.6	654	26.9 - 27.4	923
15.6 - 16.2	1140	27.4 - 28.2	628
16.2 - 16.9	722	28.2 - 28.9	496
16.9 - 17.6	659	28.9 - 29.4	453
17.6 - 18.2	734	29.5 - 30.2	393
18.2 - 18.9	847	30.2 - 30.8	334
18.9 - 19.6	1140	30.8 - 31.5	317
19.6 - 20.2	1230	31.5 - 32.2	287
20.2 - 20.9	1620	32.2 - 32.8	261
20.9 - 21.6	2460	32.8 - 33.5	263
21.6 - 22.2	1370		

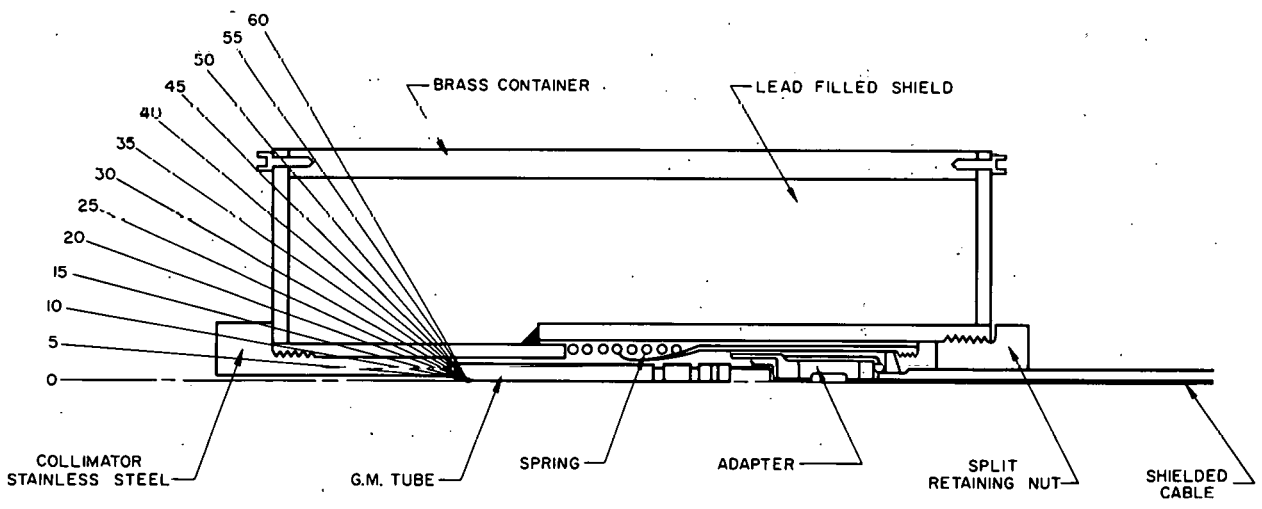

Fig. 12 Cross-Sectional View of Collimated G. M. Tube and Shield

TABLE XXII

LOCATION OF MULTIPLE SOURCES—SECOND RUN

Sources	Crud (mg)	Actual Position of Sources (cm)
A	51.9	19.6 - 19.9
B	53.5	31.1 - 31.4
C	181.9	42.1 - 42.7

Travel (cm)	Activity (Net Counts in Distance Traveled)	Travel (cm)	Activity (Net Counts in Distance Traveled)
9.7 - 12.0	750	32.7 - 35.0	1620
12.0 - 14.3	850	35.0 - 37.3	1000
14.3 - 16.6	1030	37.3 - 39.6	1520
16.6 - 18.9	1780	39.6 - 41.9	4230
18.9 - 21.2	3080	41.9 - 44.2	7660
21.2 - 23.5	1620	44.2 - 46.5	2710
23.5 - 25.8	1200	46.5 - 48.8	1180
25.8 - 28.1	1240	48.8 - 50.1	920
28.1 - 30.4	2090	50.1 - 52.4	650
30.4 - 32.7	3320	52.4 - 54.7	500

TABLE XXIII

RESOLUTION OF ADJACENT SOURCES

Sources	Crud (mg)	Actual Position of Sources (cm)
A	51.9	20.1 - 20.3
B	181.3	25.2 - 25.8
C	53.5	31.3 - 31.6

Travel (cm)	Activity (Net Counts in Distance Traveled)	Travel (cm)	Activity (Net Counts in Distance Traveled)
9.5 - 11.8	1100	26.9 - 29.2	2440
11.8 - 13.1	1170	29.2 - 31.5	2580
13.1 - 15.4	1200	31.5 - 33.8	1610
15.4 - 17.7	1400	33.8 - 36.1	1510
17.7 - 20.0	2410	36.1 - 38.4	1090
20.0 - 22.3	2640	38.4 - 40.7	1040
22.3 - 24.6	4980	40.7 - 43.0	1000
24.6 - 26.9	5720	43.0 - 45.3	1080

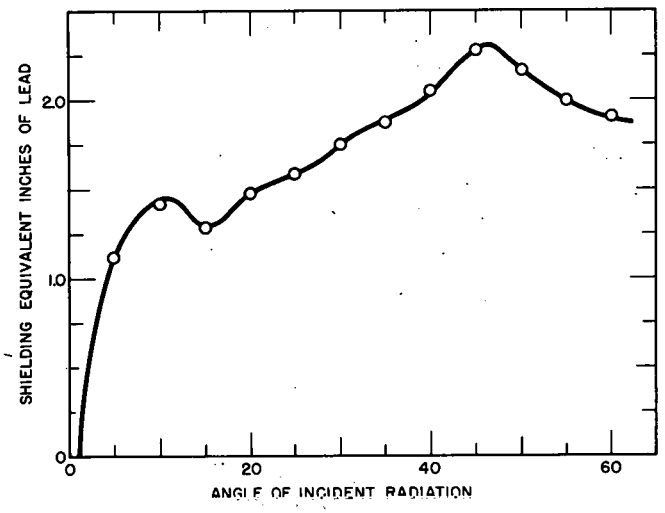

Fig. 13 Equivalent Lead Shielding and Collimation for G. M. Probe

TABLE XXIV

COMPARISON OF ACTUAL AND OBSERVED SOURCE POSITIONS

Source Crud (mg)	Mean Actual Position (cm)	Mean Observed Position (cm)	Difference (cm)
51.9	20.2	20	0.2
181.3	25.5	25	0.5
53.5	31.4	29.5	0.9

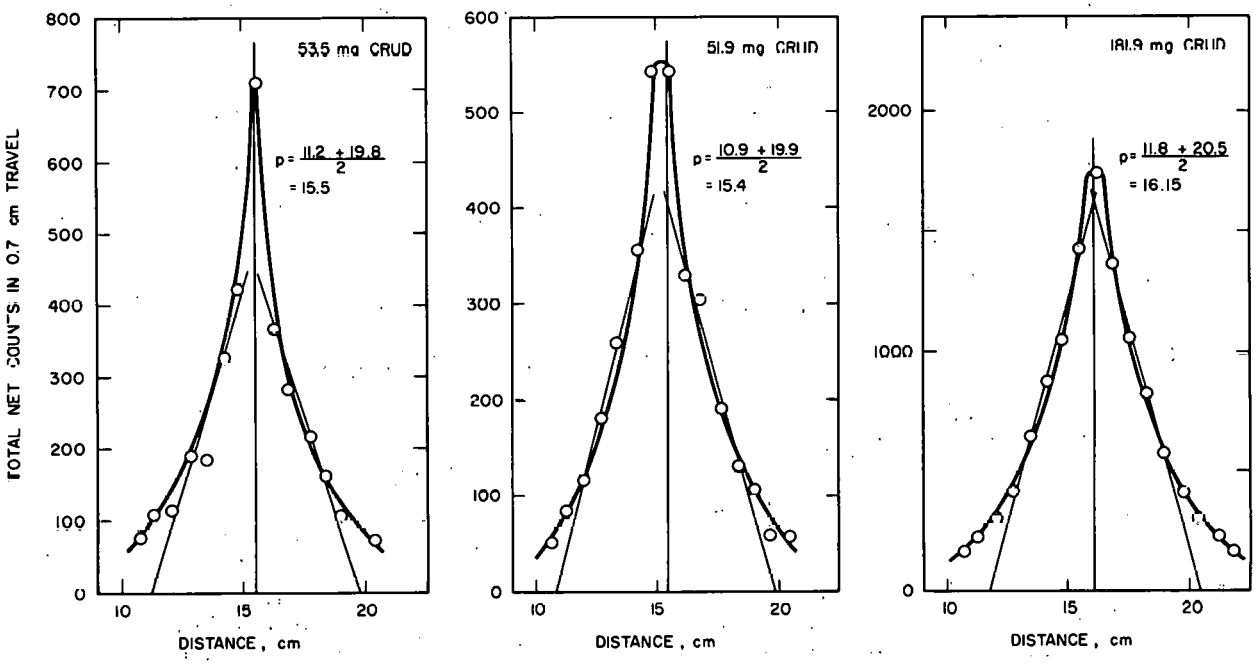

Fig. 14 Location of Single Sources by Collimated Scanner

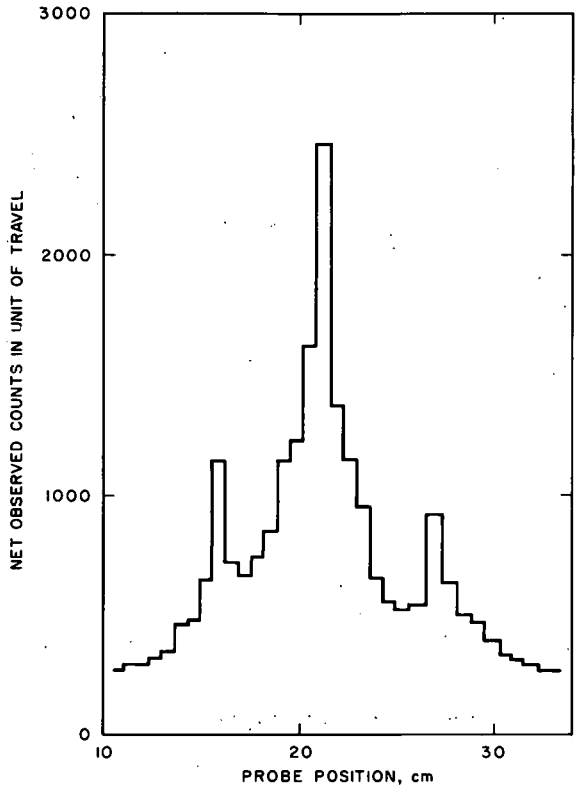

Fig. 15 Location of Multiple Sources by Collimated Scanner (First Run)

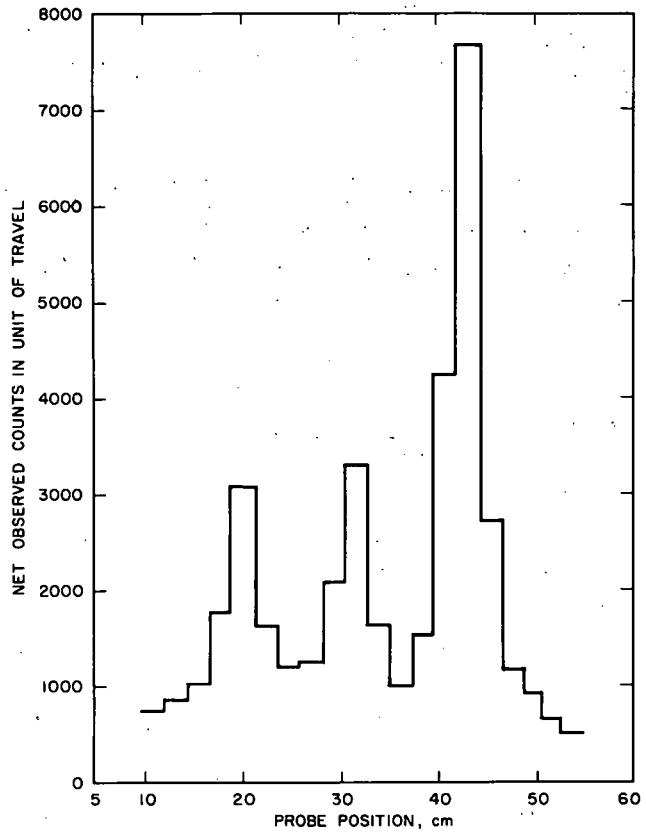

Fig. 16 Location of Multiple Sources by Collimated Scanner (Second Run)

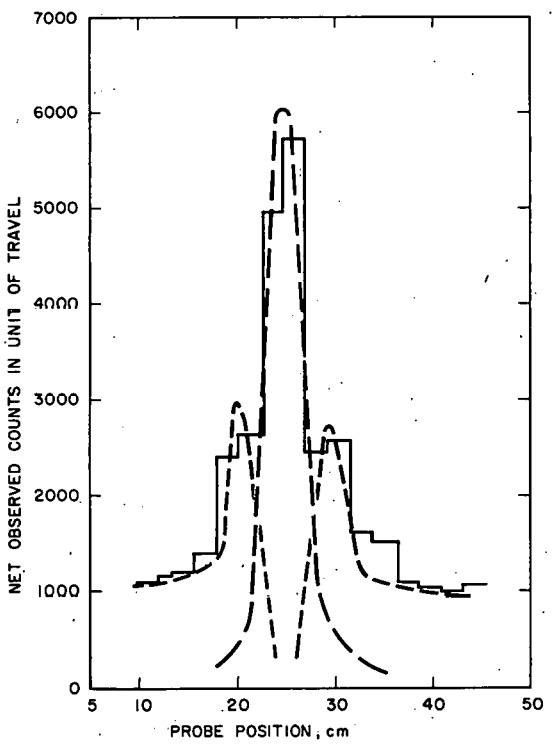

Fig. 17 Resolution of Adjacent Sources by Collimated Scanner

APPENDIX II: OPERATING HISTORIES OF LABORATORY ION EXCHANGE COLUMNS

The information contained in the tables and figures of this appendix is discussed in the text under Removal of Fission Products by Base-form Mixed Beds.

A. NH_4OH - Form Columns

TABLE XXV

OPERATING HISTORY OF NH_4OH RESIN WITH Sr^{90}-Y^{90} ACTIVITY

Column Volumes	Column Equivalents of NH_4OH	Influent Activity* (c/min-ml)	Effluent Activity* (c/min-ml)	Decontamination Factor*
300	0.037	5128	147	34.9
375	0.047	3327	28	119
450	0.056	3327	139	23.9
525	0.065	3327	178	18.7
600	0.075	3327	193	17.2
675	0.084	6810	243	28.0
825	0.103	6810	546	12.5
900	0.112	6810	654	10.4
1050	0.131	5829	552	10.6
1135	0.140	5830	898	6.5
1260	0.157	5829	960	6.1
1600	0.199	20,406	178	115
1830	0.236	10,640	820	13
1980	0.246	10,640	970	11

*Counting procedures did not distinguish between Sr^{90} and Y^{90}. Results are questionable because of probable separation of Sr^{90}. See discussion under Laboratory Column Experiments.

Note: Column Size - 1.05-cm ID x 76 cm deep
Influent pH - 9.5 (NH_4OH)
Flow loading - 7.5 gpm/ft^2

TABLE XXVI

OPERATING HISTORY OF NH_4 OH RESIN WITH Cs^{137}-Ba^{137} ACTIVITY

Column Volumes	Column Equivalents of NH_4OH	Influent Activity (c/min-ml)	Effluent Activity (c/min-ml)	Decontamination Factor
300	0.037	6950	1	6950
600	0.075	6600	1	6600
900	0.112	8842	1	8842
1200	0.149	8379	3	2793
1350	0.168	7275	1	7275
1500	0.187	7275	105	69.3
1650	0.205	8644	9	960
1800	0.224	8644	13	665

Note: Column Size - 1.05-cm ID x 76 cm deep
Influent pH - 9.5 (NH_4OH)
Flow Loading - 7.5 gpm/ft^2

TABLE XXVII

OPERATING HISTORY OF NH_4OH RESIN WITH Ce^{144}-Pr^{144} ACTIVITY

Column Volumes	Column Equivalents of NH_4OH	Influent Activity (c/min-ml)	Effluent Activity (c/min-ml)	Decontamination Factor
280	0.035	3212	40	80.3
360	0.045	6225	128	48.6
420	0.052	6225	220	28.3
480	0.060	6225	264	23.6
560	0.070	6225	311	20.0
600	0.075	6225	361	17.2
670	0.083	6924	361	19.2
730	0.091	6924	485	14.3
880	0.109	6924	486	14.2
950	0.118	6924	623	11.1
1200	0.149	5679	885	6.4
1400	0.174	733	242	3.0

Note: Column Size - 1.05-cm ID x 76 cm deep
Influcnt pH - 9.5 (NH_4OH)
Flow Loading - 7.5 gpm/ft^2

B. KOH - Form Columns

TABLE XXVIII

OPERATING HISTORY OF KOH RESIN COLUMN WITH Sr^{90}-Y^{90} ACTIVITY

Column Volumes	Column Equivalents of KOH	Influent Activity* (c/min-ml)	Effluent Activity* (c/min-ml)	Decontamination Factor
100	0.029	15,914	541	29.4
220	0.063	15,914	707	22.5
330	0.094	15,567	2,915	5.3
450	0.128	15,567	5,420	2.9
550	0.157	15,567	7,694	2.0
660	0.188	30,310	9,967	3.0
770	0.219	30,920	18,752	1.6
890	0.254	30,920	15,907	1.9
1000	0.285	45,462	15,576	2.9
1110	0.316	45,720	15,530	2.9

* Counting procedures did not distinguish between Sr^{90} and Y^{90}. Results are questionable because of probable separation of Sr^{90}. See discussion under Laboratory Column Experiments.

Note: Influent pH - 10.3 (KOH)
Flow Loading - 7.5 gpm/ft^2
Column Size - 1.05 cm ID x 76 cm deep

TABLE XXIX

OPERATING HISTORY OF KOH RESIN COLUMN WITH Cs^{137}-Ba^{137} ACTIVITY

Column Volumes	Column Equivalents of KOH	Influent Activity (c/min-ml)	Effluent Activity (c/min-ml)	Decontamination Factor
100	0.029	14,671	513	28.6
220	0.063	14,671	3	4890
330	0.094	14,960	204	73.3
450	0.128	14,960	10,970	1.4
550	0.157	14,960	14,602	1.0

TABLE XXIX

OPERATING HISTORY OF KOH RESIN COLUMN
WITH Cs^{137}-Ba^{137} ACTIVITY (Continued)

Column Volumes	Column Equivalents of KOH	Influent Activity (c/min-ml)	Effluent Activity (c/min-ml)	Decontamination Factor
660	0.188	23,970	19,526	1.2
770	0.219	24,450	13,657	1.8
890	0.254	24,450	19,556	1.2
1000	0.285	44,756	55,970	0.8
1100	0.316	46,051	43,644	1.1

Note: Influent pH - 10.3 (KOH)
Flow Loading - 7.5 gpm/ft^2
Column Size - 1.05 cm ID x 76 cm deep

TABLE XXX

OPERATING HISTORY OF KOH RESIN COLUMN
WITH Ce^{144}-Pr^{144} ACTIVITY

Influent pH - 10.3 (KOH)
Flow Loading - 7.5 gpm/ft^2
Column Size - 1.05 cm ID x 76 cm deep

Column Volumes	Column Equivalents of KOH	Influent Activity (c/min-ml)	Effluent Activity (c/min-ml)	Decontamination Factor
100	0.029	13,968	313	44.6
200	0.063	13,968	617	22.6
330	0.094	14,256	12,380	1.2
450	0.128	14,256	12,648	1.1
550	0.157	14,256	18,562	0.8
660	0.188	25,205	19,525	1.4
770	0.219	36,968	31,537	1.2
890	0.254	35,099	35,029	1.0
1000	0.285	46,202	43,272	1.1
1100	0.316	51,153	44,557	1.1

C. LiOH - Form Columns

TABLE XXXI

OPERATING HISTORY OF LiOH RESIN COLUMN WITH Sr^{90}-Y^{90} ACTIVITY

Flow Loading - 7.5 gpm/ft^2

Column Size - 1.05-cm ID x 76 cm deep

Column Volumes	Column Equivalents of LiOH	Influent Activity (c/min-ml)	Effluent* Activity (c/min-ml)	Decontamination Factor
		Influent adjusted to pH 9.5 with LiOH		
65	0.003	1,000	46	21.7
885	0.040	16,970	434	39.1
1060	0.048	12,375	1,110	11.2
1215	0.055	12,375	776	15.9
1435	0.065	12,560	398	31.6
1700	0.077	12,560	761	16.5
1920	0.087	10,302	365	28.2
2190	0.099	7,894	596	13.2
2385	0.108	7,894	521	14.9
2520	0.114	6,550	584	11.2
2920	0.132	8,658	831	10.4
		Influent adjusted to pH 10.5 with LiOH		
90	0.04	9,500	778	12.2
1130	0.51	20,108	690	29.1
1370	0.62	9,894	1,311	7.6
1635	0.73	9,894	2,306	4.3
1900	0.86	8,652	2,949	2.9
2100	0.95	9,928	3,526	2.8
2230	1.01	9,928	3,327	3.0
2585	1.17	10,844	1,785	6.1
2785	1.26	6,867	1,958	3.5
3095	1.40	7,313	2,824	2.6

* Counting procedures did not distinguish between Sr^{90} and Y^{90}. Results are questionable because of probable separation of Sr^{90}. See discussion under Laboratory Column Experiments.

TABLE XXXII

OPERATING HISTORY OF LiOH RESIN COLUMN WITH Sr^{90}-Y^{90} ACTIVITY

Flow Loading - 7.5 gpm/ft^2

Column Size - 1.05-cm ID x 12.5 cm deep

Column Volumes	Column Equivalents of LiOH	Influent Activity* (c/min-ml)	Effluent Activity* (c/min-ml)	Decontamination Factor*
	Influent adjusted to pH 10.5 with LiOH			
175	0.08	5000	856	5.8
795	0.36	5000	2087	2.4
1855	0.84	5000	2143	2.3
3800	1.72	8708	4205	2.1
4245	1.92	8708	2255	3.9
5130	2.32	8708	2345	3.7

* Counting procedures did not distinguish between Sr^{90} and Y^{90}. Results are questionable because of probable separation of Sr^{90}. See discussion under Laboratory Column Experiments.

TABLE XXXIII

OPERATING HISTORY OF LiOH RESIN COLUMN WITH Cs^{137}-Ba^{137} ACTIVITY

Flow Loading - 7.5 gpm/ft^2

Column Size - 1.05-cm ID x 76 cm deep

Column Volumes	Column Equivalents of LiOH	Influent Activity (c/min-ml)	Effluent Activity (c/min-ml)	Decontamination Factor
	Influent adjusted to pH 9.5 with LiOH			
65	0.003	3500	4	875
375	0.017	3500	19	184
1040	0.047	3500	172	20.4
1305	0.059	2567	110	23.3
680	0.076	3132	89	35.2
1835	0.083	5340	105	50.8
2080	0.094	5359	55	97.4
2390	0.108	5359	21	283
2985	0.135	6532	11	594
3315	0.150	6132	8	767

TABLE XXXIII

OPERATING HISTORY OF LiOH RESIN COLUMN WITH Cs^{137}-Ba^{137} ACTIVITY
(Continued)

Flow Loading - 7.5 gpm/ft^2
Column Size - 1.05-cm ID x 76 cm deep

Column Volumes	Column Equivalents of LiOH	Influent Activity (c/min-ml)	Effluent Activity (c/min-ml)	Decontamination Factor
		Influent adjusted to pH 10.5 with LiOH		
45	0.03	3500	6	583
1105	0.50	3712	37	100
1435	0.65	1756	15	117
1550	0.70	1756	10	176
1770	0.80	2872	110	26.1
2320	1.05	4783	23	208
2540	1.15	6223	15	415
2920	1.32	6223	13	479
3270	1.48	6194	27	229
3870	1.75	7271	16	454

TABLE XXXIV

OPERATING HISTORY OF LiOH RESIN COLUMN WITH Cs^{137}-Ba^{137} ACTIVITY

Flow Loading - 7.5 gpm/ft^2
Column Size - 1.05-cm ID x 12.5 cm deep

Column Volumes	Column Equivalents of LiOH	Influent Activity (c/min-ml)	Effluent Activity (c/min-ml)	Decontamination Factor
		Influent adjusted to pH 9.5 with LiOH		
135	0.006	7636	266	28.7
440	0.020	7636	564	13.5
1525	0.069	7636	1226	6.2
1725	0.078	9650	765	12.6
2035	0.092	9650	817	11.8
4945	0.194	12,148	1433	8.5
6495	0.294	13,939	1458	8.3
7335	0.332	13,939	1428	9.8
9105	0.412	13,939	983	14.2

TABLE XXXIV

OPERATING HISTORY OF LiOH RESIN COLUMN WITH Cs^{137}-Ba^{137} ACTIVITY
(Continued)

Flow Loading - 7.5 gpm/ft^2
Column Size - 1.05-cm ID x 12.5 cm deep

Column Volumes	Column Equivalents of LiOH	Influent Activity (c/min-ml)	Effluent Activity (c/min-ml)	Decontamination Factor
Influent adjusted to pH 10.5 with LiOH				
265	0.12	7362	235	31.3
775	0.35	7362	404	18.2
1635	0.74	7362	453	16.3
2920	1.32	7100	1462	4.9
3710	1.68	7271	36	2.2
4930	2.23	16,000	4133	3.9
5635	2.55	16,000	4283	3.7

TABLE XXXV

OPERATING HISTORY OF LiOH RESIN COLUMN WITH Ce^{144}-Pr^{144} ACTIVITY

Flow Loading - 7.5 gpm/ft^2
Column Size - 1.05-cm ID x 76 cm deep

Column Volumes	Column Equivalents of LiOH	Influent Activity (c/min-ml)	Effluent Activity (c/min-ml)	Decontamination Factor
Influent adjusted to pH 9.5 with LiOH				
65	0.003	10,000	787	12.7
1660	0.075	2560	335	7.6
1945	0.088	7410	744	10.0
2080	0.094	7410	1928	3.8
2210	0.100	7410	1337	5.5
2385	0.108	4295	1218	3.5
2540	0.115	5192	842	6.2
2830	0.128	5192	810	6.4
3205	0.145	5651	2205	2.6
3645	0.165	2698	2180	1.2
3870	0.175	6046	3880	1.6

TABLE XXXV

OPERATING HISTORY OF LiOH RESIN COLUMN WITH Ce^{144}-Pr^{144} ACTIVITY
(Continued)

Flow Loading - 7.5 gpm/ft^2
Column Size - 1.05-cm ID x 76 cm deep

Column Volumes	Column Equivalents of LiOH	Influent Activity (c/min-ml)	Effluent Activity (c/min-ml)	Decontamination Factor
		Influent adjusted to pH 10.5 with LiOH		
55	0.025	18,000	281	64.1
730	0.33	2340	616	3.8
1280	0.58	5312	1862	2.9
1500	0.68	8013	3836	2.1
1725	0.78	8013	3990	2.0
1945	0.88	4650	2328	2.0
2075	0.94	5566	3223	1.7
2210	1.00	5566	3225	1.7
2610	1.18	6323	3413	1.8
3050	1.38	7148	3289	2.2
3315	1.50	5719	2849	2.0

TABLE XXXVI

OPERATING HISTORY OF LiOH RESIN COLUMN WITH Ce^{144}-Pr^{144} ACTIVITY

Flow Loading - 7.5 gpm/ft^2
Column Size - 1.05-cm ID x 12.5 cm deep

Column Volumes	Column Equivalents of LiOH	Influent Activity (c/min-ml)	Effluent Activity (c/min-ml)	Decontamination Factor
		Influent adjusted to pH 9.5 with LiOH		
165	0.0075	10,853	5200	2.1
995	0.045	10,853	6867	1.6
1545	0.070	10,853	7800	1.4
3935	0.178	4221	4361	1.0
5480	0.248	2838	2662	1.1
5810	0.263	2838	2741	1.0
6740	0.305	2200	1793	1.2
7735	0.350	2200	1330	1.7

TABLE XXXVI

OPERATING HISTORY OF LiOH RESIN COLUMN WITH Ce^{144}-Pr^{144} ACTIVITY
(Continued)

Flow Loading - 7.5 gpm/ft^2
Column Size - 1.05-cm ID x 12.5 cm deep

Column Volumes	Column Equivalents of LiOH	Influent Activity (c/min-ml)	Effluent Activity (c/min-ml)	Decontamination Factor
		Influent adjusted to pH 10.5 with LiOH		
220	0.10	4400	3887	1.1
600	0.27	4400	4913	0.9
995	0.45	4400	4481	1.0
1660	0.75	4400	5046	1.0
1770	0.80	4400	2415	1.8
3870	1.75	4715	979	4.8
4975	2.25	2612	2251	1.2
5900	2.69	2612	2363	1.1
7735	3.50	3187	2017	1.6

TABLE XXXVII

OPERATING HISTORY OF LiOH RESIN COLUMN WITH Ru^{106}-Rh^{106} ACTIVITY

Flow Loading - 7.5 gpm/ft^2
Column Size - 1.05-cm ID x 76 cm deep

Column Volumes	Column Equivalents of LiOH	Influent Activity (c/min-ml)	Effluent Activity (c/min-ml)	Decontamination Factor
		Influent adjusted to pH 9.5 with LiOH		
90	0.004	3100	38	81.6
930	0.042	8300	1800	4.6
1340	0.056	3700	275	13.5
1480	0.067	4550	690	6.6
1635	0.074	4550	750	6.1
1790	0.081	4200	1600	2.6
2035	0.092	4200	1880	2.2
2165	0.098	4700	1700	2.8
2430	0.110	4700	2700	1.7
2740	0.124	3650	2850	1.3
3095	0.140	7300	6500	1.1

TABLE XXXVII

OPERATING HISTORY OF LiOH RESIN COLUMN WITH Ru^{106}-Rh^{106} ACTIVITY
(Continued)

Flow Loading - 7.5 gpm/ft^2
Column Size - 1.05-cm ID x 76 cm deep

Column Volumes	Column Equivalents of LiOH	Influent Activity (c/min-ml)	Effluent Activity (c/min-ml)	Decontamination Factor
		Influent adjusted to pH 10.5 with LiOH		
65	0.03	4871	72	68.7
730	0.33	9525	1069	8.9
1170	0.53	4900	2300	2.1
1390	0.63	3418	888	3.9
1460	0.66	3418	2198	1.6
1660	0.75	3418	2289	1.5
1880	0.85	4295	3630	1.2
1990	0.90	3690	3052	1.2
2210	1.00	3690	3172	1.2
2385	1.08	3690	2885	1.3
2610	1.18	4605	3549	1.3
3050	1.38	3817	3423	1.1
3425	1.55	6693	5195	1.3

TABLE XXXVIII

OPERATING HISTORY OF LiOH RESIN COLUMN WITH Ru^{106}-Rh^{106} ACTIVITY

Flow Loading - 7.5 gpm/ft^2
Column Size - 1.05-cm ID x 12.5 cm deep

Column Volumes	Column Equivalents of LiOH	Influent Activity (c/min-ml)	Effluent Activity (c/min-ml)	Decontamination Factor
		Influent adjusted to pH 10.5 with LiOH		
220	0.10	4445	3106	1.4
795	0.36	4445	3383	1.3
1855	0.84	4445	3542	1.2
3535	1.60	3920	3668	1.1
3980	1.80	3920	2358	1.7
4970	2.25	4790	3190	1.5
5635	2.55	4790	3421	1.4
7070	3.20	4464	3748	1.2
7735	3.50	4464	2983	1.5

TABLE XXXIX

OPERATING HISTORY OF LiOH RESIN COLUMN WITH Zr^{95}-Nb^{95} ACTIVITY

Flow Loading - 7.5 gpm/ft^2

Column Size - 1.05-cm ID x 76 cm deep

Column Volumes	Column Equivalents of LiOH	Influent Activity (c/min-ml)	Effluent Activity (c/min-ml)	Decontamination Factor
	Influent adjusted to pH 9.5 with LiOH			
65	0.003	2945	56	52.6
175	0.008	2945	125	23.6
400	0.018	3356	203	16.5
665	0.030	5876	420	14.0
770	0.033	5876	299	19.7
885	0.040	5876	558	10.5
1215	0.055	5318	380	14.0
1280	0.058	5318	762	7.0
1545	0.070	3559	1542	2.3
1770	0.080	5717	2227	2.6
	Influent adjusted to pH 10.5 with LiOH			
45	0.02	3795	85	44.6
265	0.12	3795	83	45.7
400	0.18	3457	110	31.4
660	0.29	5666	310	18.3
1105	0.49	4204	432	9.7
1660	0.75	4982	530	9.4
1945	0.88	4961	562	8.8

TABLE XL

OPERATING HISTORY OF LiOH RESIN COLUMN WITH Zr^{95}-Nb^{95} ACTIVITY

Flow Loading - 7.5 gpm/ft^2

Column Size - 1.05-cm ID x 12.5 cm deep

Column Volumes	Column Equivalents of LiOH	Influent Activity (c/min-ml)	Effluent Activity (c/min-ml)	Decontamination Factor
	Influent adjusted to pH 10.5 with LiOH			
175	0.08	1924	853	2.3
775	0.35	1924	1245	1.6
1700	0.77	1924	1343	1.4
3980	1.80	2015	475	4.2
4860	2.20	647	328	2.0
5965	2.70	647	368	1.8

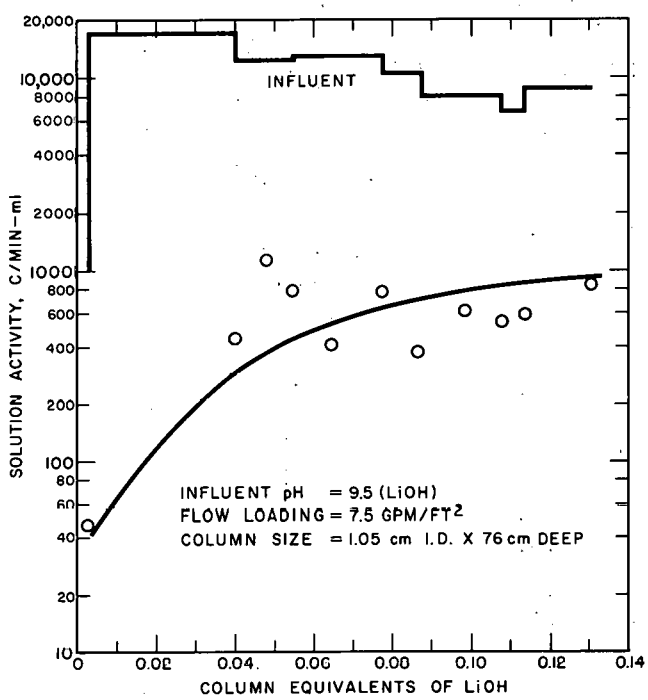

Fig. 18 Operating History of LiOH Resin Column with Sr^{90}—Y^{90} Activity (1)

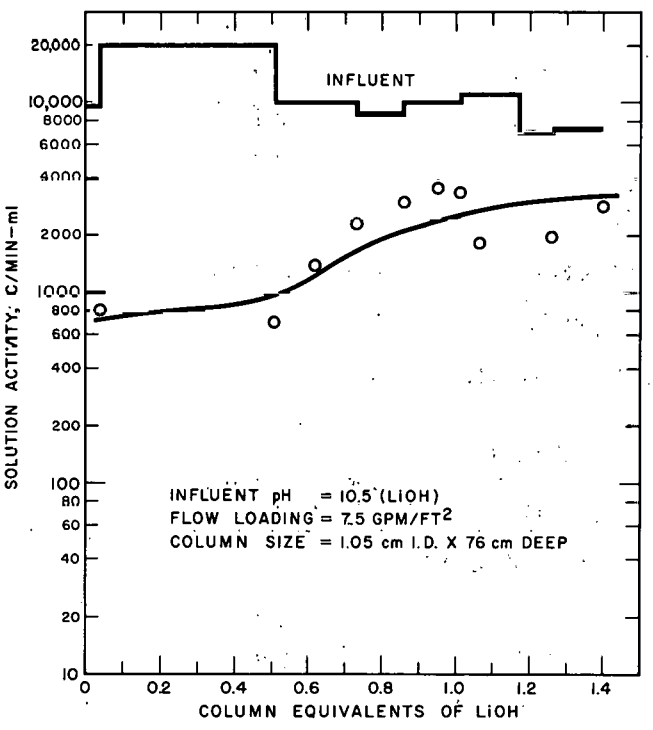

Fig. 19 Operating History of LiOH Resin Column with Sr^{90}—Y^{90} Activity (2)

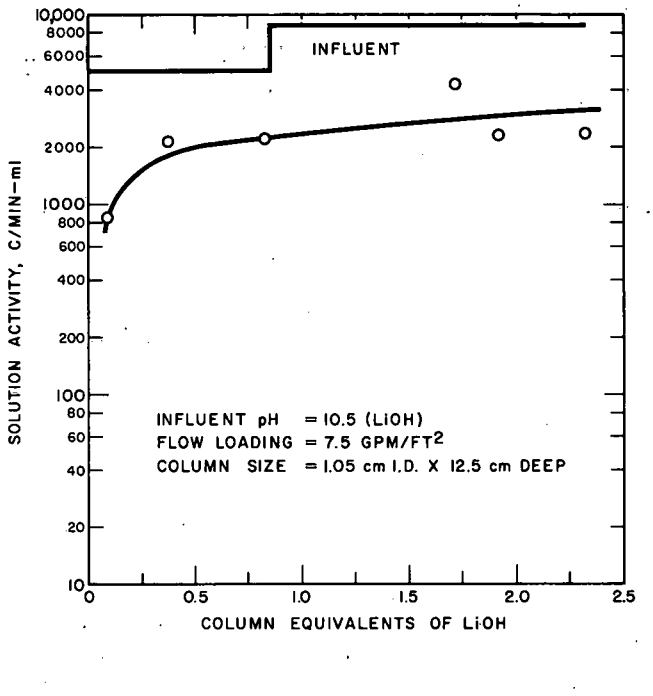

Fig. 20 Operating History of LiOH Resin Column with Sr^{90}—Y^{90} Activity (3)

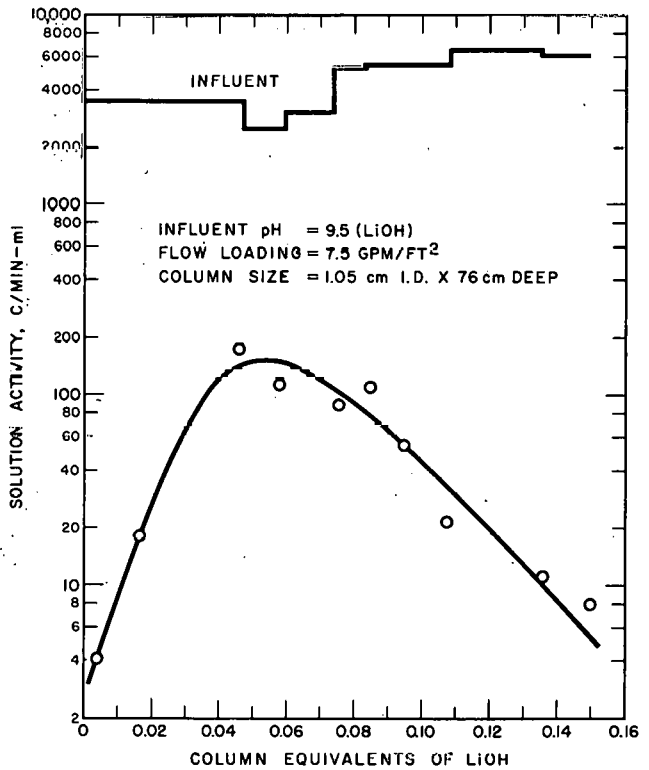

Fig. 21 Operating History of LiOH Resin Column with Cs^{137}—Ba^{137} Activity (1)

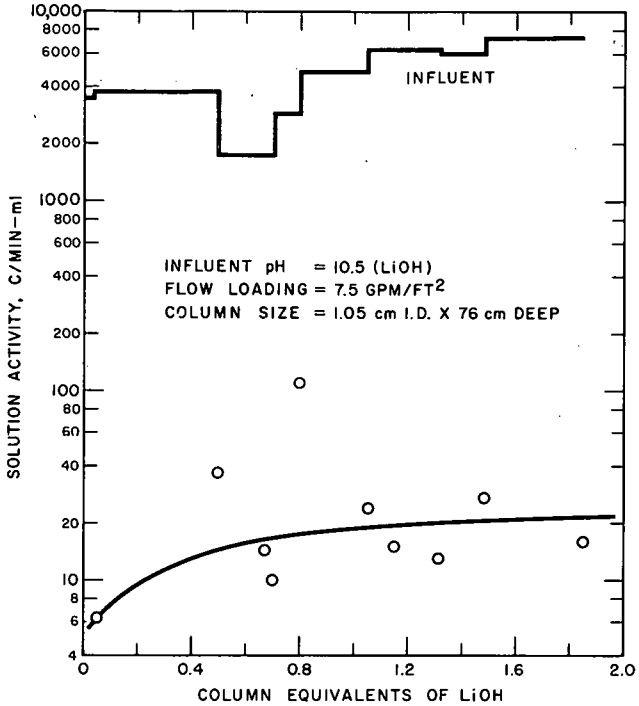

Fig. 22 Operating History of LiOH Resin Column with Cs^{137}—Ba^{137} Activity (2)

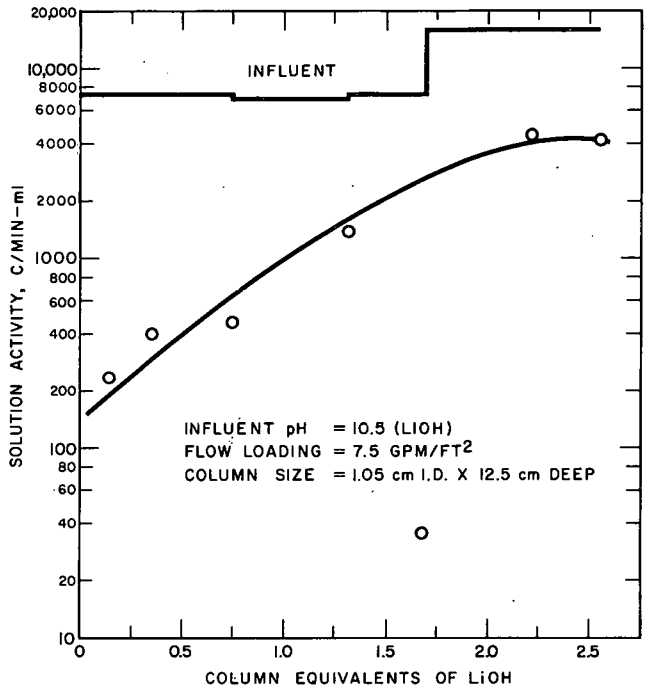

Fig. 24 Operating History of LiOH Resin Column with Cs^{137}—Ba^{137} Activity (4)

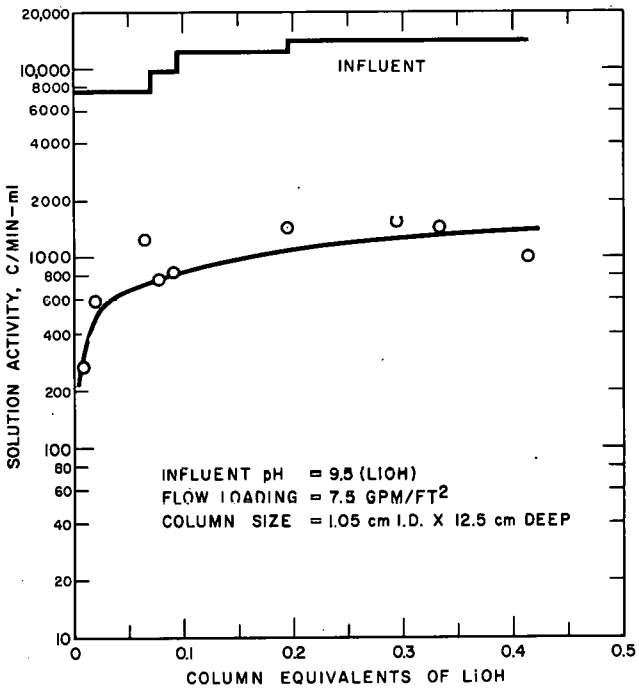

Fig. 23 Operating History of LiOH Resin Column with Cs^{137}—Ba^{137} Activity (3)

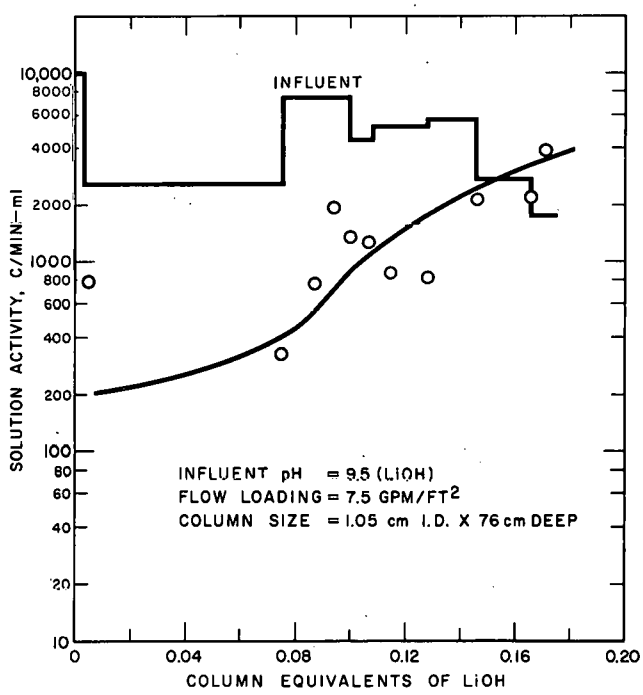

Fig. 25 Operating History of LiOH Resin Column with Ce^{144}—Pr^{144} Activity (1)

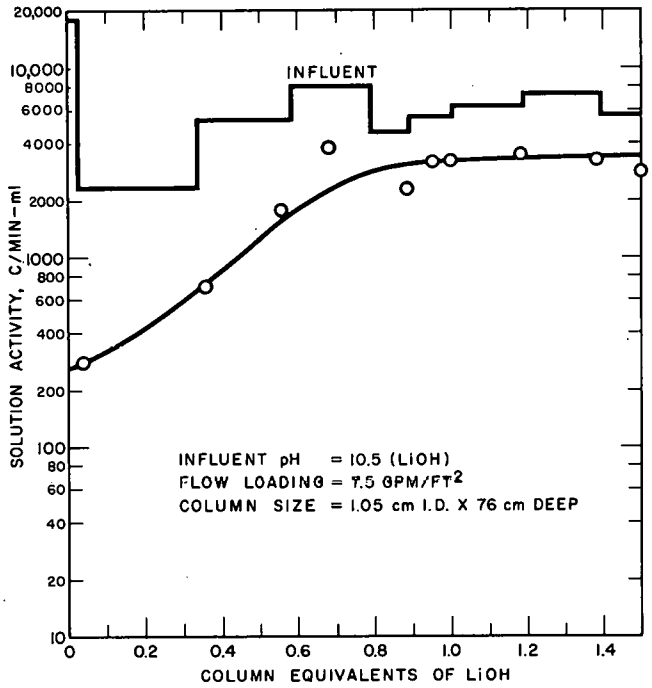

Fig. 26 Operating History of LiOH Resin Column with Ce^{144}—Pr^{144} Activity (2)

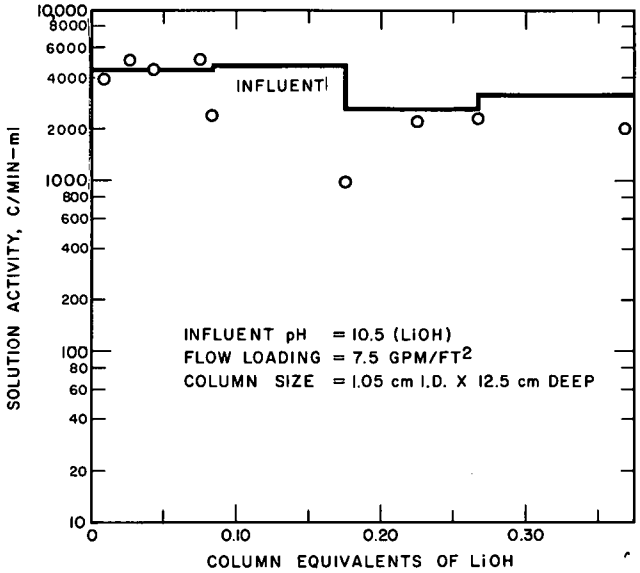

Fig. 28 Operating History of LiOH Resin Column with Ce^{144}—Pr^{144} Activity (4)

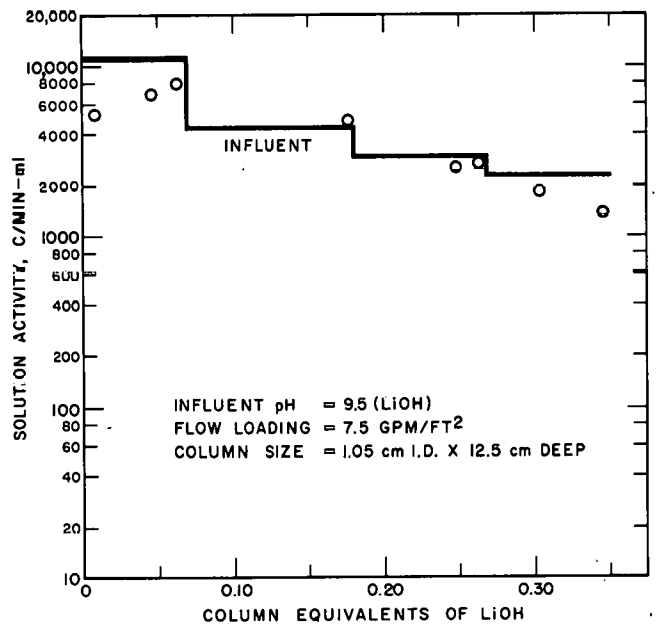

Fig. 27 Operating History of LiOH Resin Column with Ce^{144}—Pr^{144} Activity (3)

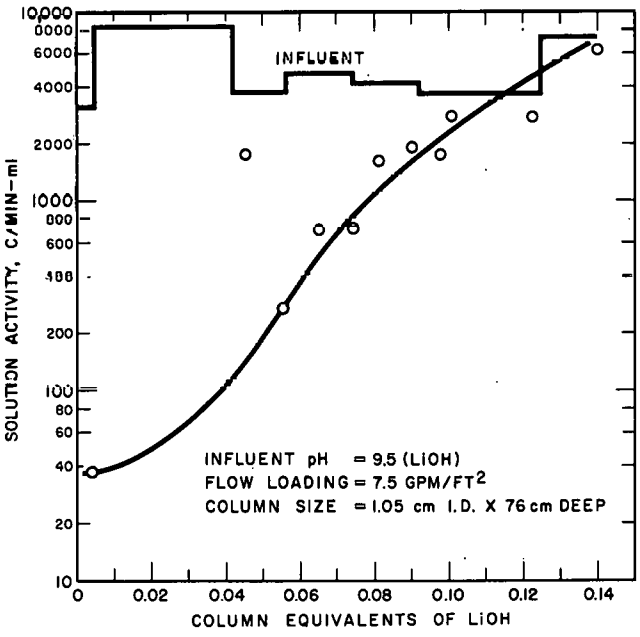

Fig. 29 Operating History of LiOH Resin Column with Ru^{106}—Rh^{106} Activity (1)

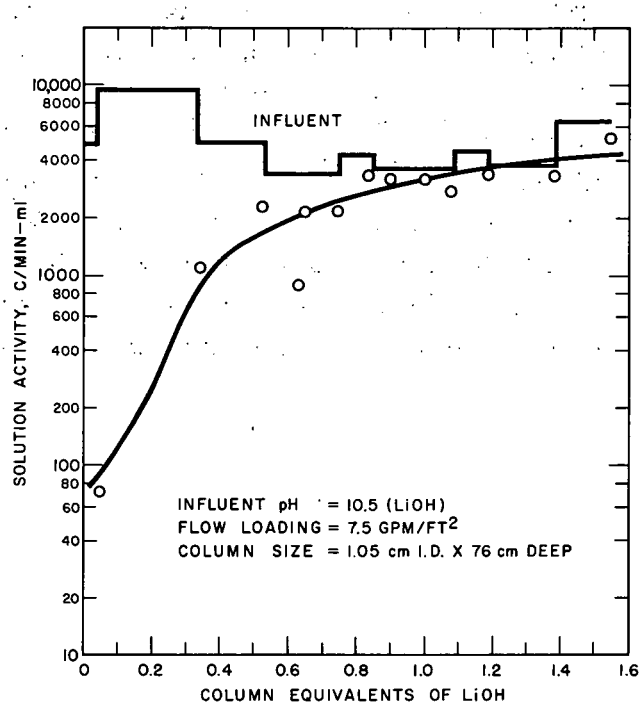

Fig. 30 Operating History of LiOH Resin Column with Ru^{106}—Rh^{106} Activity (2)

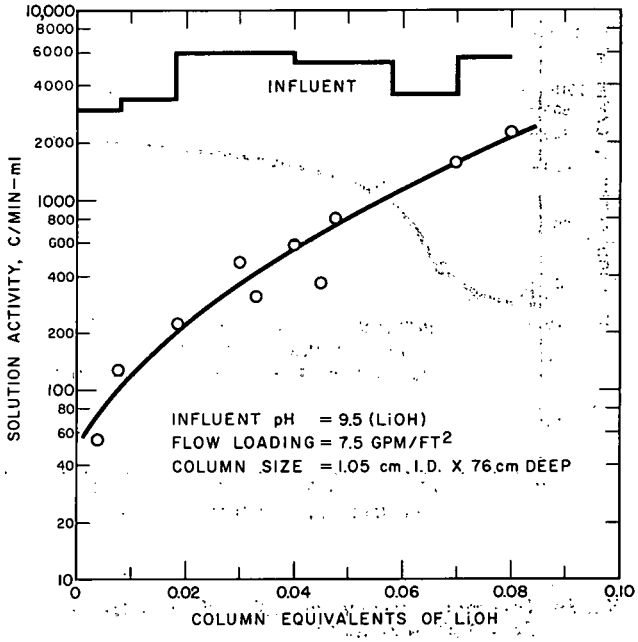

Fig. 32 Operating History of LiOH Resin Column with Zr^{95}—Nb^{95} Activity (1)

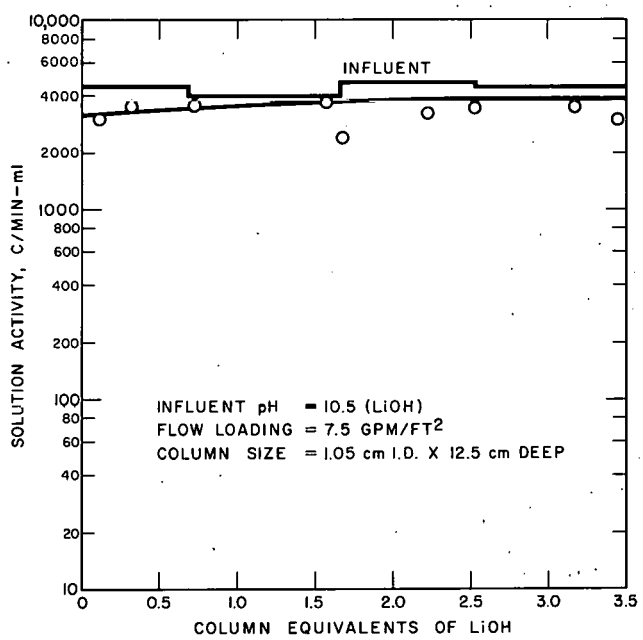

Fig. 31 Operating History of LiOH Resin Column with Ru^{106}—Rh^{106} Activity (3)

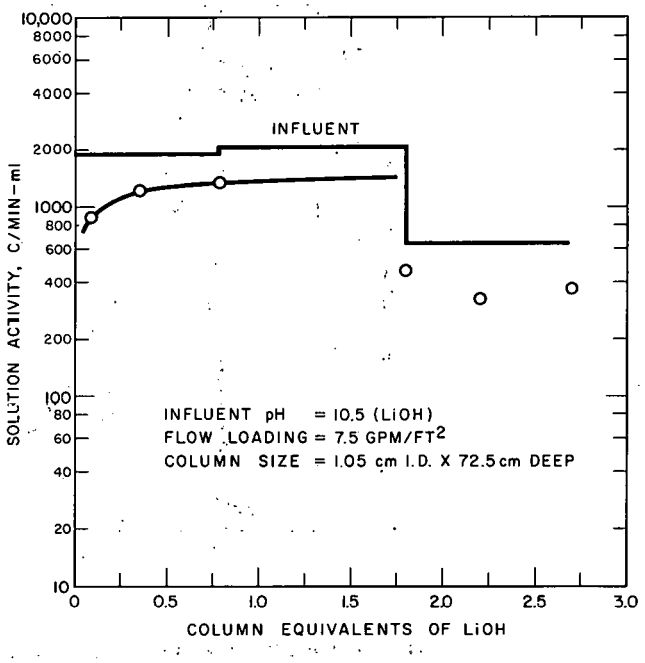

Fig. 33 Operating History of LiOH Resin Column with Zr^{95}—Nb^{95} Activity (2)

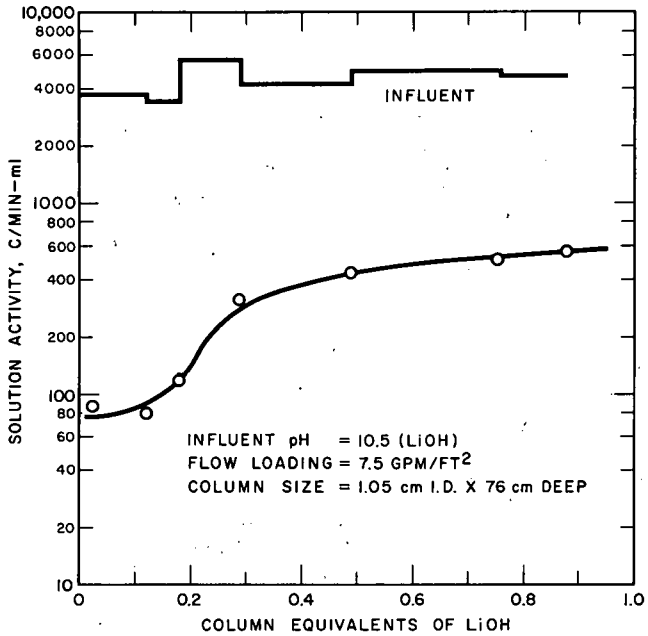

Fig. 34 Operating History of LiOH Resin Column with Zr^{95}—Nb^{95} Activity (3)

APPENDIX III: DISTRIBUTION OF RADIOISOTOPES ON LABORATORY COLUMNS

This appendix contains the results of collimated and uncollimated radiation surveys of the 76-cm, LiOH-form columns used with the following fission products: Sr^{90}-Y^{90}, Cs^{137}-Ba^{137}, Ce^{144}-Pr^{144}, Ru^{106}-Rh^{106}, and Zr^{95}-Nb^{95}. The surveys were made several months after processing had been stopped. The information is provided by distribution curves and is discussed in the text under Removal of Fission Products by Base-form Mixed Beds.

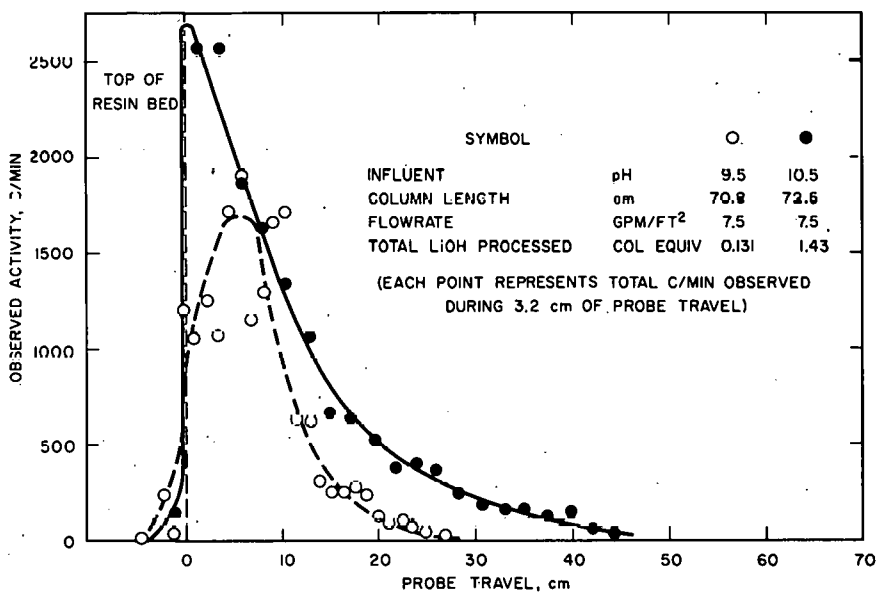

Fig. 35 Sr^{90}—Y^{90} Activity Distribution on LiOH Resin by a Collimated Probe Instrument

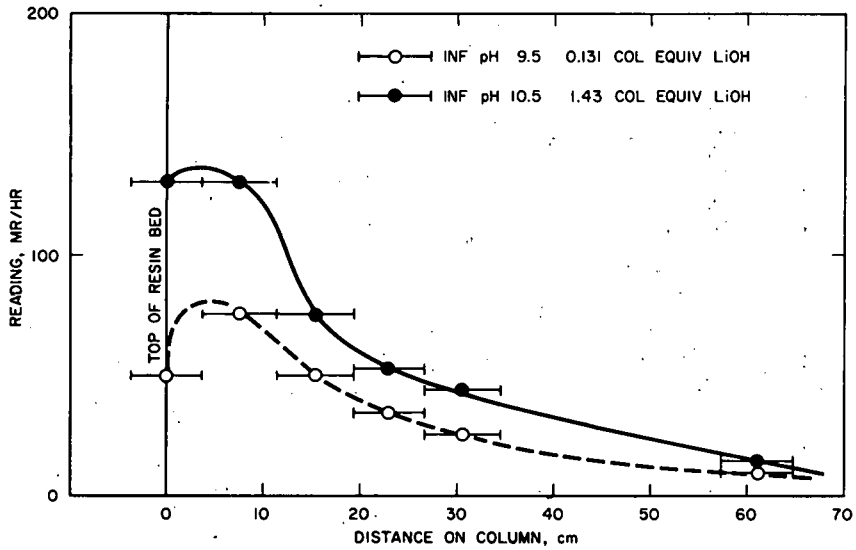

Fig. 36 Sr^{90}—Y^{90} Activity Distribution on LiOH Resin by an Uncollimated Probe Instrument

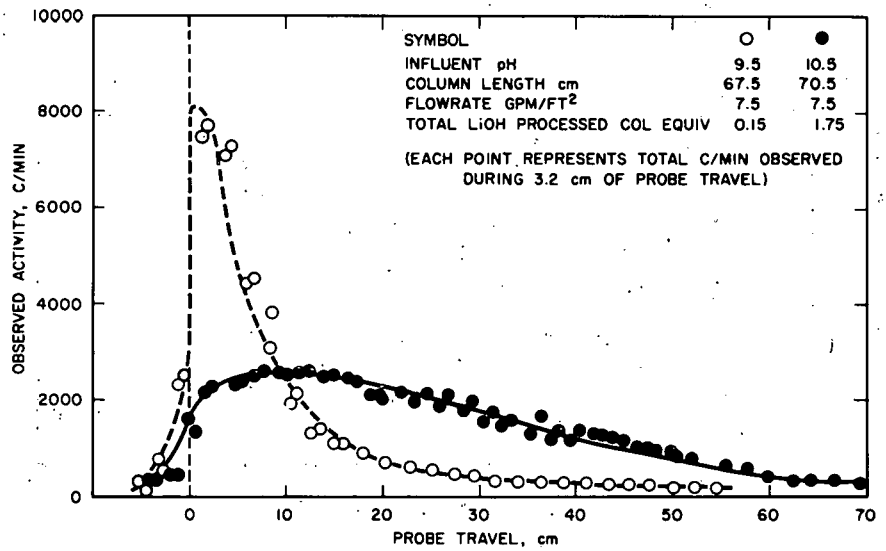

Fig. 37 Cs^{137}—Ba^{137} Activity Distribution on LiOH Resin by a Collimated Probe Instrument

THIS PAGE

WAS INTENTIONALLY

LEFT BLANK

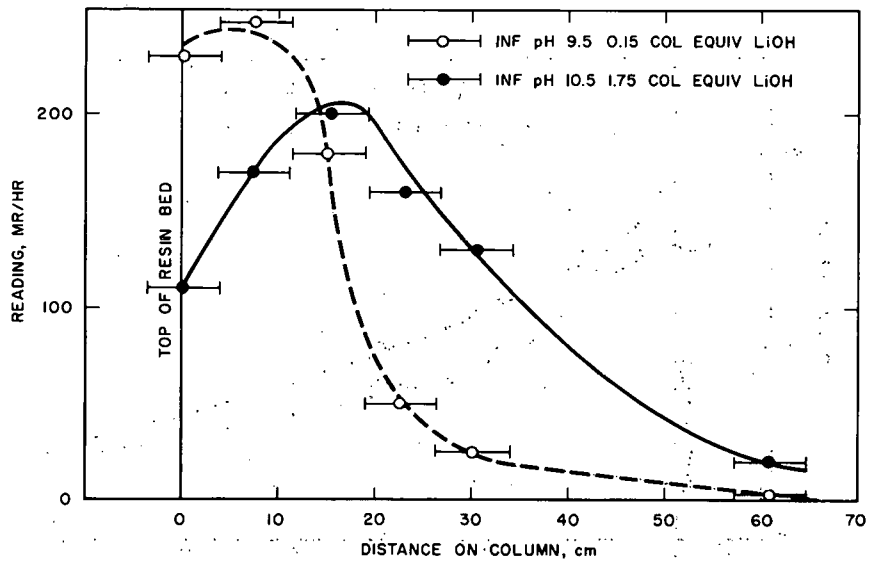

Fig. 38 Cs^{137}—Ba^{137} Activity Distribution on LiOH Resin by a Portable Survey Instrument (Uncollimated)

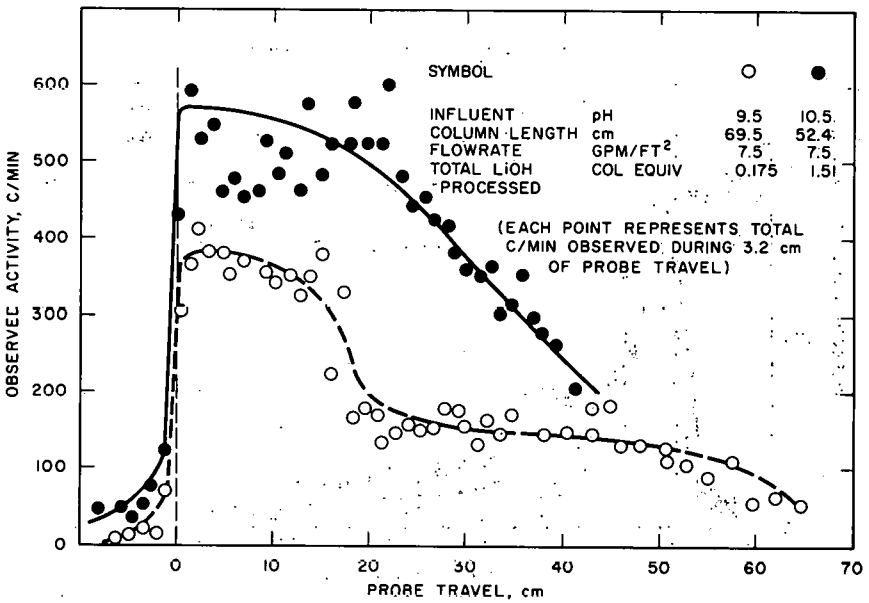

Fig. 39 Ce^{144}—Pr^{144} Activity Distribution on LiOH Resin by a Collimated Probe Instrument

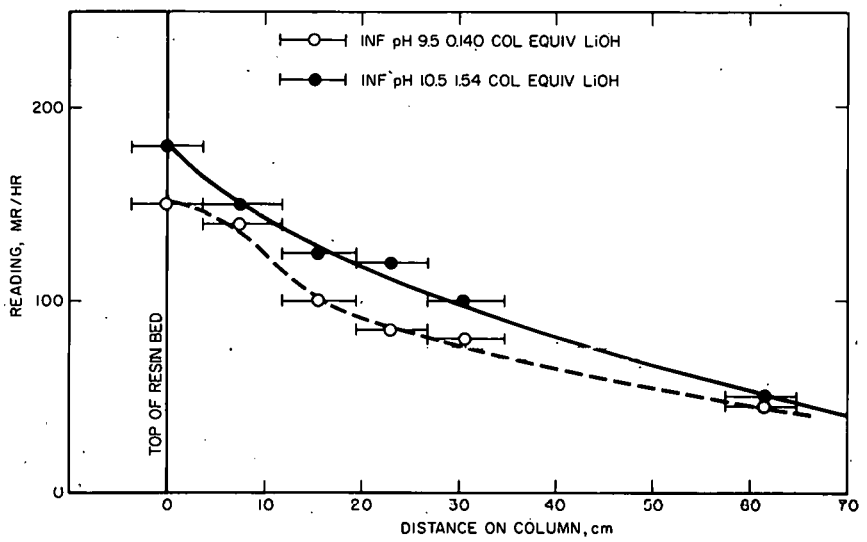

Fig. 42 Ru^{106}—Rh^{106} Activity Distribution on LiOH Resin by a Portable Survey Instrument (Uncollimated)

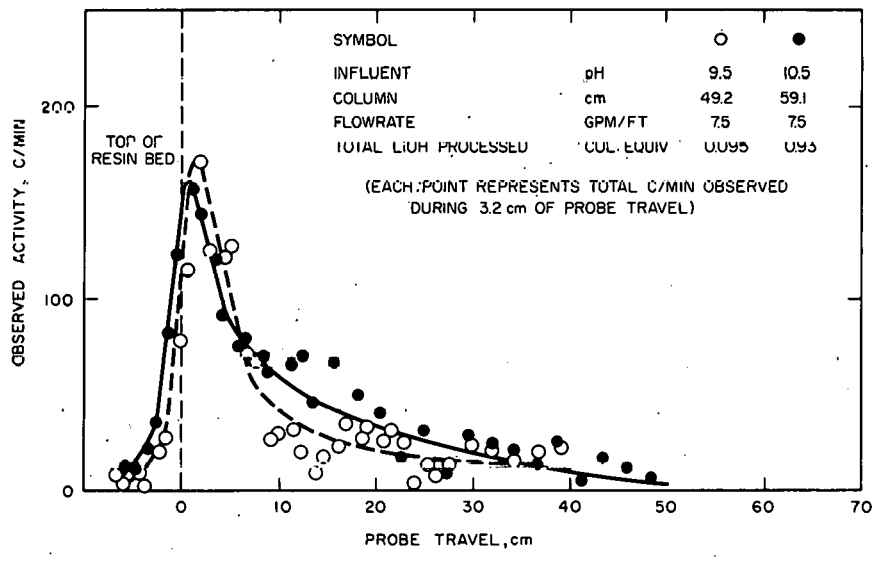

Fig. 43 Zr^{95}—Nb^{95} Activity Distribution on LiOH Resin by a Collimated Probe Instrument

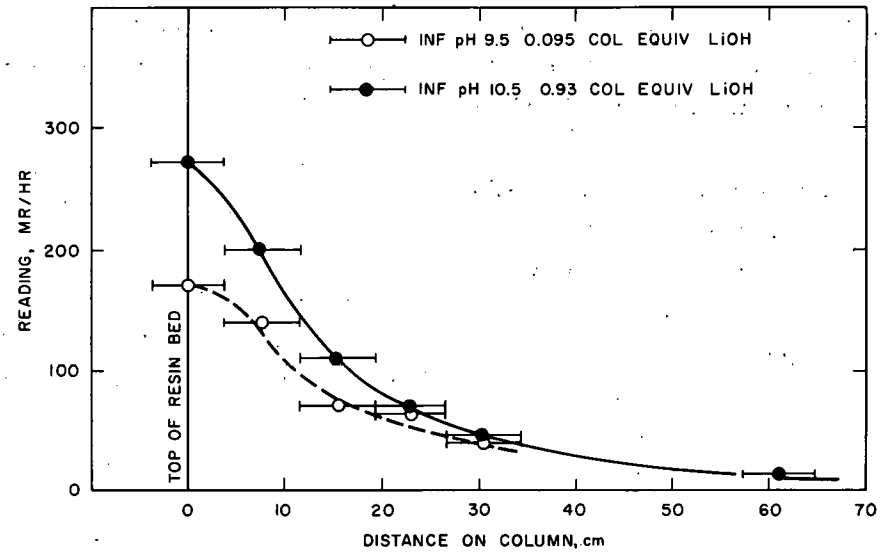

Fig. 44 Zr^{95}—Nb^{95} Activity Distribution on LiOH Resin by a Portable Survey Instrument (Uncollimated)

APPENDIX IV: MULTISTAGE COLUMN THEORY INCLUDING RADIOACTIVE DECAY OF MICRO-CONSTITUENT*

It is instructive to derive the equations applicable to a simple model for an ion exchange column and to examine the effect of decay of radioisotopes on the apparent performance of the column. The model selected for this purpose consists of a series of stages through which the solution passes in succession, coming into equilibrium with the resin phase contained in each stage.** The solution is assumed to contain a macroconstituent, say LiOH or KOH at about 10^{-4} M. For this discussion the resin phase may be considered a mixed bed of strongly acid cation resin and strongly basic anion resin in a one-to-one equivalent ratio, fully converted to the appropriate base form. An ionized, radioactive microconstituent, not previously present in solution or resin, is assumed to appear in the influent solution at time t = 0 and remain in the influent at constant concentration. The problem is now to calculate the distribution of the microconstituent in the solution and resin phases as a function of time and position along the column.

The following nomenclature has been used:

- G = total capacity of resin (eq/cc wet resin) concentration of (monovalent) major species on resin (mol/cc wet resin).
- n = number of equilibration stages in the column.
- Q = solution flowrate (cc/sec).
- V_x = bulk volume of the wet resin bed (cc resin).
- t = time (sec).
- delay constant of microconstituent (sec^{-1}).
- C'_{w_o} = concentration of microconstituent in entering solution (mol/cc).
- C'_{w_i} = concentration of microconstituent in solution in equilibrium with i^{th} stage (mol/cc).
- C'_{w_n} = concentration of microconstituent in equilibrium with final (n^{th}) stage concentration of microconstituent in effluent (mol/cc).

*W. T. Lindsay, Jr.

**A more comprehensive theory has been developed by A. S. Kesten of Bettis Laboratory to include radioactive decay in the case where either liquid film or solid-phase diffusion can be rate controlling. The equations resulting from that work are rather complicated, however, and cannot be applied to experimental results of the type reported here. Consequently, a simpler theory is given to aid in interpretation of results and in prediction of expected column performance under selected, simplified conditions.

$C_{w_o} = C_{w_i} = C_{w_n}$ = concentration of macroconstituent in solution (constant with time and throughout the column) (mol/cc).

X'_{r_i} = mole fraction of microconstituent in resin phase of i^{th} stage.

X'_{r_n} = mole fraction of microconstituent in resin phase of final (n^{th}) stage.

$X_{r_1} = X_{r_i} = X_{r_n}$ = mole fraction of macroconstituent in resin phase (constant with time and throughout the column) ~1.

$R = C'_{W_i}/X'_{r_i}$ = distribution coefficient between solution and resin phase for microconstituent (assumed constant throughout the column).

Note first that the gross composition of resin and solution phases will be essentially unchanged by the presence of the trace radioactive species. Under these conditions it is reasonable to assume that the distribution coefficient R will be independent of the concentration of this trace species. It is also assumed that the diffusion coefficient of the trace species in the solution is independent of its own concentration. This is reasonable in view of the constancy of ionic strength of the solution (Ref 5).

For a monovalent trace ion, the thermodynamic equilibrium constant K_a for the exchange reaction in the i^{th} stage, $M'^{+} + MR = M'R + M^{+}$, where M' is a radioactive trace cation, M is a cation at macroconcentration, and R represents the resin, can be written

$$K_a = \left(\frac{\gamma_{w_i}}{\gamma'_{w_i}}\right)\left(\frac{C_{w_i}}{C'_{w_i}}\right)\left(\frac{X'_{r_i}}{X_{r_i}}\right), \qquad (5)$$

where γ_{w_i} and γ'_{w_i} represent the activity coefficients of the major and minor species in the solution phase and the activities of the two species in the resin phase have been replaced by the corresponding mole fractions (Ref 6). Then,

$$K_c = \left(\frac{\gamma'_{w_i}}{\gamma_{w_i}}\right) K_a = \left(\frac{C_{w_i}}{C'_{w_i}}\right) X'_{r_i} \qquad (6)$$

when the number of moles of the microcomponent in the resin phase can be neglected relative to the number of moles of the major species in that phase. Therefore,

$$R = \frac{C'_{w_i}}{X'_{r_i}} = \frac{C_{w_o}}{K_c} = \text{constant} \qquad (7)$$

if C_{w_i} remains constant, since the activity coefficients of the ions in solution remain unchanged at the constant ionic strength. Similarly, for a divalent trace ion,

$$R = \frac{C_{w_o}^{\,2}}{K_c} = \text{constant}, \qquad (7a)$$

and for a trivalent trace ion,

$$R = \frac{C_{w_o}^{\,3}}{K_c} = \text{constant}. \qquad (7b)$$

A set of differential equations can be written for the mass balance of the trace ion in each of the n equilibration stages as follows:

$$\left.\begin{aligned}
\left(\frac{GV_x}{n}\right)\left(\frac{dX'_{r_i}}{dt}\right) &= QC'_{w_o} - \frac{\lambda GV_x X'_{r_1}}{n} - QRX'_{r_1},\\
\left(\frac{GV_x}{n}\right)\left(\frac{dX'_{r_2}}{dt}\right) &= QRX'_{r_1} - \frac{\lambda GV_x X_{r_2}}{n} - QRX'_{r_2},\\
&\vdots\\
\left(\frac{GV_x}{n}\right)\left(\frac{dX_{r_i}}{dt}\right) &= QRX'_{r_{i-1}} - \frac{\gamma GV_x X_{r_i}}{n} - QRX'_{r_i},\\
&\vdots\\
\left(\frac{GV_x}{n}\right)\left(\frac{dX_{r_n}}{dt}\right) &= QRX'_{r_{n-1}} - \frac{\gamma GV_x X'_{r_n}}{n} - QRX'_{r_n}
\end{aligned}\right\} \qquad (8)$$

Two additional assumptions have been made in writing these equations: first, that the number of moles of the trace ion in the solution phase of each stage is negligible compared with the number of moles in the resin phase and, second, that the volume of resin in each stage is independent of position in the column and equal to V_x/n. The first of these assumptions is easily justified for the case of solutions with the macrocomponent at concentrations on the order of 10^{-4} M. The second assumption implies, in addition to the constancy of the diffusion coefficient for the trace ion, that liquid film resistance is rate controlling in the ion exchange process. Boyd, Adamson, and Myers (Ref 7) found from studies of the kinetics of exchange of a trace ion in the presence of a macroconstituent that liquid film resistance was rate controlling at macro-ion concentrations of 10^{-3} M or below at the conditions of their experiments, while resin-phase diffusion did not become the controlling step unless macro-ion concentrations were 0.1 M or greater. Thus, the second assumption is probably not too inaccurate for the conditions.

The solution to Eqs (8) is found to be

$$\frac{RX'_{r_n}}{C_{w_o}} \quad \frac{C'_{w_n}}{C'_{w_o}} = \left(\frac{nQR}{\alpha GV_x}\right)^n - e^{-\alpha t}$$

$$\left(C_1 + C_2 t + \ldots C_n t^{n-1}\right), \qquad (9)$$

where $\alpha = \lambda + \frac{nQR}{GV_x}$,

and C_1, C_2, $\ldots C_n$ are constants.

The constants are identified by the condition that $X'_{r_n} = 0$ when $t = 0$ and by the requirement that, as V_x/n approaches zero and n approaches infinity, C'_{w_n}/C'_{w_o} remains zero until some time at which sharp breakthrough occurs and C'_{w_n}/C'_{w_o} becomes unity. Substitution of the constants in Eq (9) and rearranging gives, as the result,

$$\frac{C'_{w_n}}{C'_{w_o}} = \frac{RX'_{r_n}}{C'_{w_o}} = \left(\frac{nQR}{\alpha GV_x}\right)^n \left\{1 - e^{-\alpha t}\left[1 + \alpha t + \ldots + \frac{(\alpha t)^{n-1}}{(n-1)\,!}\right]\right\} \qquad (10)^*$$

This equation predicts the familiar S-shaped curve for breakthrough of the trace species, with the time of breakthrough and the sharpness of breakthrough governed by the parameters n, Q, R, G, V_x, and λ. Of these, Q and V_x are independently variable, λ is determined by the radioisotope in question, G is a property of the type of resin used, and n and R are parameters appropriate to the particular conditions of operation. The number of equilibration stages (n) will depend on the linear velocity of solution through the interstices of the bed, the resin particle size, the nature of the trace ion, and the nature and concentration of the macro-ion in solution. The distribution coefficient R will depend on the nature and concentration of the macro-ion in solution, the nature of the trace ion, and the type of resin. For a given type of resin, bed depth, area flow loading, and concentration range for the macroconstituent in solution, it should be possible to determine the parameters n and R for a variety of macroconstituents such as LiOH, KOH and NH_4OH and microconstituents such as Cs, Ba, Sr, I, etc., and then to predict the apparent performance of columns operating under these conditions for removal of isotopes of trace species of various half-lives.

By setting the second derivative of Eq (10) equal to zero, the time t_m is obtained for the maximum in the slope of the breakthrough curve:

$$t_m = \frac{n-1}{\alpha} . \qquad (11)$$

Note that if $\lambda << \frac{nQR}{GV_x}$,

* Equation (10) has been confirmed by independent derivation by A. S. Kesten by the method of Laplace transforms.

$$t_m = \left(\frac{n-1}{n}\right)\frac{GV_x}{QR}, \quad \text{and} \tag{12}$$

$$t_m \sim \frac{GV_x}{QR} \tag{13}$$

when n is large. This result, as expected, provides R and K_c from the results of column tests on long-lived radioisotopes. For the case of a monovalent trace ion, K_c is equal to $QC_{w_o}t_m/GV_x$, the total number of column equivalents passed into the column at the time t_m. If K_c is on the order of unity (as for isotopic exchange or for exchange of alkali metal ions), it is predicted that breakthrough will occur after passage of about one column equivalent. As λ increases relative to nQR/GV_x, the time of the maximum slope of the breakthrough curve becomes earlier, being equal to the time when 1/2 column equivalent has passed through the column in the isotopic exchange case for monovalent ions when $\lambda = nQR/GV_x$. It is informative to note that, for this case, the quantity nQR/GV_x is the reciprocal of the time required to pass one equilibration stage equivalent (i.e., 1/n column equivalents) into the column.

The magnitude of the slope of the breakthrough curve at t_m is obtained by substituting Eq (11) into the first derivative of Eq (10):

$$\left[\frac{d\left(C'_{w_n}/C'_{w_o}\right)}{dt}\right]_{t_m} = \frac{\left(\frac{nQR}{GV_x}\right)^n e^{-(n-1)}(n-1)^{(n-1)}}{\alpha^{n-1}(n-1)!} \tag{14}$$

If n is 10 or greater, Stirling's approximation can be used without great error to give

$$\left[\frac{d\left(C'_{w_n}/C'_{w_o}\right)}{dt}\right]_{t_m} = \frac{\alpha\left(\frac{nQR}{\alpha GV_x}\right)^n}{\sqrt{2\pi(n-1)}} \tag{15}$$

Again, when $\lambda \ll \frac{nQR}{GV_x}$, a simple result is obtained:

$$\left[\frac{d\left(C'_{w_n}/C'_{w_o}\right)}{dt}\right]_{t_m} = \frac{QR}{GV_x}\frac{n}{\sqrt{2\pi(n-1)}} \sim \frac{QR\sqrt{n}}{GV_x\sqrt{2\pi}} \tag{16}$$

Substituting Eq (12) in Eq (16),

$$\left[\frac{d\left(C'_{w_n}/C'_{w_o}\right)}{dt}\right]_{t_m} = \frac{\sqrt{n-1}}{t_m\sqrt{2\pi}} \tag{17}$$

from which n can be obtained from column experiments with long-lived radioisotopes. As λ increases relative to nQR/GV_x, the slope of the breakthrough curve at t_m becomes smaller, equaling $1/2^{(n-1)}$ times the value of the slope for $\lambda = 0$ when λ becomes equal to nQR/GV_x.

Returning to Eq (10), it can be seen that

$$\frac{C'_{w_n}}{C'_{w_o}} = \frac{RX'_{r_n}}{C'_{w_o}}$$

is equal to the ratio of the number of moles of the trace species in the n^{th} stage to the total number of moles of this species that would be contained in the final stage, if it were equilibrated with the incoming solution. Therefore, the distribution of the trace species on the column, normalized to the total possible content of each stage when equilibrated with the influent, will be given by RX'_{r_i}/C'_{w_o}. At any given time t before breakthrough, it can be shown from Eq (10) that the maximum in the derivative of the distribution curve with respect to x, the fraction of the total bed length, will be at $x_m = QRt/GV_x$ when $\lambda \ll nQR/GV_x$. The magnitude of the derivative at this point, assuming i_m (which is equal to $x_m n$) is large enough so that Stirling's approximation can be

used, will be $-\sqrt{n}/(x_m\sqrt{2\pi})$ for this case. Thus, n and R can also be determined from the distribution of activity on a column at times before breakthrough when long-lived radioisotopes are used.

The steady-state ratio for effluent to influent concentration of the trace species, which is equal to the reciprocal of the decontamination factor, is obtained by setting $t = \infty$ in Eq (10). Thus,

$$\left(\frac{C'_{w_n}}{C'_{w_o}}\right)_{SS} = \left(\frac{1}{D.F.}\right)_{SS} = \left(\frac{nQR}{\alpha GV_x}\right)^n \quad (18)$$

When $\lambda = 0$, the steady-state decontamination factor is unity, but when λ has some finite value, the steady-state decontamination factor will be greater than one, owing to decay of the trace species on the column during the average time required for an ion, alternately residing in the solution and resin phases, to pass through the column.

Equation (18) can be rewritten:

$$(D.F.)_{SS} = 1 + \left(\frac{\lambda GV_x}{nQr}\right)^n \quad (19)$$

It can be seen that if the reciprocal of the decay constant is of the order of the time required to pass 1/n column equivalents, the steady-state decontamination factor will be very large. For instance, if $\lambda = GV_x/nQR$ and $n = 10$, $(D.F.)_{SS} = 2^{10} \approx 10^3$. It is of interest to determine the steady-state decontamination factor for isotopes with longer half-lives such that $\lambda GV_x/nQR \leqq 0.1$. For this case,

$$\ln (D.F.)_{SS} = n \ln \left(1 + \frac{\lambda GV_x}{nQR}\right) \quad (20)$$

$$\left.\begin{aligned} \ln(D.F.)_{SS} &\propto \frac{\lambda GV_x}{QR} \\ (D.F.)_{SS} &\propto e^{\lambda GV_x/QR} \end{aligned}\right\}$$

This is as expected, since GV_x/QR is the average time required for an atom of the radioactive species to pass through the column. For the special case of isotopic exchange of monovalent ions in a 29-in. column of MB-1 resin, treating a 10^{-4} M solution at a flow loading of 7.5 gpm/ft^2, $GV_x/QR = 10^6$ sec. Thus, if $\lambda/n \leqq 10^{-7}$ sec^{-1}, $\ln(D.F.)_{SS} = 10^6 \lambda$; and, if n is 10 or any number greater, an isotope with a half-life of 8 days will have a steady-state decontamination factor equal to e. The factor will be greater for shorter half-lives. In a reactor coolant system with a recirculating bypass purification system, a decontamination factor of the order of e or greater is one of the requirements for the purification system to exert effective control over the concentration of a radioactive species in the coolant.

APPENDIX V: SURVEY OF HIGH pH OPERATION OF IN-PILE AND OUT-OF-PILE LOOPS

The information contained in this survey is discussed in the text under Experience with Base Form Resins. Additional information has been obtained with high pH operation in both test loops and reactor plants since the original information presented in this report was gathered.

LOOP M-3 — BETTIS LABORATORY

Stainless Steel

Total Volume: 15 liters

pH Range: 9.2 to 10.5

LiOH Resin

This work consisted primarily of corrosion tests. No pertinent data were available on the operations except for the fact that no additions of LiOH reagent were necessary to maintain the pH after the original adjustment.

LOOP HB-5—MATERIALS TESTING REACTOR

Test—WAPD-29-1

Stainless Steel Piping

Dates: December 1, 1956 to January 14, 1957

Hours of Operation: approximately 900

Leakage Rate: low until January 7; 3 gal/day after this date

Volume of Loop: 1.11 ft^3 or 8.30 gal

Volume of Purification System: 0.061 ft^3 or 0.45 gal

Total Volume: 12 gal

Surface Area: 60.6 ft^2

Volume of Resin: 426 ml

Flow through Ion Exchange Bed: 0.1 gpm

pH Range: 9.3 to 10.5

LiOH Resin

The first cycle was started on December 1, 1956, and completed on December 21. No addition of LiOH reagent was necessary to maintain the pH during this period which was equivalent to 500 hours. The second cycle was completed on January 14, 1957. Two additions of LiOH reagent were necessary during the second cycle. The leakage was low during the first cycle and was high (3 gal/day = 0.25 system volumes /day) for the second cycle. The leakage rate for the second cycle necessitated the two additions of LiOH solution.

The LiOH resin was changed at the end of each cycle. This change was requested by Bettis Laboratory for radiochemical analyses; the change was not the result of resin exhaustion.

LOOP HT-1—MATERIALS TESTING REACTOR

Test—WAPD-26-1

Stainless Steel Piping

Dates: January 22, 1956 to April 4, 1956

Hours of Operation: approximately 1700

Leakage Rate: unknown

Volume of Loop: 9.4 ft^3 or 70.3 gal

Volume of Purification System: 0.196 ft^3 or 1.46 gal

Total volume: 71.5 gal

Surface Area: 216 ft^2

Volume of Resin: 426 cm^3

Flow through Ion Exchange Bed: 0.1 gpm

System Volumes per Second: 2.3 x 10^{-5}

pH Range: 7.8 to 9.4

KOH Resin

The KOH resin was used one day every two weeks to increase the pH. The test was at low power and low activity was present in the water. This test is of little interest in determining the effectiveness of a KOH bed in maintaining pH.

Test—WAPD-30-1

All parameters are the same as the WAPD-26-1 test except for the following:

Dates: October 24, 1956 to January 24, 1957

Hours of Operation: approximately 2000

Leakage Rate: high, but unknown.

pH Range: 9.5 to 10.5

The leakage was high and the loop was drained a number of times and KOH solution added at 12 different time intervals. The evidence is not sufficient for any conclusion because of the large volume of water lost or drained from the loop.

KAPL LOOPS—MATERIALS TESTING REACTOR

TF-33

Carbon Steel

Dates: November 6, 1956 to January 24, 1957

Hours of Operation: >2000

Leakage Rate: unknown

Volume of Loop: >70 gal

Surface Area: 93 ft^2

Volume of Resin: 1026 cm^3

Flow through Ion Exchange Bed: 0.23 gpm

System Volumes per Second: 5.5 x 10^{-5}

pH Range: 9.2 to 9.7

LiOH Resin

There were no difficulties in maintaining the pH without additions of LiOH solution.

TF-37

Stainless Steel

Dates: January 11, 1957 to January 24, 1957

Hours of Operation: 300

Volume of System: >20 gal

Surface Area: 102 ft^2

Volume of Resin: 1287 cm^3

Flow through Ion Exchange Bed: 0.5 gpm

System Volumes per Second: 4.0 x 10^{-4}

pH: 10.1

LiOH Resin

There were no additions of LiOH solution to maintain pH during this test.

BETTIS TEST FACILITY

Stainless Steel

Dates: December, 1953 to June, 1954

Hours of Operation: 1022 hours above 440°F, 548 hours below 400°F

Leakage Rate: unknown

System Volume: 515 ft^3 or 3852 gal

Volume of Resin: 5 ft^3 or 37.4 gal

Flow through Ion Exchange Bed: approximately 10 gpm

System Volumes per Second: 5.5×10^{-5}

pH Range: 9.2 to 9.7

LiOH Resin

During this test program there was no difficulty in maintaining the pH. The reagent, LiOH, was added four times, approximately once a month. The additions were necessary due to a high leakage rate during facility startup.

X-1 LOOP—CHALK RIVER

Test—X-1-d

Stainless Steel

Dates: May 9, 1955 to November 7, 1955

Leakage Rate: fluctuated from 10 to 400 ml/hr; for the last 700 hours with KOH resin, 10 ml/hr

System Volume: 18 gal

Surface Area: 112 ft^2

Volume of Resin: 360 cm^3

Flow through Ion Exchange Bed: 0.1 gpm

System Volumes per Second: 9.3×10^{-5}

pH Range: neutral and 9.5 to 10.5

KOH resin

After the loop had operated for a period of time, a high pressure drop resulted in the system. A KOH resin bed was introduced into the system and the pH rose from 7 to 11 within 8 days. At this time, a HOH resin bed was valved in and, after 7 hours, KOH resin was valved in again. For 300 hours the pH was steady and on July 26, 1955, the resin was removed and shipped to Bettis Laboratory. HOH and KOH resins were valved in and out (with no pertinent information available) until October 9. At this time, the KOH resin was used until the end of the test. The pH was easily maintained for 600 to 700 hours at pH 9.5 to 10.5 without any additions of KOH solution.

Test—X-1-j

Same parameters as the X-1-d test except for the following:

Dates: December 10, 1956 to January 11, 1957

Hours of Operation: >600

Loop Volume: 25 gal

System Volumes per Second: 6.7×10^{-5}

Leakage Rate: 150 ml/hr

pH Range: 9.5 to 10.5

The pH was maintained easily without the addition of LiOH solution.

X-2 LOOP—CHALK RIVER

Test—X-2-a

Stainless Steel

Dates: November 22, 1954 to April 14, 1955

Surface Area: 112 ft^2

Loop Volume: 18 gal

Leakage Rate: approximately 100 ml/hr November to January; 160 to 240 ml/hr February to April

Flow through Ion Exchange Bed: 0.1 gpm

System Volumes per Second: 9.3×10^{-5}

KOH Resin

The loop water was neutral until December 18, 1954. On December 21, a KOH resin bed was valved in and the pH was 9.2 to 9.7; 3 g of KOH in solution were added. The pH was 9.5 to 10.5 for 1000 hours; at this time, 3 g of KOH solution were added. For 500 hours the pH was constant. Five additions of KOH solution were necessary within a week-March 18, 20, 21, 23, and 24. It was discovered that valve LW-14 was open. Thermal syphon (upflow) through the surge tank had been concentrating KOH solution in the tank. Closing the valve eliminated any further need for KOH solution for the remainder of the test. The excessive additions of KOH solution were necessary because of mechanical malfunction, and were not the result of a resin deficiency.

Test—X-2-c

Same parameters as the X-2-a test except for the following:

Dates: June 27, 1955 to February 15, 1956

Hours of Operation: approximately 4500 hours

Leakage Rate: 80 ml/hr

pH Range: 9.5 to 10.5

Volume of Resin: 1500 ml

Flow through Ion Exchange Bed: 0.15 gpm

KOH Resin

The pH was maintained between 9.5 to 10.5 without any addition of KOH solution or replacement of the resin bed.

Test—X-2-f

Same parameters as the X-2-a test except for the following:

Dates: August 14, 1956 to October 9, 1956

Hours of Operation: 1200

Leakage Rate: 400 ml/hr

Flow through Ion Exchange Bed: 0.17 gpm

System Volumes per Second: 1.6×10^{-4}

KOH Resin

pH Range: 9.5 to 10.5

The pH was maintained without any additions of KOH solution.

X-3 LOOP—CHALK RIVER

This loop has the same dimensions as the X-2 loop.

Dates: December 10, 1956 to January 23, 1957

Hours of Operation: 1000

Leakage Rate: 125 ml/hr

pH: 10.0

KOH Resin

No additions of KOH solution were necessary.

LOOP CR-VI—CHALK RIVER

This loop has the same parameters as the X-2 loop.

Test—CR-VI-A

Carbon Steel

Dates: February 14, 1956 to September 10, 1956

Loop Volume: 18 gal

Flow through Ion Exchange Bed: 0.05 gpm

System Volumes per Second: 4.6×10^{-5}

KOH Resin

Leakage Rates: 1700 ml/hr, February 29; 4000 ml/hr, March 2; 1750 ml/hr, April 14; 2000 ml/hr, May 23

On February 15, 1956, KOH solution was added to the loop to raise the pH; KOH solution was added again on February 18. There was no resin flow during this period. After the column was valved in, the pH was steady for 300 hours. Until March 5, there were high leakage rates and KOH was added again. For 2000 hours the pH was maintained at 9.5 to 10.5 with KOH addition. The resin bed was replaced. For 800 hours no KOH solution was necessary with the large ion exchange column valved in; for 1000 hours with the same column valved in, no KOH solution was added.

Test—CR-VI-B

Same parameters as the CR-VI-A test except for the following:

Dates: November 3, 1956 to December 27, 1956

Leakage Rate: 620 ml/hr

The pH was initially raised to 10 with KOH resin. On November 8, a demineralizer containing a Nalcite (SO_4) hot resin bed was put on; on November 16, a KOH bed was valved in. There was poor flow through the Nalcite column (malfunctioning Neva-Clog filter). On November 26, the Nalcite column was valved in. On November 30, it was discovered that both resin columns had no O-rings, and those were repaired on December 6. Prior to this date there was practically no flow through the demineralizer. Because of the difficulties encountered during the test, no conclusions can be drawn.

LOOP CR-V—CHALK RIVER

Test—CR-V-B

Little information was supplied for this test. From the available date, it appears that the pH was maintained at 9.5 to 10.5, and without KOH addition for 1000 hours using a KOH resin.

GENERAL COMMENTS ON CHALK RIVER TESTS

In the nine in-pile tests run at pH 9.5 to 10.5, no difficulty was experienced in maintaining the pH using KOH or LiOH resin beds in the loop purification system. The two exceptions were: the case of the X-2-a test during the period accidental upflow through the surge tank concentrated the KOH solution in the tank, and the case of the CR-VI-A test when the leakage rate exceeded 2000 ml/hr (equivalent to 0.7 system volumes per day). The problem was readily solved on CR-VI-A by replacing the HOH resin in the makeup system for the loop with KOH resin, so that all make-up water was added at the proper pH.

LOOP R-1P—BETTIS LABORATORY

Test on Hydrogen Instrument Analysis Using LiOH Resin

Stainless Steel

Dates: December 4, 1956 to December 21, 1956

Hours of Operation: approximately 350

Loop Volume: 1 gal

Flow through Ion Exchange Bed: 0.05 gpm

System Volumes per Second: 8×10^{-4}

pH Range: 9.1 to 10.2

LiOH Resin

LiOH reagent was added at the startup. No further additions were necessary.

LOOP R-2—BETTIS LABORATORY

Stainless Steel

Dates: May 14, 1956 to May 21, 1956

Hours of Operation: 161

Volume of Loop: 11 liters

Flow through Ion Exchange Bed: 0.05 gpm

System Volumes per Second: 2.8×10^{-4}

LiOH Resin

The LiOH resin column was not constantly on. The pH varied from 9.1 to 10.8. One addition of LiOH was used, but did not seem to be necessary since the pH at that time was 9.3.

In a test from November 14, 1956, to November 21, 1956 (168 hours), the LiOH resin was only put on-stream for approximately 40 hours, but no addition of LiOH solution was necessary. This was also true for tests adding up to 488 hours.

ACKNOWLEDGMENTS

The authors wish to acknowledge the many contributions of others to the work reported here. They are indebted to K. H. Vogel, of Bettis Laboratory, and his staff, to personnel of Atomic Energy of Canada, Ltd., and to members of Bettis radiochemistry groups for the results of the Chalk River test. The laboratory work at Bettis was carried out by W. Schmoutz, D. Kelly, R. P. Roush, D. J. Stiteler, L. S. Lasher, R. W. Holloway, and M. J. Hendrickson, with assistance from others of the Bettis PWR Chemistry and Advanced Development Chemistry Groups. A. S. Kesten provided confirmation of some of the equations given in the report by independent derivation. Many valuable discussions with P. Cohen are appreciated.

REFERENCES

1. G. P. Simon, B. G. Schultz, and Y. Solomon, "Van de Graaff Study, Second Interim Report on the Deposition of Corrosion Products Under Irradiation," WAPD-BT-7 (March 1958).

2. G. P. Simon, "Van de Graaff Study, Third Interim Report on the Deposition of Corrosion Products Under Irradiation," WAPD-BT-11 (December 1958).

3. T. J. Kisiel "Observations on the Thermal Performance of Uranium Oxide Rod Specimens from Post-Irradiation Examinations," WAPD-BT-6 (January 1958).

4. W. T. Lindsay, Jr. and C. S. Abrams, "Ion Exchange Removal of Fission Products from High Purity Water," WAPD-BT-16 (December 1959).

5. H. E. Harned, Physical Chemistry of Electrolytic Solutions, (New York: Reinhold, 2nd Ed., 1950), p 86.

6. G. E. Boyd, J. Schubert, and A. W. Adamson, "The Exchange Adsorption of Ions from Aqueous Solutions by Organic Zeolites, I. Ion-Exchange Equilibria," J. Am. Chem. Soc. 69 2818 (1947).

7. G. E. Boyd, A. W. Adamson, and L. S. Myers, Jr., "The Exchange Adsorption of Ions from Aqueous Solutions by Organic Zeolites, II. Kinetics," J. Am. Chem. Soc. 69 2836 (1947).